HIV gp120-induced synaptic changes – modulation by the endocannabinoid system and NMDARs

A DISSERTATION

SUBMITTED TO THE FACULTY OF THE

UNIVERSITY OF MINNESOTA

BY

XINWEN ZHANG

IN PARTIAL FULFILLMENT OF THE REQUIREMENTS

FOR THE DEGREE OF

DOCTOR OF PHILOSOPHY

STANLEY A. THAYER, ADVISOR

OCTOBER 2019

Acknowledgements

Thank you, first and foremost, to my thesis advisor, Dr. Stanley Thayer. Thank you for accepting me to our lab and for always being patient, supportive and giving me good advice on my research and career. You not only showed me how to conduct rigorous scientific research, but also helped me to become a nice, happy and compassionate person. I feel so lucky to have you as my advisor and life role model.

Thank you to all the past and present members of the Thayer lab for your friendship, advice and collaboration. You made my graduate school life much easier. Thank you, Dr. Kelly Krogh, for mentoring me during my rotation and first several months in the lab, and for all the good advice on my research and career decisions. Thank you, Mariah Wu, for introducing American culture to me and for all the happiness and crying moments together. Thank you, Dr. Jonathan Raybuck, for all the advice and help.

Thank you to my thesis committee members, Dr. Jonathan Marchant, Dr. Anna Lee, and Dr. Robert Meisel. Thank you for your time, support and genuine guidance for my research. Thank you for always arranging time for me and supporting my career development.

I would also like to thank Dr. Colin Campbell, the DGS, for your guidance and help for my graduate study and career. And thank you to Jim Shoemaker, our education coordinator, for helping me deal with all the graduation, internship, and immigration problems.

Thank you to all my friends and family for all the love and support. And special thanks to my mother for always encouraging me and teaching me to be brave and try my best.

The work in this dissertation would not be possible without the grant from the National Institute on Drug Abuse, National Institutes of Health (DA07304) awarded to Dr. Stanley Thayer.

Summary of Publications

1. Wu MM, **Zhang X**, Asher MJ, Thayer SA (2019) Druggable targets of the endocannabinoid system: Implications for the treatment of HIV-associated neurocognitive disorder. Brain Res. [Epub ahead of print]
2. **Zhang X**, Green MV, Thayer SA (2019) HIV gp120-induced neuroinflammation potentiates NMDA receptors to overcome basal suppression of inhibitory synapses by p38 MAPK. J Neurochem. 148(4):499-515
3. Green MV, Raybuck JD, **Zhang X**, Wu MM, and Thayer SA (2019) Scaling Synapses in the Presence of HIV. Neurochemical Research. 44(1):234-246
4. **Zhang X**, Thayer SA (2018) Monoacylglycerol lipase inhibitor JZL184 prevents HIV-1 gp120-induced synapse loss by altering endocannabinoid signaling. Neuropharmacology. 128:269-281.

Abstract

37.9 million people worldwide are living with HIV. Nearly half of these individuals develop HIV-associated neurocognitive disorder (HAND). Symptoms range from subclinical cognitive deficits to severe dementia that impairs daily function and may cause death. Combination antiretroviral therapy (cART) has significantly decreased the incidence of severe HIV dementia and encephalitis; however, HAND prevalence remains high and may be increasing due to the prolonged life span of HIV patients. Currently, there is no effective treatment for improving cognitive function in HAND patients. Thus, understanding the mechanism and possible avenues for modulating HIV-induced cognitive decline is important. HIV neurotoxicity is mainly mediated by factors released by infected cells. The HIV envelope protein, gp120, is shed by infected cells and is a potent neurotoxin causing excitotoxicity and loss of excitatory synapses. Synaptic damage is reversible and correlates with cognitive decline in HAND patients.

In this dissertation, I explored mechanisms of HIV gp120-induced changes in the number of excitatory and inhibitory synapses. Balance between excitatory and inhibitory synapses is important for controlling network excitability and maintaining normal neural function. The endocannabinoid (eCB) system and NMDA receptors (NMDARs) were investigated for their role in gp120-induced synaptotoxicity. HIV gp120 induces loss of excitatory synapses via a neuroinflammatory pathway; the endocannabinoid (eCB) system is a potential target to modulate neuroinflammation. In the first study, I demonstrated that inhibition of monoacylglycerol lipase (MGL), the enzyme that degrades the eCB 2-arachidonoylglycerol (2-AG), using the specific inhibitor JZL184, blocked gp120-induced excitatory synapse loss. Inhibition of MGL suppressed gp120-induced release of the inflammatory cytokine interleukin-1β (IL-1β) through enhanced activation of cannabinoid type 2 receptors (CB2Rs), and decreased production of prostaglandin E_2 (PGE_2) further decreases neuroinflammation.

In the second study, I showed that gp120 increases the number of inhibitory synapses through the same IL-1β-mediated neuroinflammatory pathway. Activation of the tyrosine kinase Src potentiated GluN2A NMDARs to overcome a tonic suppression of inhibitory synapses by p38 mitogen-activated protein kinase.

In the third study, a mechanism for excitatory synaptogenesis was examined. I showed that presynaptic GluN2B NMDARs control spontaneous glutamate release, and

inhibition of these receptors induces synaptogenesis when evoked neurotransmission is impaired.

Taken together, these studies elucidate mechanisms of gp120-induced synaptotoxicity. Decreased excitatory and increased inhibitory synaptic input may be adaptive mechanisms through which neurons counteract excessive excitation-induced by HIV neurotoxins. Because these synaptic changes correlate with cognitive decline, they may indicate that a neuroprotective mechanism has gone awry. By determining the pathways activated by HIV gp120, this dissertation provides new insight into synaptotoxicity-associated with HAND and identifies novel targets for therapeutic agents that provide neuroprotection.

Table of Contents

List of Figures

Abbreviations

AA, arachidonic acid

AEA, anandamide

AH6809, 9-oxo-6-propan-2-yloxyxanthene-2-carboxylic acid

AIDS, acquired immunodeficiency syndrome

AM630, 6-iodopravadoline

ANI, asymptomatic neurocognitive impairment

APs, action potentials

BBB, blood-brain barrier

CaMKII, Ca^{2+}/calmodulin-dependent protein kinase II

cART, combination antiretroviral therapy

CB, cannabinoid

CB1R, cannabinoid type 1 receptor

CB2R, cannabinoid type 2 receptor

CREB, cAMP response element-binding protein

CXCR4, C-X-C chemokine receptor type 4

CCR5, C-C chemokine receptor type 5

CNS, central nervous system

COX, cyclooxygenase enzymes

DMEM, Dulbecco's modified Eagle's Medium

DSE, depolarization-induced suppression of excitation

DSI, depolarization-induced suppression of inhibition

eCB, endocannabinoid

EGFP, enhanced green fluorescent protein

$EP_{1\text{-}2}R$, prostaglandin 1 and 2 receptors

FAAH, fatty acid amide hydrolase

GABA, γ-aminobutyric acid

$GABA_AR$, γ-aminobutyric acid type A receptor

GFP, green fluorescent protein

HHSS, HEPES Hanks' salt solution

HIV, human immunodeficiency virus

HAD, HIV-associated dementia

HAND, HIV-associated neurocognitive disorder

IL-1β, interleukin-1β

IL1R, interleukin-1 receptor

JZL184, 4-nitrophenyl 4-(dibenzo[d][1,3]dioxol-5-yl(hydroxy)methyl)piperidine-1-carboxylate

LPS, lipopolysaccharide

LRP, lipoprotein receptor-related protein

LTP, long term potentiation

MAP2, microtubule-associated protein 2

MDM2, murine double minute 2

MND, mild neurocognitive disorder

MGL, monoacylglycerol lipase

M-tropic, macrophage-tropic

mIPSC, miniature inhibitory post-synaptic current

Nef, negative regulatory factor

NMDAR, N-methyl-D-aspartate receptor

nNOS, neuronal nitric oxide synthase

PG, prostaglandin

PGE_2, prostaglandin E_2

PSD95, post-synaptic density protein 95

p38 MAPK, p38 mitogen-activated protein kinase

qRT-PCR, quantitative reverse transcription real-time polymerase chain reaction

RRID, Research Resource Identifier (see scicrunch.org)

ROIs, regions of interest

SSCTs, spontaneous spine calcium transients

T-tropic, T cells-tropic

2-AG, 2-arachidonoylglycerol

Tat, trans-activator of transcription

TNF-α, tumor necrosis factor-α

Chapter One: Introduction

I. HIV pathogenesis, virology and treatment

Human immunodeficiency virus (HIV) attacks the immune system and, in advanced stages, causes acquired immunodeficiency syndrome (AIDS), one of the deadliest diseases in human history. Currently, about 37.9 million people are infected with HIV including 1.7 million children (<15 years old) (UNAIDS, 2019). 0.8 % of adults among 15 – 49-year-olds worldwide are living with HIV (WHO Global Health Observatory, 2018). About 59 % of the infected patients are receiving effective antiretroviral therapy and the prevention of HIV has improved greatly over the years (WHO Global Health Observatory, 2018). Despite that, the fight against HIV/AIDS continues.

HIV is mainly transmitted through sexual contact across mucosal surfaces, maternal-infant exposure, and percutaneous inoculation (Shaw and Hunter, 2012). Ordinary day-to-day contacts such as shaking hands, hugging or sharing personal objects will not cause infection. Primary HIV infection causes non-specific symptoms such as fever, headache, fatigue, rash, and joint pain (Bollinger et al., 1997; Vanhems et al., 1999; Lavreys et al., 2000). As disease progresses, decreased CD4-positive lymphocytes and increased plasma viral load are detected (Mellors et al., 1997). Without treatment, HIV further advances to AIDS by depleting CD4-positive lymphocytes to below 200 cells/mm^3 (Osmond et al., 1994; Vlahov et al., 1998). Marked immune activation and inflammation accompany HIV infection. Natural killer cells and neutralizing antibodies mediate an increase in innate host immune response shortly after infection; residual inflammation is induced by HIV proteins and co-infections during chronic stages of the disease (Appay and Sauce, 2008; Maartens et al., 2014). Although innate immune response is critical for viral control, HIV mutations emerge and strictly limit this effect (Alter et al., 2011; Elemans et al., 2017). Immunodeficient patients can develop severe opportunistic infections, respiratory disorders, cancers, and neurological complications such as peripheral nervous system disorders and HIV-associated neurocognitive disorder (HAND) (Crowe et al., 1991; Laga et al., 1992; Wallace et al., 1993; Price, 1996; Wallace et al., 1997; McArthur et al., 2005; Silverberg et al., 2009; Letendre, 2011).

HIV is an enveloped lentivirus containing a single strand of RNA. The HIV lifecycle includes viral entry, reverse transcription, DNA integration, production of viral proteins, and viral release (Ferguson et al., 2002; Maartens et al., 2014). Viral entry is the first and the most important step of HIV infection. The viral envelope precursor glycoprotein gp160 is cleaved into gp120 and gp41 that form a trimer of heterodimers gp120/gp41 (Wilen et

al., 2012). Gp120 is the membrane surface envelope glycoprotein that identifies and interacts with coreceptors, and gp41 is the transmembrane glycoprotein that anchors gp120/gp41 complex in the membrane and facilitates the membrane fusion during viral entry (Willey et al., 1988; Freed, 2001). Gp120 binds to CD4, a surface receptor expressed on macrophages, dendritic cells and CD4-positive T cells, and induces exposure of coreceptor-binding sites. C-X-C chemokine receptor type 4 (CXCR4) and C-C chemokine receptor type 5 (CCR5) are two chemokine receptors that serve as coreceptors for gp120 binding. Binding of gp120 to coreceptors further triggers membrane fusion and viral entry (Wilen et al., 2012; Chen, 2019).

Two types of HIV virus have been identified: HIV-1 and HIV-2. HIV-1 is the most widespread and toxic, and major type of HIV and thus, the focus of many HIV related studies. HIV-2 is a less toxic form of HIV and causes fewer disease outcomes (Marlink et al., 1994). HIV tropism is mainly determined by coreceptors. Macrophage-tropic (M-tropic) HIV variants use CCR5 as coreceptor and are designated as R5. T cells-tropic (T-tropic) HIV variants use CXCR4 as coreceptor and are designated as X4 virus (Shioda et al., 1991; Berger et al., 1999).

The application of combination antiretroviral therapy (cART) has successfully transformed HIV from a fatal infection to a chronic manageable disease (Maartens et al., 2014) with dramatically increased survival rate (Johnson et al., 2013). Early initiation of cART has also been shown to decrease HIV transmission (Cohen et al., 2011). More than 40 antiretroviral drugs have been approved by the U.S. Food and Drug Administration and inhibit viral infection at various steps in virus lifecycle. The antiretroviral drugs include nucleoside reverse transcriptase inhibitors, non-nucleoside reverse transcriptase inhibitors, protease inhibitors, fusion inhibitors, CCR5 antagonists, integrase inhibitors. Typical cART contains two or more drugs from one or more drug classes.

Despite the successful management of disease symptoms, eradication of HIV from infected individuals remains unlikely. Even with patients under highly active cART treatment, resting CD4-positive T cells and the central nervous system (CNS) can serve as latent reservoirs for HIV that can be reactivated and initialize systemic infection (Finzi et al., 1997; Lambotte et al., 2003; Siliciano et al., 2003; Thompson et al., 2011). CNS viral escape can possibly be attributed to the relatively low brain penetration of antiretroviral drugs (Kerza-Kwiatecki and Amini, 1999; Thomas, 2004), infected long-living microglia and macrophages in the brain with low turn-over rates (Crowe et al., 2003), and

integration of HIV-1 to terminally differentiated cells such as astrocytes (Churchill et al., 2006). CNS reservoirs account for the wide prevalence of HAND despite of successful control of plasma viral load in patients receiving cART.

II. HIV-associated neurocognitive disorders

HIV-associated neurocognitive disorder (HAND) represents a spectrum of neurocognitive dysfunction caused by HIV infection. HIV-associated dementia (HAD), mild neurocognitive disorder (MND), and asymptomatic neurocognitive impairment (ANI) are three major forms of HAND. They are categorized based on the interference of daily function using neuropsychological and functional assessment (Antinori et al., 2007; Saylor et al., 2016).

About half of HIV-infected individuals develop HAND (Ellis et al., 2007). Before the wide application of cART, HAD was the most common form of HAND and almost inevitably led to death (Ellis et al., 1997). Deployment of highly active cART treatment has dramatically decreased the incidence of severe HAD form of cognitive dysfunction; however, the prevalence HAND remains high and will likely increase due to the increased life span of HIV-infected patients (Maschke et al., 2000; Valcour et al., 2004; Tozzi et al., 2007; Heaton et al., 2010; McArthur et al., 2010; Joska et al., 2011).

HAND is characterized by marked cognitive dysfunction including diminished performance on attention measurements, slow speed of information processing, and impaired task-dependent functions (Baldewicz et al., 2004; Heaton et al., 2004); motor dysfunction and depressive symptoms are also observed (Reger et al., 2002). These symptoms seriously impair life quality, everyday function and even survival (Heaton et al., 1994; Heaton et al., 2004; Albert and Martin, 2014). Additionally, conversion from ANI to more severe forms of cognitive dysfunction is common in the later stages of HAND patients under cART (Grant et al., 2014). Thus, early clinical intervention in addition to cART is important for controlling HAND progression.

III. HAND pathogenesis and mechanism of HIV neurotoxicity

Introduction of cART has fundamentally shifted the pathophysiology of HAND. Neuronal loss and encephalitis, historically considered to play central role, are no longer the main pathophysiological foundation for HAND (Gelman, 2015) and do not correspond closely to cognitive impairment in HAND patients (Adle-Biassette et al., 1999). In contrast, non-apoptotic neural dysfunction such as damage to synaptodendritic connections and

disturbance in neural network homeostasis are more closely associated with cognitive impairment in patients with MND and ANI, the most prevalent forms of HAND (Masliah et al., 1997; Everall et al., 1999; Ellis et al., 2009). Neural dysfunction rather than neuronal loss is an emerging focus of therapeutic strategies for HAND.

HIV penetrates the blood-brain barrier (BBB) at early stages of infection (Resnick et al., 1988). Multiple mechanisms are proposed for HIV brain entry. The most commonly accepted "Trojan Horse" hypothesis dictates that infected circulating monocytes transmigrate across the BBB in response to chemotactic signals (Nath, 1999; Gonzalez-Scarano and Martin-Garcia, 2005), and subsequently infect macrophages (Fischer-Smith et al., 2008), microglia (Dickson et al., 1991) and astrocytes (Brack-Werner, 1999). Neurons are not infected by HIV (Gonzalez-Scarano and Martin-Garcia, 2005; Kovalevich and Langford, 2012); thus, HIV neurotoxicity is mainly through indirect mechanisms mediated by neurotoxic factors released by infected cells (Ellis et al., 2007).

Sustained neuroinflammation is associated with the progression of HAND (Anthony et al., 2005; Vera et al., 2016). Infected macrophages and microglia cause sustained brain HIV production and stimulate a brain immune response causing release of inflammatory cytokines such as interleukin 1-β (IL-1β) and tumor necrosis factor-α (TNF-α) (Hong and Banks, 2015); infected astrocytes, although not producing intact virus, release toxic viral proteins such as trans-activator of transcription (Tat), negative regulatory factor (Nef) and envelope protein gp120 (Brack-Werner, 1999). Viral proteins can exert direct neurotoxicity (Krogh et al., 2014), and also activate uninfected macrophages and microglia further enhancing cytokine release and neuroinflammation (Kaul et al., 2001; Li et al., 2009).

IV. Current and potential avenues for HAND treatment

Deployment of cART has significantly decreased the incidence of severe conditions of HAND; milder forms are still prevalent. This is in part due to poor penetration of most cART drugs through BBB (Strazielle and Ghersi-Egea, 2005; Ellis et al., 2009). CART drugs with better CNS-penetrating properties have been shown to reduce CNS viral load (Letendre et al., 2008) but their effect on the improvement of neurocognitive function remains questionable (Marra et al., 2009; Ellis et al., 2014). In fact, there is increasing concern that these drugs themselves are neurotoxic (Etherton et al., 2015) limiting their wide application in HAND treatment. Thus, there is great need to develop alternative or adjunctive therapeutic strategies for HAND patients.

Neuronal injury in HAND is mainly indirect and due to the inflammatory cytokines and viral proteins released by infected immune cells and astrocytes. Neuroprotective or regenerative agents targeting neuronal repair and preventing further injury have been increasingly explored for the treatment of cognitive decline in HAND. Lithium, a drug for treatment of bipolar disorder, was shown to prevent spine loss induced by gp120 in vitro (Everall et al., 2002). In humans with HAND, administration with lithium associated with increased cognitive performance in a single-arm, 12-week study (Letendre et al., 2006). However, this drug failed to demonstrate neurocognitive improvement in HAND patients in a recent 6-month randomized placebo-controlled trial (Decloedt et al., 2016). Memantine, a non-competitive antagonist of NMDA receptors, was shown to prevent tat and gp120-induced neurotoxicity in vitro and in transgenic mice (Toggas et al., 1996; Shin et al., 2012). However, in a Phase II clinical trial, it did not induce cognitive improvement in HAND patients (Schifitto et al., 2007). Intranasal insulin is being investigated as a potential therapeutic agent although the mechanism for cognitive improvement is still not well understood (Saylor et al., 2016). Minocycline, an antibiotic, was reported to suppress CNS inflammation and severity of encephalitis in SIV-infected rhesus macaques (Zink et al., 2005). Another agent suppressing neuroinflammation by inhibiting interleukin-1 receptor (IL-1R) is also being investigated but the therapeutic effect is not clear (ClinicalTrials.gov Identifier: NCT02527460). These studies indicate the potential for developing neuroprotective agents for HAND patients; however, lack of efficacy in human trials has significantly limited the further development of many drugs. Thus, more investigations to fully understand the pathophysiological mechanisms of HAND need to be conducted and novel therapeutic strategies need to be explored.

V. HIV-1 gp120: A potent neurotoxin

HIV envelope protein gp120 is one of the most toxic viral proteins released by infected cells and plays critical role in HIV neurotoxicity. The primary function of gp120 in the viral life cycle is to identify host cells and facilitate viral entry. Precursor protein gp160, encoded by env gene, is cleaved to gp120 and gp41 after translation (Ferguson et al., 2002). The non-covalently linked gp120/gp41 complex forms a “trimeric spike” on the virion surface. C-terminal gp41 contains a cytoplasmic domain, a membrane spanning domain and an extracellular domain, and mediates conformational change in viral fusion (Arrildt et al., 2012). N-terminal protein gp120 remains completely outside of the viral membrane. It consists of 25 β- and 5 α-helical loops and contains five linearly organized conserved regions (C1-C5) interspersed with five variable regions (V1-V5) (Cooley and

Lewin, 2003). HIV gp120 identifies and interacts with host cell receptors during viral fusion. Residues in the conserved regions on either side of V4 interact with host cell receptor CD4; both the apex and the base of the V3 loop interacts with coreceptors (Arrildt et al., 2012).

HIV gp120 is a potent neurotoxin shed by infected immune cells and astrocytes (Kaul et al., 2001) and detected in brain tissues of HAND patients (Jones et al., 2000; Nath, 2002). Systemic and intraventricular injection of gp120 causes neurocognitive deficits in rats (Spencer and Price, 1992; Epstein and Gendelman, 1993). In a gp120 transgenic mouse model, brain expression of gp120 closely corresponded with the severity of damage in the CNS and this model was shown to mimic the neuronal injuries in human (Toggas et al., 1994; Thaney et al., 2018). Treatment with gp120 causes disturbed glutamate homeostasis and loss of excitatory synapses in cortical and hippocampal cultures (Vesce et al., 1997; Kim et al., 2011).

HIV gp120 may induce neurotoxicity through multiple pathways. As previous mentioned, CXCR4 and CCR5 are coreceptors for gp120-mediated viral entry. These chemokine receptors are mainly G_i protein-coupled receptors that not only serve as coreceptors for virus but can be activated independently by released gp120 protein itself and other endogenous ligands (Busillo and Benovic, 2007; Wu and Yoder, 2009). CXCR4 and CCR5 are expressed in various types of brain cells including microglia, astrocytes and neurons and their activation closely associates with neuroinflammation (Mennicken et al., 1999). In fact, gp120 is shown to directly stimulate astrocytes causing glutamate mediated neurotoxicity (Vesce et al., 1997), and activate microglia causing release of inflammatory cytokines (Kim et al., 2011). It is also reported that nanomolar concentrations of gp120 can interact with the glycine binding site of N-methyl-D-aspartate receptors (NMDARs) (Fontana et al., 1997). Understanding the primary mechanism for gp120-mediated neurotoxicity is critical for deciphering mechanisms of HIV neural injury and discovering neuroprotective agents. In this work, $gp120_{IIIB}$ from a viral strain that specifically binds to CXCR4 is used to investigate the mechanism of neurotoxicity associated with gp120.

VI. Synaptic changes in HAND

Numerous studies have been conducted to characterize the pathological underpinning of HAND. Synaptodendritic damage, rather than neuronal death, corresponds well with cognitive decline in HAND (Adle-Biassette et al., 1999; Ellis et al.,

2007; Saylor et al., 2016). This damage including dendritic beading, aberrant sprouting, retraction of dendritic spines, and loss of synaptic connections (Ellis et al., 2009), happens at an early stage and milder form of HAND and precedes overt neuronal loss by months to years (Bellizzi et al., 2006).

HIV-related neuroinflammatory factors and viral proteins including gp120 have been reported to induce this type of synaptic damage. HIV gp120 induces loss of excitatory synapses at concentration as low as 600 pM *in vitro* (Kim et al., 2011). Loss of synaptic density and associated leaning deficits were also observed in transgenic mice expressing gp120; this model was shown to mimic neurodegeneration in HIV patients (Toggas et al., 1994; Thaney et al., 2018). HIV tat, another widely studied HIV viral protein, causes excitatory synapse loss at a low concentration (50 ng/ml) in vitro (Kim et al., 2008b), and synapse loss-associated cognitive deficits in transgenic mice expressing tat and in mice following intraventricular injection of tat (Fitting et al., 2013; Hahn et al., 2015; Raybuck et al., 2017). IL-1β, one of the main inflammatory cytokines released by HIV-infected cells, was also shown to induce loss of excitatory synapses and cognitive dysfunction (Mishra et al., 2012; Festa et al., 2015).

Higher cognitive behaviors require accurate coordination of neurons through a complex neural network with stable activity patterns. Such networks are not static; both physiological and pathological forces can drive destabilization of the network. For example, under physiological conditions, neurons are constantly integrating, transmitting and storing information. In long-term potentiation (LTP), the widely accepted cellular basis for learning and memory, sustained high-frequency stimulation from presynaptic terminal increases synaptic efficacy leading to unconstrained synaptic strengthening (Bliss and Collingridge, 1993; Pozo and Goda, 2010; Turrigiano, 2012). To retain excitability and maintain the homeostasis of the network, neurons can stimulate multiple mechanisms, including synaptic scaling to adjust the strength of all synapses (Turrigiano and Nelson, 2004; Marder and Goaillard, 2006), regulation of intrinsic excitability (Marder and Goaillard, 2006; Turrigiano, 2011), change of the balance between excitatory and inhibitory synaptic input (Liu, 2004; Gonzalez-Islas and Wenner, 2006), and compensatory adjustment of synapse numbers (Kirov et al., 1999; Turrigiano, 1999; Wierenga et al., 2006). These mechanisms, collectively termed as “homeostatic plasticity”, form the stabilizing force to maintain activity levels in neural network.

Gp120, tat and inflammatory cytokines such as IL-1β and TNF-α are all well-documented excitotoxins causing glutamate and Ca^{2+} influx-dependent excitotoxicity and pathologically disturb the network homeostasis (Dawson et al., 1993; Gelbard et al., 1993; Lawrence et al., 1998; Wang et al., 1999). Tat and IL-1β potentiate NMDAR-mediated Ca^{2+} influx (Viviani et al., 2003; Krogh et al., 2014). TNF-α and gp120 inhibit astrocyte glutamate reuptake (Fine et al., 1996; Wang et al., 2003); gp120 was also shown to directly stimulate astrocytes to increase glutamate release (Vesce et al., 1997). Collectively, these data suggest that the early synaptodendritic damage in HAND may be part of a coping mechanism for neurons to counteract excessive excitatory input and has gone awry leading to functional impairment. This idea is also supported by a previous study that showed that tat induced loss of excitatory synapses is through a mechanism that is distinct from that leading to neuronal death (Kim et al., 2008b).

Balance between excitatory and inhibitory synaptic input is also part of the homeostatic plasticity mechanism (Liu, 2004; D'Amour J and Froemke, 2015; Hiratani and Fukai, 2017). This balance is important for normal network function and disturbing it is associated with cognitive dysfunction in many neurological disorders such as Down syndrome, autism spectrum disorders and schizophrenia (Gao and Penzes, 2015; Nelson and Valakh, 2015; Zorrilla de San Martin et al., 2018). Activity dependent regulation of inhibitory synaptogenesis has been reported (Lin et al., 2008; Flores et al., 2015). In HAND conditions, tat was shown to increase the number of inhibitory synapses in primary hippocampal culture (Hargus and Thayer, 2013). Extra-synaptic γ-aminobutyric acid $_A$ ($GABA_A$) receptor-mediated tonic inhibition is also increased by gp120 (Green and Thayer, 2019). Immunostaining of gephyrin, a post-synaptic scaffolding protein of inhibitory synapse, was increased in transgenic mice expressing tat; however, in the same study, decreased levels of synaptotagmin 2, a marker of GABAergic pre-synaptic terminal, was also detected (Fitting et al., 2013). These studies suggest scaling of inhibitory synapse number may underly the mechanism for cognitive dysfunction in HAND.

Damage to excitatory synapses and compensatory increases in inhibitory synapses may reveal important targets for therapeutic intervention of HAND. First, these changes directly correspond to cognitive deficits in HAND and many other neurological disorders. Second, these changes happen at the early stage of disease and often precede overt neuronal death (Bellizzi et al., 2006). Neurons still maintain the ability for synaptic repair and functional recovery. In fact, studies have indicated that the loss of excitatory

and increase of inhibitory synapses are through mechanisms that are distinct from neuronal death and both are reversible (Figure 1.1) (Kim et al., 2008b; Shin et al., 2012; Hargus and Thayer, 2013; Raybuck et al., 2017). Induction of recovery of excitatory synapses was further shown to trigger improvement of cognitive function in mice (Raybuck et al., 2017). Thus, further mechanistic understanding of how inhibitory synapses are influenced in HAND and strategies to protect and induce recovery of excitatory synapses are promising research topics for the treatment of HAND.

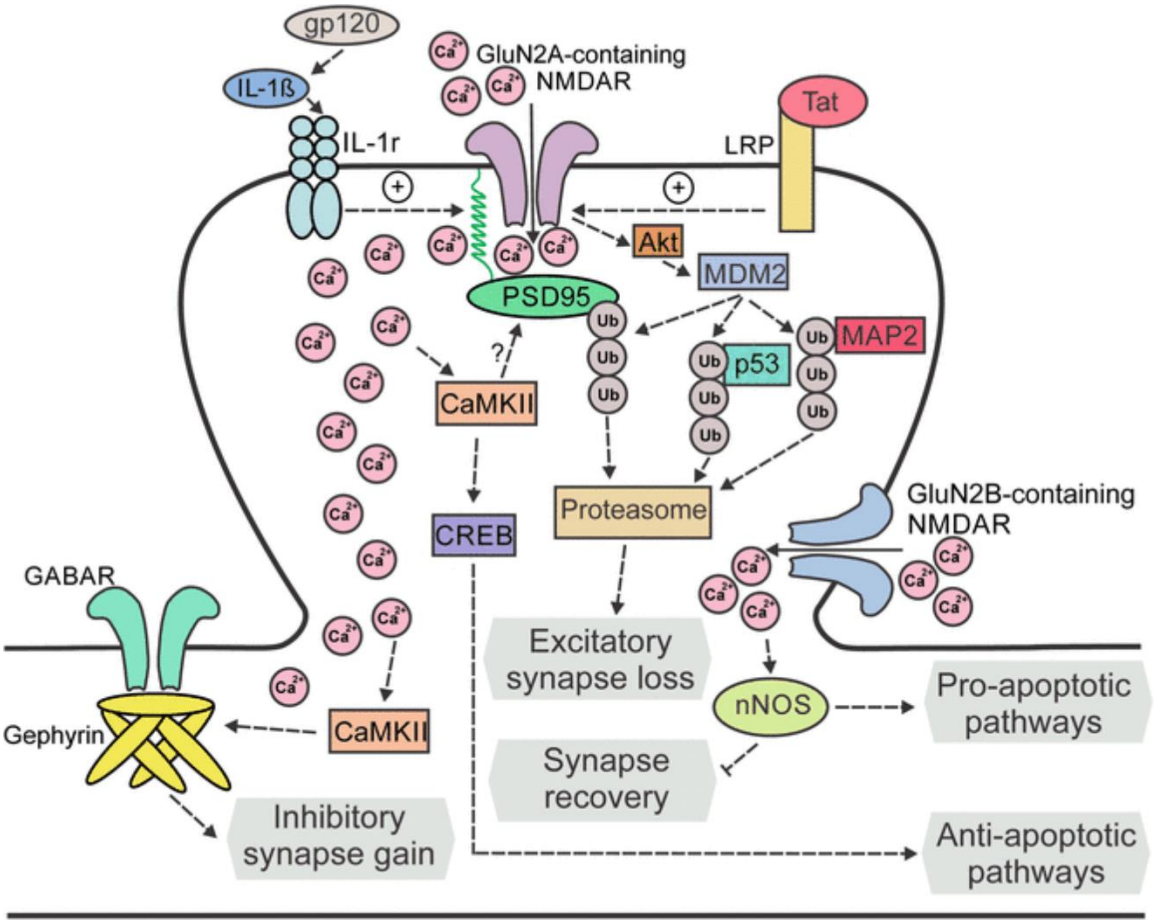

Figure 1.1 Hypothetical mechanism for HIV gp120 and tat-induced synaptic changes. Distinct pathways mediate synaptic changes and neuronal death. Gp120 induces release of IL-1β that activate IL-1Rs. Tat can directly activate lipoprotein receptor-related protein (LRP). These processes induce changes in NMDAR function leading to subsequent pathways involving activation of Ca^{2+}/calmodulin-dependent protein kinase II (CaMKII), Akt kinase, murine double minute 2 (MDM2). MDM2 mediates ubiquitination of postsynaptic density protein 95 (PSD95), p53, and microtubule-associated protein 2 (MAP2), and leads to loss of excitatory synapses. Activation of CaMKII mediates loss of excitatory synapses, increase of inhibitory synapses, and activation of cAMP response element-binding protein (CREB) which mediates anti-apoptotic pathways. GluN2A-containing NMDARs regulate changes to excitatory and inhibitory synapses. GluN2B-containing NMDARs activate neuronal nitric oxide synthase (nNOS) preventing synapse recovery, and may mediate pro-apoptotic pathways (Green et al., 2018). Reproduced with permission, © 2018, Springer Science Business Media, LLC, part of Springer Nature.

VII. Modulation of synapses: endocannabinoid system

Neuroinflammation and excitotoxicity are two hallmarks of HIV-related neurotoxicity. HIV-infected immune cells mediate neuroinflammation; viral proteins stimulate uninfected microglia and macrophages enhancing release of inflammatory cytokines. Both viral proteins and released inflammatory cytokines cause excessive excitotoxic input and induce changes in excitatory and inhibitory synapses. The endocannabinoid (eCB) system provides on-demand protection against excitotoxicity and neuroinflammation (Marsicano et al., 2003; Walter and Stella, 2004; Wu et al., 2019).

Two major cannabinoid receptors can be targeted for neuroprotection. Cannabinoid type 1 receptors (CB1Rs) are expressed in presynaptic terminals of both excitatory glutamatergic and inhibitory GABAergic synapses in hippocampus (Di Marzo et al., 2015). Cannabinoid type 2 receptors (CB2Rs) are expressed at low levels in brain under healthy conditions, with expression significantly upregulated in microglia and macrophages under neuroinflammatory conditions (Howlett et al., 2002; Nunez et al., 2004; Di Marzo et al., 2015). Both CB1Rs and CB2Rs are $G_{i/o}$ protein-coupled receptors. CB1Rs mediate a retrograde signaling pathway in which depolarized post-synaptic neurons rapidly release eCBs to stimulate presynaptic CB1Rs inhibiting further release of neurotransmitters (Wilson and Nicoll, 2001). This process causes transient suppression of excitation (depolarization-induced suppression of excitation, DSE) or inhibition (depolarization-induced suppression of inhibition, DSI) of post-synaptic neurons and is a form of short-term synaptic plasticity to control network excitability (Kano et al., 2002; Freund et al., 2003; Diana and Marty, 2004). Activation of CB1Rs was shown to alleviate excitotoxicity in seizures (Marsicano et al., 2003; Monory et al., 2006; Guggenhuber et al., 2010). CB2Rs exhibits anti-neuroinflammatory effects (Cabral and Griffin-Thomas, 2009). CB2R activation reduces the release of inflammatory cytokines (Klegeris et al., 2003; Romero-Sandoval et al., 2009), decreases microglial activation (Malek et al., 2015) and inhibits chemotaxis (Romero-Sandoval et al., 2009). In HAND models, direct stimulation of CB2Rs suppressed microglial activation and neuroinflammation (Gorantla et al., 2010; Hu et al., 2013) leading to protection from loss of excitatory synapses (Kim et al., 2011; Purohit et al., 2014). Investigation of direct activation of CB1Rs to protect HIV neurotoxicity is rare, probably because of the psychoactive properties of exogeneous cannabinoids (Howlett et al., 2002).

Modulation of the endogenous CBR ligands anandamide (AEA) and 2-arachidonoylglycerol (2-AG) provide an alternative and potentially better strategy for neuroprotection. AEA is a low-efficacy agonist for CB1Rs and has even lower efficacy for CB2Rs. 2-AG is a full agonist for both CB1Rs and CB2Rs (Di Marzo et al., 2015). AEA and 2-AG are degraded by fatty acid amide hydrolase (FAAH) and monoacylglycerol lipase (MGL) respectively, both generating arachidonic acid (AA) (Blankman and Cravatt, 2013). AA is the precursor for cyclooxygenase enzymes (COX1 and COX2)-mediated production of pro-inflammatory prostaglandins (PGs) in brain (Simmons et al., 2004; Rouzer and Marnett, 2009). Thus, inhibiting the degradation of eCBs may enhance the activation of CB receptors and decrease production of PGs producing dual protective effects on neurons. And because the protective effect is “on-demand” and dependent on transient production of eCBs; this strategy will likely exhibit fewer side effects than direct activation of CB receptors. Inhibition of MGL may exert more powerful protective effect than inhibiting FAAH because 2-AG is a full against for both CB1Rs and CB2Rs, and the AA generated by 2-AG degradation is the main pool for brain production of PGs (Nomura et al., 2011; Viader et al., 2015).

In fact, inhibition of MGL induces potent anti-neuroinflammatory effects (Nomura et al., 2011; Grabner et al., 2016). In an Alzheimer’s disease model, MGL inhibition induced the recovery of excitatory synaptic spines and this effect was associated with cognitive recovery in transgenic mice (Chen et al., 2012). These data suggest a potential protective effect of MGL inhibition in HIV-associated synaptodendritic damage with potential multiple protective pathways and reduced psychoactive side effects.

VIII. Modulation of synapses: NMDARs

The NMDAR is a neuron-specific ionotropic glutamate receptor mediating Ca^{2+} influx into neurons. NMDARs play important roles in regulation of learning and memory (Malhotra et al., 1996; Tang et al., 1999; Newcomer and Krystal, 2001) and its dysfunction is associated with many neurodegenerative diseases such as Alzheimer’s disease, (Snyder et al., 2005), multiple sclerosis (Rossi et al., 2013), and bipolar disorder (Clinton and Meador-Woodruff, 2004). HIV neurotoxins cause biphasic changes in NMDAR-mediated Ca^{2+} influx (Krogh et al., 2014; Green and Thayer, 2016). These functional changes in NMDARs mediate HIV neurotoxin-induced loss of excitatory synapses and increase of inhibitory synapses (Kim et al., 2008b; Kim et al., 2011; Hargus and Thayer, 2013).

NMDARs are tetramers composed of two obligatory GluN1 subunits and two GluN2 subunits (Cull-Candy et al., 2001). Four types of GluN2 subunits exist: GluN2A, GluN2B, GluN2C and GluN2D (Cull-Candy et al., 2001). GluN2A and GluN2B are the most abundant forms expressed in hippocampus, an important region controlling learning and memory (Monyer et al., 1994; Shipton and Paulsen, 2014). NMDARs are expressed on synaptic and extra-synaptic sites of neurons (Papouin et al., 2012). Synaptic NMDARs localize to both pre- and post-synaptic terminals (Corlew et al., 2008).

Previous studies focusing on the non-selective NMDAR antagonist memantine (Johnson et al., 2015) showed that the drug induced excitatory synapse recovery in vitro (Shin et al., 2012) but, failed to demonstrate effective cognitive improvement in HAND patients (Schifitto et al., 2007). Different subtypes of NMDARs with different locations are coupled to different pathways and thus, play different roles in regulating neural function. Inhibiting GluN2A NMDARs blocked tat-induced loss of excitatory synapses in hippocampal neurons but failed to rescue synapses after loss; inhibition of GluN2B NMDARs induced recovery of synapses after tat-induced loss but did not block the initial loss (Figure 1.1) (Shin et al., 2012; Hargus and Thayer, 2013; Raybuck et al., 2017). Post-synaptic NMDARs undergo switch from GluN2B to GluN2A during development (Stocca and Vicini, 1998); while presynaptic sites retain GluN2B receptors and these receptors regulate glutamate release. In particular that regulation of spontaneous release of glutamate (Abrahamsson et al., 2017) is important for regulating synaptic strength and formation of synapses during development (Crawford et al., 2017; Ramirez et al., 2017).

Thus, further understanding of the role of different subtypes and locations of NMDARs in modulation of HIV-related excitatory and inhibitory synaptic changes will provide insight for research on the protection and rescue of synapses.

IX. Summary of introduction and current studies

In summary, HAND is a worldwide public health issue influencing nearly half of the 37.9 million HIV-infected population. CART decreased life-threatening HAD but did not change the prevalence of HAND and the drugs may cause neuronal injury themselves. Effective symptom-improving agents are not available, creating a great need for thorough understanding of mechanisms for cognitive dysfunction and exploration of novel therapeutic strategies. Synaptic damage is the most relevant pathological underpinning for cognitive deficits in HAND, and HIV neurotoxicity is mainly mediated by released viral proteins and inflammatory cytokines. This dissertation focuses on HIV neurotoxin gp120-

induced changes in excitatory and inhibitory synapses. The eCB system and NMDARs, two promising targets for modulating the synaptotoxicity of HIV neurotoxins, were examined.

HIV gp120 is a potent neurotoxin inducing loss of excitatory synapses. Enhancing the function of the eCB system induces anti-neuroinflammatory effects in many neurological diseases models. In the first study, I used a novel fluorescent recombinant antibody-like protein (intrabody) to label excitatory synapses. My study discovered that a neuroinflammatory pathway involving activation of microglia and release of inflammatory cytokine IL-1β mediates gp120-induced loss of excitatory synapses. Subsequent potentiation of NMDARs is also involved in the pathway for synapse loss. A selective inhibitor for MGL, JZL184, blocked the loss through both activation of CB2Rs (but not CB1Rs) and reduced production of prostaglandin E_2 (PGE_2).

My work also discovered that gp120 increases the number of functional inhibitory synapses. The same microglia-mediated neuroinflammatory pathway is involved. Subsequent Src family kinase-induced potentiation of GluN2A NMDARs mediates the upregulation. This pathway overcomes a basal suppression of inhibitory synaptogenesis provided by p38 mitogen-activated protein kinase (MAPK). This work is consistent with previous work demonstrating that HIV tat treatment increases inhibitory synapse number and further supports the idea that a mechanism that controls the homeostasis of neural network is stimulated to counteract the excessive excitation that result from exposure to HIV proteins (Hargus and Thayer, 2013).

Finally, to investigate the possible role of NMDARs in synaptogenesis, I used a novel spine calcium imaging method. I demonstrated that GluN2B NMDARs on presynaptic terminals controls spontaneous release of glutamate. Inhibiting this process, when evoked network activity is blocked, induces excitatory synaptogenesis. Previously our lab reported that blocking GluN2B-containing NMDARs induces recovery of excitatory synapses after the network is impaired (Shin et al., 2012; Raybuck et al., 2017). This work supports those findings and may present a mechanism for the regeneration of synapses after HIV neurotoxin-induced loss.

These studies expand our understanding of the neurotoxic mechanisms of HIV gp120. Drug discovery focusing on subtypes of NMDARs with specific locations may

provide a novel view for the field. Modulation of neuroinflammation through eCB system is also a promising therapeutic strategy and may be well tolerated by patients.

Chapter Two:

Monoacylglycerol lipase inhibitor JZL184 prevents HIV-1 gp120-induced synapse loss by altering endocannabinoid signaling.

Xinwen Zhang, Stanley A. Thayer*

Department of Pharmacology, University of Minnesota Medical School Minneapolis, MN

Content adapted from published article: Zhang X, Thayer SA (2018) Monoacylglycerol lipase inhibitor JZL184 prevents HIV-1 gp120-induced synapse loss by altering endocannabinoid signaling. Neuropharmacology. 128:269-281.

Contributions: XZ and SAT designed the study; XZ performed experiments and collected data; XZ and SAT analyzed data and wrote the manuscript; SAT provided reagents and conceptual advice.

I. Introduction

Monoacylglycerol lipase (MGL) hydrolyzes the endocannabinoid, 2-arachidonoylglycerol (2-AG), to arachidonic acid (AA) and glycerol (Blankman and Cravatt, 2013). In the brain, hydrolysis of 2-AG by MGL is the principal source of AA for the production of prostaglandins (PGs) (Nomura et al., 2011). Thus, inhibition of MGL can affect neuronal function by enhancing endocannabinoid signaling (Viader et al., 2015) and decreasing PG-mediated inflammation (Nomura et al., 2011; Grabner et al., 2016). Both of these actions might protect the CNS from excitotoxic insult. Activation of the endocannabinoid system protects neuronal function in animal models of epilepsy, stroke and Alzheimer's disease (Pacher et al., 2006; Chen et al., 2012). Neuroinflammation impairs neuronal function (Heneka et al., 2015), and elevated PG levels contribute to neuronal dysfunction in animal models of status epilepticus (Jiang et al., 2013), pain (Zhao et al., 2007) and Alzheimer's disease (Johansson et al., 2015). Here we examined the effects of MGL inhibition in an *in vitro* model of a neuroinflammatory disorder using JZL184, a potent and selective inhibitor of MGL (Pan et al., 2009; Grabner et al., 2016).

HIV-associated neurocognitive disorder (HAND) afflicts almost half of HIV-infected individuals (Ellis et al., 2007; Saylor et al., 2016). Cognitive decline in HAND correlates closely with synaptodendritic damage such as dendritic pruning and degradation of synaptic proteins (Ellis et al., 2007; Ellis et al., 2009). Because HIV does not infect neurons, HIV neurotoxicity is indirect and thought to be mediated by a neuroinflammatory response to viral proteins and inflammatory cytokines released by infected microglia and macrophages (Kaul et al., 2001; Ellis et al., 2007; Saylor et al., 2016). The HIV envelope protein, gp120, has been detected in the brain tissue of HAND patients (Jones et al., 2000; Nath, 2002), is shed by infected cells (Kaul et al., 2001), and is a potent neurotoxin (Toggas et al., 1994).

Synapse loss is the hallmark of HAND and gp120 induces significant loss of synapses in both primary neuronal cultures and transgenic mice (Toggas et al., 1994; Iskander et al., 2004; Kim et al., 2011). When applied to hippocampal cultures composed of microglia, astrocytes and neurons, $gp120_{IIIB}$ binds to CXCR4 on microglia evoking the release of the inflammatory cytokine interleukin-1β (IL-1β) (Viviani et al., 2006; Kim et al., 2011). HIV gp120-induced synapse loss is blocked by an IL-1 receptor antagonist (Kim et al., 2011). Whether modulating endocannabinoid tone affects this process of neuroinflammatory synapse loss is not known. Thus, gp120-induced loss of synapses between hippocampal

neurons in culture provides a model to study the potential for inhibition of MGL to protect synaptic function.

The present study demonstrates that JZL184 completely protects from gp120-induced synapse loss. The contributions of enhanced endocannabinoid tone and reduced PGE_2-mediated neuroinflammation to synapse protection were determined. The dual mechanisms of protection that result from MGL inhibition might be particularly beneficial in neurodegenerative disorders with a strong neuroinflammatory component like HAND.

II. Materials and methods

Materials

Drugs used in this study and their pharmacological targets are summarized in supplementary Table 1. Materials were obtained from the following sources: JZL184 from the NIDA Drug Supply Program (Research Triangle Institute, Research Triangle Park, NC, USA) and Cayman Chemical (Ann Arbor, MI, USA); IL-1β and IL-1ra from R&D System (Minneapolis, MN, USA); AM630, AH6809, JZL 195, LY320135, rimonabant, and SR144528 from Tocris Bioscience (Bristol, UK); arachidonoyl-AMC from Enzo Life Sciences (Farmingdale, NY, USA); 4-nitrophenylacetate (4-NPA) from Cayman Chemical (catalog number: 705193; Ann Arbor, MI, USA); Dulbecco's modified Eagle's medium (DMEM), Hanks' balanced salt solution, fetal bovine serum, horse serum, penicillin/streptomycin, fura-2 AM, and glycine from Invitrogen (Carlsbad, CA, USA). The PSD95.FingR-eGFP expression vector (pCAG-PSD95.FingR-eGFP) was generated in the laboratory of Don Arnold and obtained from Addgene (catalog number: 46295; Cambridge, MA, USA). The expression vector for tdTomato driven by the synapsin promoter was generated by excising tdTomato from pLVX-tdTomato-N1 (Clontech-Takara Bio, Mountain View, CA, USA) and inserting it into the pSyn backbone of pSyn-PSD95-GFP kindly provided by Kirill Martemyanov (Scripps Research Institute, Jupiter, FL, USA). HIV-1 $gp120_{IIIB}$ was obtained through the National Institutes of Health (NIH) AIDS Reagent Program, Division of AIDS, National Institute of Allergy and Infectious Diseases, NIH (catalog number:11784).

Cell culture

All animal care and experimental procedures conformed to the Guide for the Care and Use of Laboratory Animals published by the U.S. National Institutes of Health. Ethical approval was granted by the Institutional Animal Care and Use Committee of the University of Minnesota (protocol 1612-34372A). Primary neuronal cultures were prepared from fetal tissue collected from 70 timed pregnant Sprague Dawley rats (250-300 g when mated) supplied by Charles River Laboratories (Raleigh, North Carolina, USA). Because multiple dishes of cells are produced from a single plating, this method reduced the number of animals required to complete the study. Prior to tissue collection, the animals were housed in the University of Minnesota vivarium for 2–6 d at constant temperature and humidity on a 12 h light/dark cycle, with free access to water and standard rat chow.

Primary rat hippocampal neurons were grown as described previously (Waataja et al., 2008) with minor modifications. Dams were killed by CO_2 inhalation in an institutionally approved and calibrated CO_2 chamber. Embryonic day 17 fetuses were rapidly decapitated with sharp scissors then hippocampi dissected and placed in Ca^{2+} and Mg^{2+} free Hanks' Balanced salt solution. Hippocampi were suspended in DMEM without glutamine, supplemented with 10% fetal bovine serum and penicillin/streptomycin (100 U mL^{-1} and 100 µg mL^{-1}, respectively) and dissociated by trituration through flame-narrowed Pasteur pipettes of decreasing aperture. Dissociated cells were then plated onto either a 25 mm round cover glass or a 25 mm round cover glass glued to cover a 19 mm diameter opening drilled in the bottom of a 35 mm Petri dish. The cover glass was pre-coated with Matrigel (150 µL, 0.2 mg mL^{-1}) (BD Biosciences, Billerica, MA, USA). Cells were grown in a humidified atmosphere of 10% CO_2 and 90% air (pH 7.4) at 37 °C. On day 1 and day 8 *in vitro*, cells were fed by exchanging 75% of the media with DMEM, supplemented with 10% horse serum and penicillin/ streptomycin. Cells used in this study were grown for 12 to 16 days in vitro without mitotic inhibitors, resulting in a mixed glial-neuronal culture. Using previously described immunocytochemistry methods (Kim et al., 2011), we found that these cultures are composed of 24 $\pm$ 4% neurons, 55 $\pm$ 4% astrocytes and 13 $\pm$ 6% microglia.

MGL Activity Assay

MGL activity was measured using a previously described assay (Muccioli et al., 2008) with minor modifications. Rat hippocampal cultures were untreated or pretreated

with various concentrations of JZL184 for 24 h. After pre-treatment, cells were scraped and collected in buffer containing 50 mM HEPES (pH 7.4), 1 mM EDTA, 1 µM pepstatin, 100 µM leupeptin, and 0.1 mg mL^{-1} aprotinin. The cells were sonicated on ice five times for 10 s at 15 s intervals and then centrifuged at 100,000 x g for 50 min at 4 ℃. After resuspending the pellet, the membranes were mixed with the colorimetric substrate for lipid hydrolases 4-NPA (catalog number: 705193; Cayman Chemical, Ann Arbor, MI, USA) to a final concentration of 202 µM. The mixture was transferred immediately into an Infinite M1000 PRO Microplate Reader (Tecan, Männedorf, Switzerland), and absorbance at 405 nm was monitored every 5 min for 180 min at 37 °C. Protein concentration was measured using Pierce Coomassie (Bradford) Protein Assay Kit (catalog number: 23200; ThermoFisher Scientific, Minneapolis, MN, USA) according to the manufacturer's instructions. Enzyme activity was determined from the linear phase of the reaction (15-55 min) and normalized to protein concentration.

FAAH Activity Assay

FAAH activity was measured using a previously described assay (Ramarao et al., 2005) with minor modifications. Rat hippocampal cultures were untreated or pretreated with 1 µM JZL195, or 1 µM JZL184 for 24 h. After pre-treatment, cells were scraped and collected in buffer containing 50 mM HEPES (pH 7.4), 1 mM EDTA, 1 µM pepstatin, 100 µM leupeptin, and 0.1 mg mL^{-1} aprotinin. The cells were then sonicated on ice five times for 10 s at 15 s intervals and then mixed with the fluorogenic substrate of FAAH, arachidonoyl-AMC (Enzo Life Science, Farmingdale, NY, USA), to a final concentration of 100 µM. The mixture was transferred immediately into an Infinite M1000 PRO Microplate Reader (Tecan, Männedorf, Switzerland), and fluorescence monitored every 5 min for 200 min at 37 °C (355 nm excitation, 460 nm emission). Enzyme activity was determined from the linear phase of the reaction (0-75 min) and normalized to protein concentration.

Transfection

Transfection of cultured rat hippocampal neurons was conducted between 11 and 12 days *in vitro* using a previously described protocol with minor modifications (Kim et al., 2011). Briefly, a DNA/calcium phosphate precipitate containing 0.5 µg of total plasmid

DNA per well was prepared and allowed to form for 90 min at room temperature. The media (conditioned media) was exchanged with DMEM supplemented with 1 mM kynurenic acid, 10 mM $MgCl_2$, and 5 mM HEPES to reduce neurotoxicity. The DNA/calcium phosphate precipitate was added dropwise to the cells and allowed to incubate for 30 min. After the incubation, cells were washed twice with DMEM supplemented with 10 mM $MgCl_2$ and 5 mM HEPES to remove leftover precipitate. After washing, conditioned media that had been saved at the beginning of the procedure was returned to the cells. Experiments were started 48-72 h after transfection. The calcium phosphate method of transfection was chosen because of its low toxicity.

Confocal imaging and image processing

Transfected cells were imaged with an inverted laser scanning confocal microscope (Nikon A1, Melville, NY, USA) using a 60× (1.4 numerical aperture) oil-immersion objective. Petri dishes containing cells were place in a stage-top incubator (LCI, Seoul, Korea) and maintained at 37° C and 10% CO_2 during imaging. After imaging, the cells were then returned to the cell culture incubator and the coordinates of the computer controlled stage were saved to enable repeated imaging of the same neuron for 24-48 h. A custom machined jig allowed the Petri dish to be returned to the same location on the microscope stage. GFP was excited at 488 nm and emission collected from 500 to 550 nm. TdTomato was excited at 561 nm and emission collected from 570 nm to 620 nm. Optical sections spanning 8 µm in the z-dimension were collected (1 µm per step) and combined through the z-axis into a maximum z-projection. GFP puncta were counted in an unbiased manner using an algorithm written in MetaMorph 6.2 image processing software (Waataja et al., 2008). A threshold set 0.25 times 1 standard deviation above the image mean was applied to the tdTomato image. This created a 1 bit image, which was used as a mask via a logical AND function with the GFP maximum *z*-projection. A top-hat filter (80 pixels) was applied to the masked GFP image. A threshold set 1.5 standard deviations above the mean intensity inside the mask was then applied to the contrast enhanced image. Structures between 12 and 80 pixels (0.13-0.86 μm^2) were counted as postsynaptic densities. The structures were then dilated and superimposed on the tdTomato maximum *z*-projection for visualization. The change in the number of PSD95.FingR puncta from 2-3 microscopic fields, each containing one tdTomato filled

neuronal soma, from a single dish were averaged and defined as an individual sample (n=1).

$[Ca^{2+}]_i$ imaging and analysis

Intracellular Ca^{2+} concentration ($[Ca^{2+}]_i$) was measured as previously described (Krogh et al., 2014). Briefly, cells were incubated in 10 μM fura-2 acetoxymethyl ester (fura-2 AM) in 0.04% pluronic acid in HEPES Hanks' salt solution (HHSS), pH 7.45, for 30 min at 37 °C. HHSS contained the following (in mM): HEPES 20, NaCl 137, $CaCl_2$ 1.3, $MgSO_4$ 0.4, $MgCl_2$ 0.5, KCl 5.0, KH_2PO_4 0.4, Na_2HPO_4 0.6, $NaHCO_3$ 3.0, and glucose 5.6. After loading with indicator, cells were washed in HHSS without fura-2 AM at 37 °C for 10 min. The cover glass containing loaded and washed cells was transferred to a recording chamber, and placed on the stage of an IX71 microscope (Olympus, Melville, NY, USA). Cells were imaged using a 20× (0.75 numerical aperture) objective. $[Ca^{2+}]_i$ was measured by sequential excitation of fura-2 at 340 and 380 nm (8 nm slit width) and emission was collected from 490 to 530 nm; image pairs were collected every 1 s. Cells were superfused at a rate of 2 mL min^{-1} with HHSS and responses evoked by exchanging the bath with Mg^{2+}-free HHSS containing 10 μM NMDA and 200 μM glycine for 60 s. After background subtraction, the 340 and 380 nm image pairs were converted to $[Ca^{2+}]_i$ using the formula $[Ca^{2+}]_i = K_d\beta(R-R_{min})/(R_{max} - R)$ (Grynkiewicz et al., 1985). The dissociation constant (K_d) for fura-2 was 145 nM. β is the ratio of fluorescence intensity acquired with 380 nm excitation measured in Ca^{2+}-free buffer (1 mM EGTA) and buffer containing saturating Ca^{2+} (5 mM). R is the fluorescence intensity ratio of images collected at 340 nm and 380 nm excitation. R_{min}, R_{max}, and β were determined in a series of calibration experiments on intact cells. R_{min} and R_{max} values were generated by applying 10 μM ionomycin in Ca^{2+}-free buffer (1 mM EGTA) and saturating Ca^{2+} (5 mM), respectively. Values for R_{min}, R_{max}, and β were 0.37, 9.38, and 6.46, respectively. These calibration constants were applied to all experimental recordings. The neuronal cell body was selected as the region of interest for all recordings. All neurons within the imaging field were included in the analysis and no exclusions were made. An individual sample (n=1) was defined as the average change in $[Ca^{2+}]_i$ from all the neurons imaged on a single coverslip.

Treatments

In synaptic imaging experiments an initial image (t = 0 h) was collected then HIV gp120 and drug treatments were applied directly to the cell culture media. When present, JZL184, IL-1ra, and AH6809 were added 15 min prior to addition of gp120. Selective CB receptor inverse agonists/antagonists were applied 5 min prior to the addition of JZL184. The cells were then returned to the cell culture incubator for 24 h. A second image (t = 24 h) of the same field was collected and the change in the number of synapses presented as a percentage of the initial puncta count. For $[Ca^{2+}]_i$ imaging experiments HIV gp120, IL-1β and drug treatments were applied directly to the cell culture media. JZL184, IL-1ra, and AH6809 were added 15 min prior to addition of gp120 or IL-1β. $[Ca^{2+}]_i$ responses were evoked by superfusing 10 µM NMDA and 200 µM glycine for 60 s.

Immunocytochemistry

Hippocampal cultures were transfected with PSD95.FingR-eGFP after 11 days *in vitro* as described above. 48 h after transfection, cells were washed with PBS and then fixed with 4% paraformaldehyde for 10 min. Cells were then washed with PBS three times and permeabilized with 0.2% Triton X-100 (Sigma, St. Louis, MO, USA) for 10 min. Cells were blocked in 10% BSA and 0.2% Triton X-100 for 30 min at room temperature with slow shaking. After blocking, cells were incubated with mouse anti-Bassoon monoclonal antibody (1:200, Enzo Life Sciences, Farmingdale, NY, USA) in blocking buffer at 4 °C overnight. Cells were then washed 3 times with PBS and incubated with tetramethylrhodamine (TRITC)-conjugated goat anti-mouse antibody (1:500; Millipore, Billerica, MA, USA) in blocking solution at room temperature for 1 h. Cells were imaged after three washes. PSD95.FingR-eGFP was excited at 488 nm and emission was collected from 500 to 550 nm. TRITC was excited at 561 nm and emission was collected from 570 nm to 620 nm.

ELISA

Secreted PGE_2 levels in the culture media were determined using a commercially available PGE_2 ELISA kit (catalog number: ADI-930-001; Enzo Life Sciences, Farmingdale, NY, USA). Each sample was from a single well of a 6-well plate. Two reactions for each sample were run in parallel and averaged (n=1). The assays were

performed according to the manufacturer's instructions. Absorbance was read at 405 nm using an Infinite M1000 PRO Microplate Reader (Tecan, Männedorf, Switzerland).

Quantitative Reverse Transcription Real-Time PCR (qRT-PCR)

RNA was extracted from cultures grown in 6-well plates using a commercially available RNA extraction kit (RNeasy Plus Mini Kit; catalog number: 74134; QIAGEN, Hilden, Germany), according to the manufacturer's instructions. Each sample was collected from 3 wells under the same treatment. For qRT-PCR, a SuperScript III Platinum SYBR Green One-Step qPCR Kit (catalog number: 11746; Invitrogen, Carlsbad, CA, USA) was used following the manufacturer's recommendations with minor modifications. Briefly, for each reaction, 5 uL of SYBR Green Reaction Mix with ROX was mixed with 0.2 uL Taq, 1 uL extracted RNA (containing 40-50 ng RNA), 0.2 uL primers (to make a final concentration 200 nM). The reaction was performed using a StepOnePlus Real-Time PCR System (ThermoFisher Scientific, Minneapolis, MN, USA). Synthesis of cDNA (50 °C for 3 min) was immediately followed by PCR amplification (95 °C for 5 min, followed by 40 cycles of 95 °C for 15 s and 60 °C for 1 min). IL-1β cDNA was amplified using the following primers: 5'-TCCTTGTGCAAGTGTCTGAAG-3' and 5'-GTCTGTCAGCCTCAAAGAACA-3' (IDT Integrated DNA Technologies, Coralville, IA, USA). Glyceraldehyde-3-phosphate dehydrogenase (GAPDH) was used as internal reference using the following primers: 5'-AATGGTGAAGGTCGGTGTG-3' and 5'-GTGGAGTCATACTGGAACATGTAG-3' (IDT Integrated DNA Technologies, Coralville, IA, USA). For each sample, two IL-1β reactions and two GAPDH reactions were run in parallel and averaged (n=1). Quantitative analysis was performed using the $2^{-\Delta\Delta Ct}$ method.

Statistics

All data are presented as mean ± SEM. For all treatment groups, there were at least 6 samples. Data were first tested for unequal variance using Levene's test (OriginPro v8.5, Northampton, MA, USA); no samples were found to be of unequal variance. For data sets with multiple comparisons a one-way or two-way ANOVA was performed. If gp120 treatment exerted a significant interaction with other treatment groups, or if only one treatment (gp120 alone) was used, statistical significance was determined using one-way

ANOVA with a Tukey's *post-hoc* test (Prism, GraphPad 5, La Jolla, CA 92037 USA). Time course data were analyzed with a repeated measures ANOVA using R under Rcmdr (Baier and Neuwirth, 2007).

III. Results

JZL184 inhibits rat MGL enzyme activity but not FAAH activity

JZL184 completely inhibits MGL in mouse brain cultures at a concentration of 1 µM (Grabner et al., 2016). Here we tested the effects of JZL184 on rat hippocampal cultures. Mixed cultures containing neurons, astrocytes and microglia were treated with various concentrations of JZL184 for 24 h, the cells were lysed and an enzyme assay performed on isolated membranes (Figure 2.1A). JZL184 inhibited the degradation of the colorimetric substrate 4-NPA with an IC_{50} of 0.22 ± 0.06 µM (Figure 2.1B). A concentration of 1 µM produced maximal inhibition, consistent with previous studies (Grabner et al., 2016), and was used for subsequent experiments.

This concentration of JZL184 did not significantly influence the activity of fatty acid amide hydrolase (FAAH) (Figure 2.1C and D). Cultures were treated for 24 h with 1 µM JZL184 or 1 µM JZL195, a potent inhibitor of FAAH and MGL. Cells were lysed and FAAH enzymatic activity assessed by measuring the degradation of the fluorogenic substrate, arachidonoyl-AMC. Thus, the 1 µM concentration of JZL184 used in these studies is selective for MGL relative to FAAH.

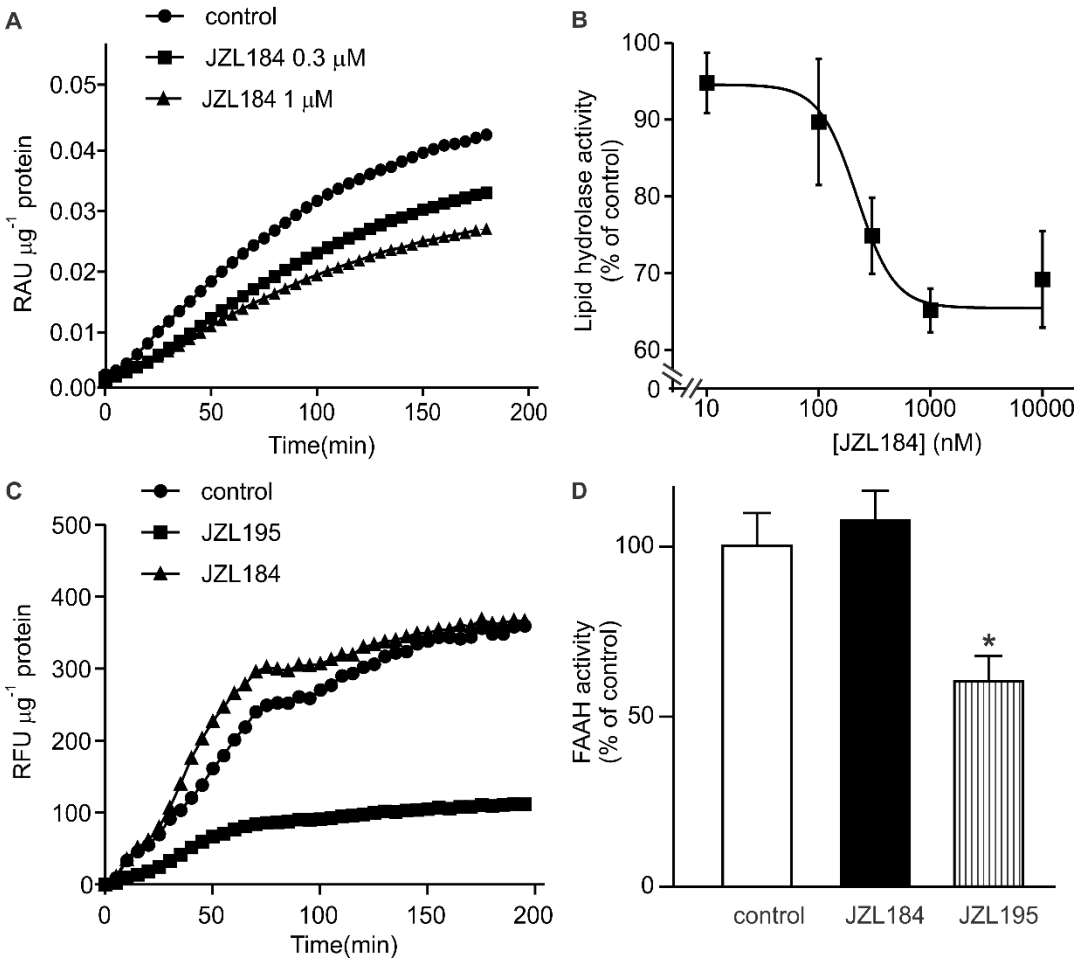

Figure 2.1 JZL184 inhibits MGL enzyme activity but not FAAH activity. (A) Representative traces show MGL enzymatic activity during incubation with the colorimetric substrate, 4-NPA. Cultures were treated for 24 h with 0, 0.3 or 1 μM JZL184. Cells were lysed and incubated with 4-NPA as described in Materials and Methods. Absorbance was monitored every 5 min for 180 min and presented as relative absorbance units (RAU) normalized to μg protein. (B) Plot shows concentration dependent inhibition of MGL activity by JZL184. Enzyme activity was determined from the linear phase of the reaction (15-55 min in A). The concentration response curve was generated using a nonlinear, least-squares curve fitting program (Origin 6.0, OriginLab Corp.) to fit a logistic equation of the form % of Control $= [(A_1 - A_2)/(1 + (X/IC_{50})^p)] + A_2$ where X = drug concentration, IC_{50} = 219 ± 62 nM, A_1 = 95 ± 3 % inhibition without drug, A_2 = 65 ± 2 % inhibition at a maximally effective drug concentration and p = 3 ± 2 slope factor. Values are expressed as mean ± SEM from 5 separate enzyme assays. The incomplete inhibition produced by a maximal concentration of JZL184 is due to the hydrolysis of 4-NPA by lipid hydrolases other than MGL present in the crude membrane preparation isolated from neuronal cell cultures. (C) Representative traces show FAAH enzymatic activity during incubation with the fluorogenic substrate, arachidonoyl-AMC. Cultures were treated for 24 h with 1 μM JZL184 or 1 μM JZL 195, a potent inhibitor of FAAH and MGL. Cells were lysed and incubated with arachidonoyl-AMC as described below. Fluorescence was monitored every 5 min for 200 min and presented as relative fluorescence units (RFU) normalized to μg protein. (D) Bar graph summarizes FAAH activity relative to untreated cultures (control) during the

linear phase of the reaction (0-75 min). FAAH activity in the presence of JZL184 was not significantly different from control. *$p<0.05$ relative to control (one-way ANOVA with Tukey's post-test, n=6).

PSD95.FingR-eGFP labels functional synapses

The HIV-1 envelope protein gp120 is a potent neurotoxin *in vitro* that mimics the synapse loss observed in HAND via a neuroinflammatory mechanism (Kim et al., 2011; Mishra et al., 2012). Here we examined the effects of inhibiting MGL with JZL184 on synapse loss induced by gp120 and assessed the mechanism of action. To monitor changes in the number of synapses, rat hippocampal cultures were transfected with expression plasmids for a recombinant antibody-like protein, PSD95.FingR-eGFP, and tdTomato, as previously described (Gross et al., 2013). Transfected cells were imaged using a laser scanning confocal microscope as described in Methods. The PSD95.FingR-eGFP construct expressed a GFP-tagged fibronectin intrabody that specifically bound to the endogenous postsynaptic scaffolding protein PSD95, labelling glutamatergic synapses in a punctate pattern (Figure 2.2A). The red tdTomato protein filled the cytoplasm enabling visualization of the transfected cell's morphology. This method was previously shown to label functional synapses without interfering with normal synaptic function. In extensive characterization experiments Gross et al. (2013) showed that PSD95.FingR-eGFP expressed in primary neuronal cultures co-immunoprecipitated with native PSD-95, that the eGFP puncta co-localized with PSD-95 immunoreactivity, and that siRNA knock down of endogenous PSD-95 produced a comparable knockdown of PSD95.FingR-eGFP labelling. Here, we used immunocytochemistry to confirm that green fluorescent puncta labelled synaptic structures. Immunoreactivity for the presynaptic scaffolding protein Bassoon co-localized with PSD95.FingR labeled postsynaptic sites (Figure 2.2B). 83 ± 1 % (n=5) of the green fluorescent puncta co-localized with Bassoon immunoreactive puncta. To track individual synapses in live cells, image stacks compressed in the z dimension were processed using an algorithm that counted green fluorescent puncta that met size (area between 0.13 μm^2 and 0.86 μm^2) and intensity criteria, and were in contact with a binary mask derived from the red tdTomato image. This method enabled the same neuron to be imaged before and after treatment to measure changes in the number of synapses.

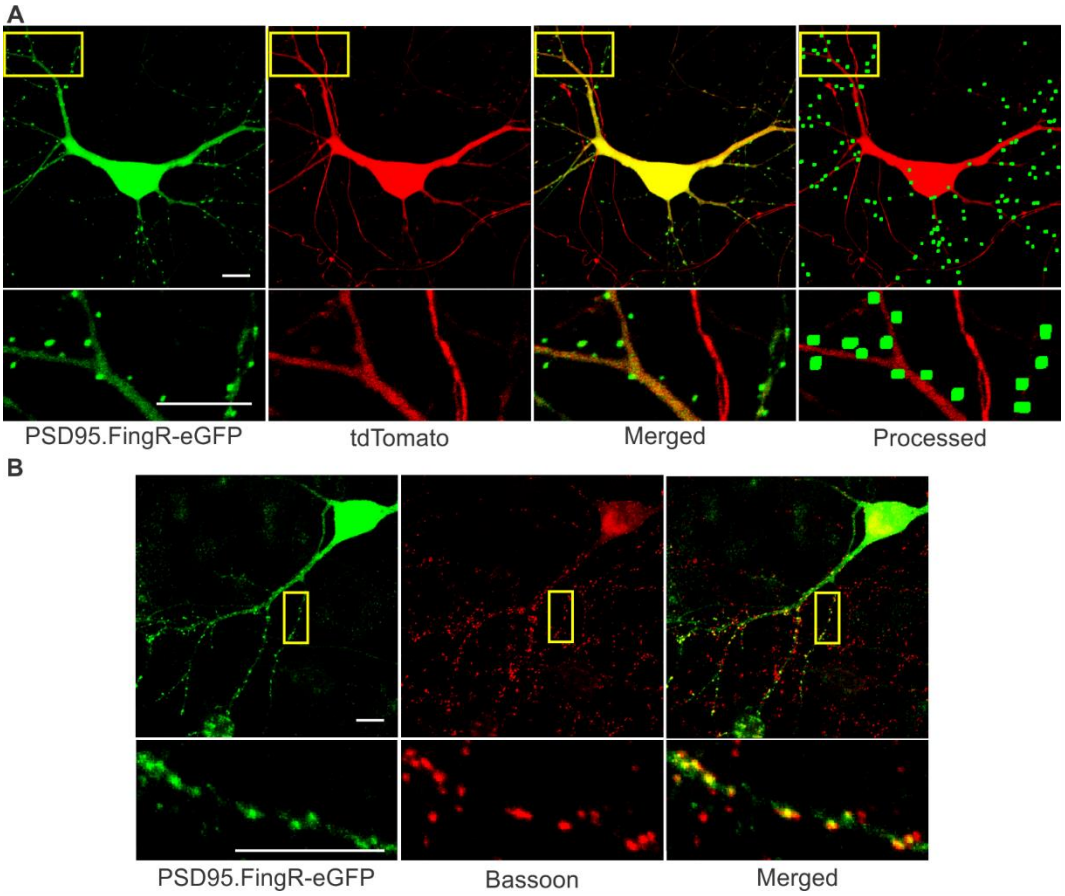

Figure 2.2 PSD95.FingR-eGFP (Intrabody) labels postsynaptic terminals at excitatory synapses. (A) Representative confocal images of a neuron expressing PSD95.FingR-eGFP and tdTomato were acquired and processed as described in Methods. PSD95.FingR-eGFP puncta were identified by filtering compressed z-stacks (8 µm) of confocal images. All puncta that met size (between 0.13-0.86 μm^2) and intensity criteria, and were in contact with a binary mask derived from the tdTomato image were counted as synapses. Puncta were dilated and overlaid on the tdTomato maximum projection (Processed) for display purposes. Insets are enlarged images of the boxed regions. Scale bars represent 10 µm. (B) Representative confocal images of a neuron expressing PSD95.FingR-eGFP (green) and immunolabeled for Bassoon (red). PSD95.FingR-eGFP puncta co-localized with Bassoon immunoreactivity (yellow, Merged). Note that non-transfected cells were also present in the field, and thus not all Bassoon immunoreactive puncta (red) co-localized with PSD95.FingR-eGFP (green) puncta. Insets are enlarged images of the boxed regions. Scale bars represent 10 µm.

gp120-induced synapse loss was blocked by inhibition of MGL

Treating hippocampal neurons in culture with the HIV-1 envelope protein $gp120_{IIIB}$ induces the loss of synaptic connections via a mechanism that requires microglial production of the inflammatory cytokine IL-1β (Kim et al., 2011). Treating the culture with 600 pM gp120 for 24 h produced a 15 ± 3% loss of PSD95.FingR labeled postsynaptic sites (Figure 2.3A). Synapse loss was maximal by 24 h and it persisted for 48 h (Figure 2.3A). The time course of gp120 induced synapse loss shown here is in good agreement with previous studies using a PSD95-GFP fusion protein to report glutamatergic synapses (Kim et al., 2011). Advantages of the intrabody approach relative to imaging the expressed fusion protein are that the intrabody construct incorporates a transcriptional control mechanism to reduce the expression of excess intrabody, reducing background fluorescence, and intrabody expression does not drive increased synapse formation as does the PSD95-GFP fusion protein.

To determine whether altering endocannabinoid tone would modulate the process of gp120-induced synapse loss, we examined the effects of inhibiting the breakdown of the endocannabinoid 2-AG to AA and glycerol by MGL. Inhibition of MGL has been shown to suppress neuroinflammation induced by neurotoxins (Nomura et al., 2011; Viader et al., 2015; Grabner et al., 2016). To determine whether inhibition of MGL could attenuate gp120-induced synapse loss, the cultures were treated with the selective MGL inhibitor, JZL184, 15 min prior to and during exposure to gp120 (Figure 2.3B and C). JZL184 (1 μM) treatment completely blocked synapse loss induced by 24 h exposure to 600 pM gp120, suggesting that inhibition of MGL protects synapses from gp120-induced loss (Figure 2.3B and C). JZL184 alone did not affect the number of synapses.

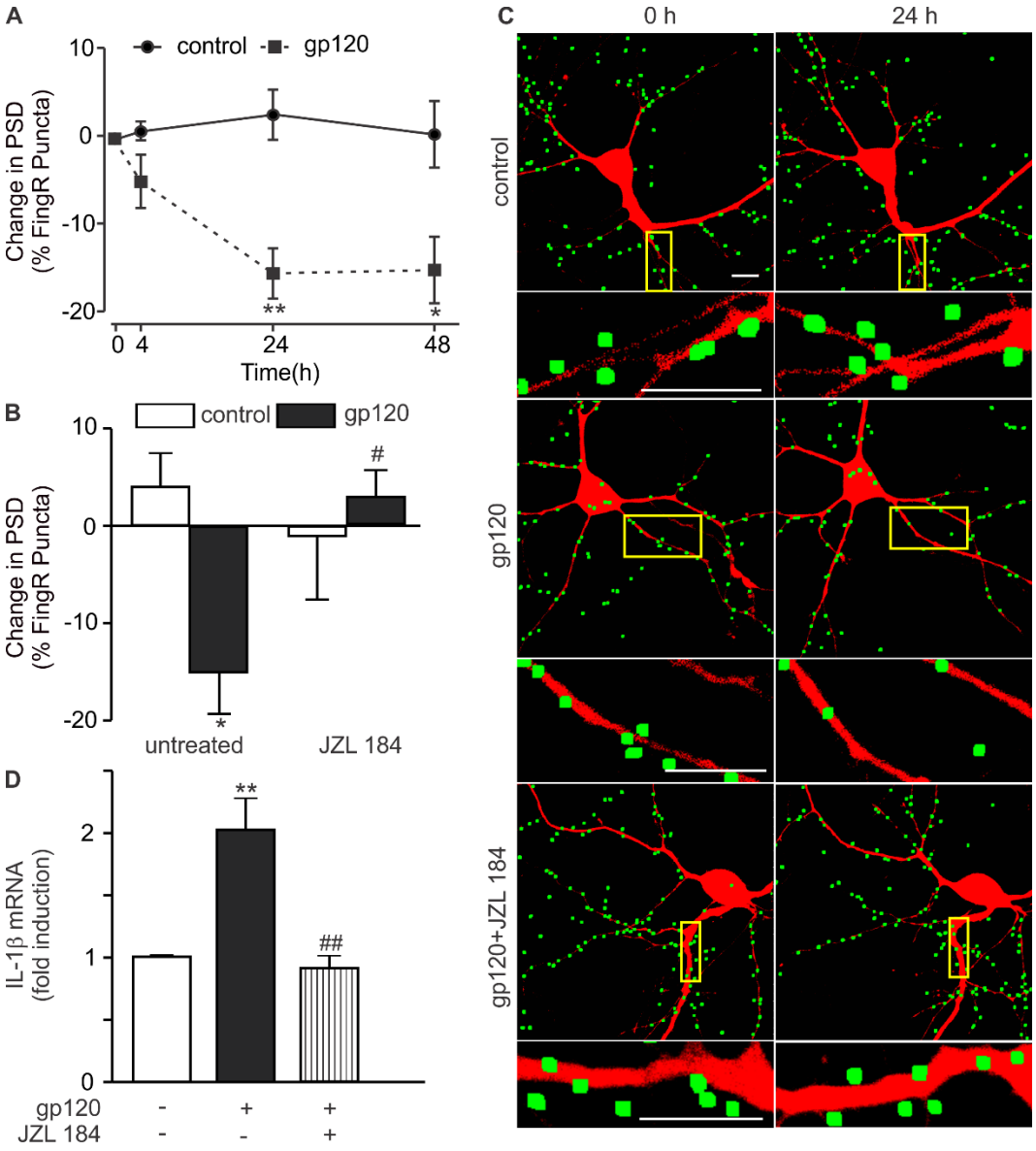

Figure 2.3 HIV gp120-induced loss of synapses and IL-1β expression were blocked by inhibition of MGL. (A) Graph shows time-dependent changes in the number of PSD95.FingR-eGFP puncta for untreated cells (control, circles) and cells treated with 600 pM gp120 (gp120, squares). Data are expressed as mean ± SEM. Repeated measures ANOVA revealed gp120 by time interactions [$F_{3, 35}$ = 6.25, p<0.01]. *p<0.05, **p<0.01 relative to control at the same time-point (Tukey's post-test, n = 7). (B) Bar graph summarizes changes in PSD95.FingR-eGFP puncta after 24 h treatment under control conditions (open bars) in the absence (n = 8) or presence (n = 6) of 1 µM JZL184 or treated with 600 pM gp120 (solid bars) in the absence (n = 7) or presence (n = 6) of JZL184. JZL184 was added 15 min prior to gp120 for all experiments. Data are expressed as mean ± SEM. *p<0.05 relative to untreated control, #p<0.05 relative to untreated gp120 (one-way ANOVA with Tukey's post-test). (C) Representative processed images of neurons with no treatment (control), or treated with 600 pM gp120 in the absence or presence of 1 µM JZL184 for 24 h. The insets are enlarged images of the boxed region. Scale bars represent 10 µm. (D) Bar graph summarizes IL-1β mRNA expression relative to control (n

= 12) after treatment with 600 pM gp120 and in the absence (n = 18) or presence of 1 μM JZL184 (n = 16) for 4 h. Data are expressed as mean ± SEM. **p<0.01 relative to control, ##p<0.01 relative to gp120 treated group (one-way ANOVA with Tukey's post-test).

JZL184 blocks gp120-induced IL-1β production

We next studied the effects of JZL184 on gp120-induced IL-1β production. In a previous study we showed that gp120 evoked the secretion of IL-1β protein, detected by ELISA, and increased the expression of IL-1β mRNA, detected by qRT-PCR (Kim et al., 2011). Here, we used the qRT-PCR assay because of its higher sensitivity. Gp120-induced increases in IL-1β mRNA levels were measured in the absence and presence of JZL184 to determine whether inhibition of MGL suppressed IL-1β production. Figure 3D shows that 4 h treatment with 600 pM gp120 increased the expression of IL-1β mRNA by 2.0 ± 0.2-fold. This increase was significant and completely blocked by treatment with JZL184 (1 μM). These results suggest that inhibition of MGL decreases IL-1β production which might contribute to the protection from gp120-induced synapse loss afforded by JZL184.

JZL184 blocks gp120-induced potentiation of NMDA-evoked Ca^{2+} influx

The HIV protein Tat and the inflammatory cytokine IL-1β potentiate NMDARs by activating Src family tyrosine kinases (Viviani et al., 2003; Krogh et al., 2014), which are known to phosphorylate NMDARs resulting in potentiated currents (Yu and Salter, 1999). Synapse loss induced by gp120 requires activation of NMDARs (Kim et al., 2011). Here we determined whether exposure to gp120 would increase the amplitude of NMDA-evoked changes in $[Ca^{2+}]_i$. Fura-2-based $[Ca^{2+}]_i$ imaging was performed as described in Methods. Cells were superfused with HEPES Hank's salt solution (HHSS) at a flow rate of 2 mL min^{-1} for 60 s and then the bath was exchanged to Mg^{2+}-free HHSS containing 200 μM glycine and 10 μM NMDA for 60 s. As shown in Figure 4A, NMDA evoked a transient increase in the $[Ca^{2+}]_i$ that rose from a mean basal level of 68 ± 3 nM to peak at 241 ± 25 nM in control cells (t = 0 h). Treatment with 600 pM gp120 produced a time-dependent increase in the amplitude of the NMDA-evoked response (Figure 2.4A and B). The gp120-induced potentiation of the NMDA-evoked response peaked after 4 h exposure to gp120 and then adapted. This time course is consistent with potentiated NMDA-mediated Ca^{2+} influx driving cellular adaptations such as synapse loss (Figure 2.3A) and downregulation of NMDAR-mediated synaptic currents (Green and Thayer, 2016). The net NMDA-evoked $[Ca^{2+}]_i$ response was increased by 113 % in cells treated for 4 h with 600 pM gp120 relative to control cells (Figure 2.4C). In the presence of IL-1ra (1 μg mL^{-1}),

an IL-1 receptor antagonist, the gp120-induced potentiation was significantly reduced (Figure 2.4D). This result is consistent with gp120 evoking the release of IL-1β from microglia; the released IL-1β then activates IL-1 receptors on neurons leading to potentiation of NMDARs. If JZL184 inhibited synapse loss by reducing the production of IL-1β as suggested by the qRT-PCR data shown in Figure 2.3D, we would expect JZL184 to prevent gp120-induced potentiation of NMDARs but not necessarily potentiation induced by direct application of IL-1β. As shown in Figure 2.4E and F, 1 μM JZL184 completely blocked the gp120-induced potentiation of the NMDA-evoked increase in $[Ca^{2+}]_i$. If the effects of JZL184 were mediated entirely by decreased production of IL-1β, then direct application of IL-1β to the culture should potentiate NMDA receptors in manner insensitive to inhibition of MGL. As shown in Figure 2.4G and H, treating the culture with IL-1β for 4 h potentiated the amplitude of the NMDA evoked $[Ca^{2+}]_i$ increase. In this cohort of cells NMDA increased the $[Ca^{2+}]_i$ in untreated cells from a mean level of 41 ± 3 nM to peak at 458 ± 28 nM. The net NMDA-evoked $[Ca^{2+}]_i$ response increased by 60 % in cells treated with 3 ng mL^{-1} IL-1β for 4 h. As hypothesized, treatment with 1 μM JZL184 together with IL-1β for 4 h did not significantly affect the IL-1β-induced potentiation of the NMDA-evoked $[Ca^{2+}]_i$ response. Thus, JZL184 blocks gp120-induced IL-1β production preventing potentiation of NMDARs.

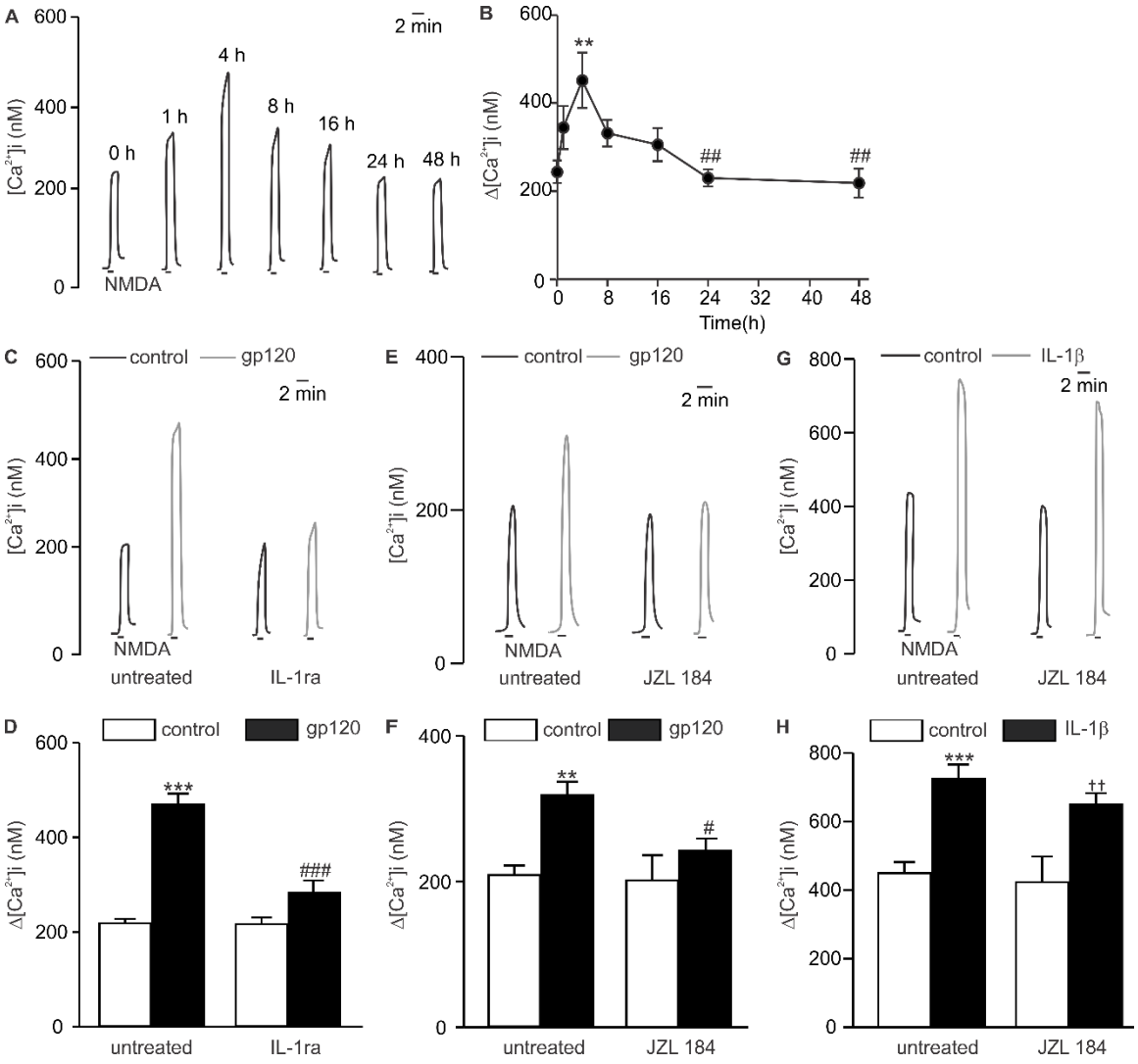

Figure 2.4 Inhibition of MGL suppresses gp120-induced potentiation of NMDA receptors by blocking IL-1β production. (A-B) HIV-1 gp120-induced a biphasic change in NMDA-evoked $[Ca^{2+}]_i$ responses. (A) representative traces show NMDA-evoked $[Ca^{2+}]_i$ (10 μM x 60 s) increases from a control neuron (0 h) or neurons treated with 600 pM gp120 for the times indicated above the traces. (B) plot summarizes NMDA-evoked $[Ca^{2+}]_i$ responses after treatment with gp120 for 0 to 48 h. Data are expressed as mean ± SEM. **p<0.01 relative to 0 h time-point, ##p<0.01 relative to 4 h time-point (ANOVA with Tukey's post-test, n ≥ 6). (C) Representative traces show increase in $[Ca^{2+}]_i$ evoked by application of 10 μM NMDA (60s) to control neurons and neurons treated with 600 pM gp120 for 4 h in the absence and presence of 1 μg mL^{-1} IL-1ra. IL-1ra was added 15 min before gp120. (D) Bar graph summarizes net $[Ca^{2+}]_i$ increase ($\Delta[Ca^{2+}]_i$) evoked by 10 μM NMDA for control and neurons treated with 600 pM gp120 for 4 h in the absence and presence of 1 μg mL^{-1} IL-1ra. ***p<0.001 relative to untreated control; ###p<0.001 relative to gp120 only treatment (one-way ANOVA with Tukey's post-test, n=16). (E) Representative traces show increase in $[Ca^{2+}]_i$ evoked by application of 10 μM NMDA (60s) to control neurons and neurons treated with 600 pM gp120 for 4 h in the absence and presence of 1 μM JZL184. JZL184 was added 15 min before gp120. (F) Bar graph summarizes Δ $[Ca^{2+}]_i$ evoked by 10 μM NMDA for control neurons in the absence (n=10)

and presence (n=6) of 1 µM JZL184 and neurons treated with 600 pM gp120 for 4 h in the absence (n=13) and presence (n=11) of 1 µM JZL184. **p<0.01 relative to untreated control; #p<0.05, relative to the group only treated with gp120 (one-way ANOVA with Tukey's post-test). (G) Representative traces show NMDA-evoked increase in $[Ca^{2+}]_i$ for control neurons and neurons treated with 3 ng mL^{-1} IL-1β for 4 h in the absence or presence of 1 µM JZL184. JZL184 was added 15 min before IL-1β. (H) Bar graph shows Δ $[Ca^{2+}]_i$ evoked by 10 µM NMDA for control neurons in the absence (n=17) and presence (n=10) of 1 µM JZL184 and neurons treated with 3 ng mL^{-1} IL-1β for 4 h in the absence (n=20) and presence of 1 µM JZL184 (n=19). ***p<0.001 relative to untreated control, ††p<0.01 relative to JZL184 treated control (one-way ANOVA with Tukey's post-test).

JZL184 activated CB_2Rs blocks gp120-induced synapse loss

JZL184 could prevent gp120-induced synapse loss by activating cannabinoid receptors secondary to the accumulation of 2-AG and/or its neuroprotective effects could result from reduced PG production as a result of decreased conversion of 2-AG to AA (Nomura et al., 2011; Ueda et al., 2011; Blankman and Cravatt, 2013). To determine whether the protective effect of JZL184 resulted from increased 2-AG that subsequently activated CB_2R, we examined the effects of JZL184 on gp120-induced synapse loss in the absence and presence of 100 nM AM630, a selective CB_2R inverse agonist/antagonist. We have shown previously that this concentration of AM630 selectively and completely blocks CB_2R function in rat hippocampal cultures (Kim et al., 2011). AM630 (100 nM) reversed the effect of JZL184 and restored the synapse loss-induced by gp120 (Figure 2.5A). We confirmed that the effect of JZL184 was mediated CB_2R using another structurally distinct CB_2R inverse agonist/antagonist. SR144528 has been shown previously to selectively block CB_2R at a concentration of 100 nM (Dhopeshwarkar and Mackie, 2016). As shown in Figure 5B, SR144528 completely blocked the effects of JZL184. AM630 and SR144528 alone produced 8 ± 6 % and 3 ± 5 % change in synapses, respectively, which is not significantly different from control. In contrast, treatment with rimonabant, a CB_1R inverse agonist/antagonist that we have shown previously to selectively and completely block CB_1R function in rat hippocampal cultures (Roloff and Thayer), did not affect JZL184-mediated protection (Figure 2.5C). Similarly, the structurally distinct CB_1R inverse agonist/antagonist LY320135, at a concentration of 1 μM, which has been shown previously to selectively inhibit CB_1R function (Felder et al., 1998), also failed to affect JZL184-mediated protection (Figure 2.5D). Thus, the effects of JZL184 were not through activation of CB_1R. Rimonabant and LY320135 alone produced -2 ± 9 % and 9 ± 6 % change in synapses, respectively, which is not significantly different from control. JZL184 suppression of IL-1β mRNA expression was partially reversed by AM630 (100 nM) (Figure 2.5E). In the presence of both JZL184 and AM630, gp120-evoked IL-1β production was significantly less than that evoked by gp120 alone. Additionally, in cells treated with both JZL184 and AM630, gp120-evoked IL-1β production was significantly greater than that evoked by gp120 in the presence of JZL184. AM630 alone had no effect on IL-1β mRNA level (1.1 ± 0.2 -fold induction). These results suggest that JZL184 attenuates gp120-induced synapse loss, in part, through activation of CB_2R and subsequent suppression of IL-1β production.

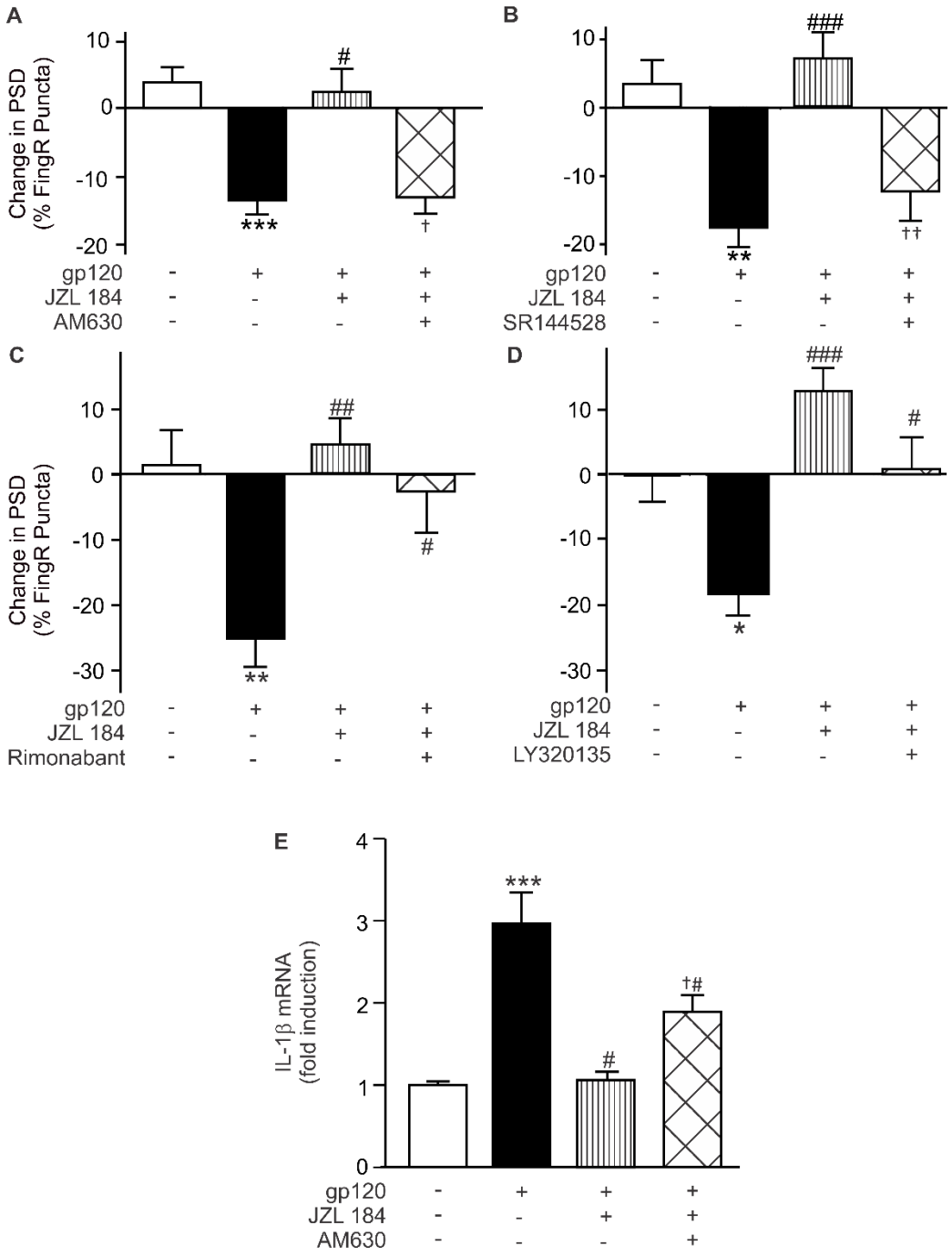

Figure 2.5 Activation of CB_2R but not CB_1R was required for JZL184 inhibition of gp120-induced neurotoxicity. (A) Bar graph shows changes in PSD95.FingR-eGFP puncta number after 24 h treatment with the indicated treatment groups: untreated (n=12), 600 pM gp120 (n=16), gp120 + 1 μM JZL184 (n=9), and gp120 + JZL184 + 100 nM AM630 (n=8). The CB_2R inverse agonist/antagonist AM630 was added 5 min prior to JZL184. ***p<0.001 relative to untreated, #p<0.05 relative to the group only treated with gp120, †p<0.05 relative the group treated with gp120 + JZL184 (one-way ANOVA with Tukey's post-test). (B) Bar graph shows changes in PSD95.FingR-eGFP puncta number after 24 h treatment with the indicated treatment groups: untreated (n=10), 600 pM gp120 (n=10),

gp120 + 1 μM JZL184 (n=10), and gp120 + JZL184 + 100 nM SR144528 (n=10). The CB_2R inverse agonist SR144528 was added 5 min prior to JZL184. **p<0.01 relative to untreated, ###p<0.001 relative to the group only treated with gp120, ††p<0.01 relative the group treated with gp120 + JZL184 (one-way ANOVA with Tukey's post-test). (C) Bar graph shows changes in PSD95.FingR-eGFP puncta number after 24 h treatment with the indicated treatment groups: untreated (n=8), 600 pM gp120 (n=8), gp120 + 1 μM JZL184 (n=7), and gp120 + JZL184 + 100 nM rimonabant (n=9). The CB_1R inverse agonist rimonabant was added 5 min prior to JZL184. **p<0.01 relative to untreated; #p<0.05, ##p<0.01 relative to the group only treated with gp120 (one-way ANOVA with Tukey's post-test). (D) Bar graph shows changes in PSD95.FingR-eGFP puncta number after 24 h treatment with the indicated treatment groups: untreated (n=9), 600 pM gp120 (n=8), gp120 + 1 μM JZL184 (n=9), and gp120 + JZL184 + 1 μM LY320135 (n=8). The CB_1R inverse agonist LY320135 was added 5 min prior to JZL184. *p<0.05 relative to untreated; #p<0.05, ###p<0.001 relative to the group only treated with gp120 (one-way ANOVA with Tukey's post-test). (E) Bar graph summarizes IL-1β mRNA expression measured using qRT-PCR assay after 4 h treatment with the indicated treatments: untreated (n=10), 600 pM gp120 (n=13), gp120 + 1 μM JZL184 (n=9), and gp120 + JZL184 + 100 nM AM630 (n=9). AM630 was added 5 min prior to JZL184. ***p<0.001 relative to untreated group, #p<0.05 relative to the group only treated with gp120, †p<0.05 relative to the group treated with gp120 and JZL184 (one-way ANOVA with Tukey's post-test).

JZL184 suppresses gp120-induced PGE_2 production

Because AM630 only partially reversed JZL184 inhibition of gp120-induced IL-1β expression, JZL184 might protect synapses through a mechanism in addition to activation of CB_2R. A potential role for reduced PG production in the protection of synapses was considered because JZL184 decreases the conversion of 2-AG to AA which is the precursor for PGs (Nomura et al., 2011). PGE_2 contributes to neuroinflammation (Johansson et al., 2013; Johansson et al., 2015); thus, we first determined whether gp120 treatment can induce the production of PGE_2. Treatment with 600 pM gp120 stimulated PGE_2 production and this effect was blocked in the presence of 1 µM JZL184 (Figure 2.6A). PGE_2 (56 ± 5 pg mL^{-1}) was present in media from untreated cultures. Treatment (4 h) with HIV gp120 increased PGE_2 to 80 ± 7 pg mL^{-1}. Note that PGE2 levels were measured in the relatively large volume of the cell culture well and might be higher in the cell monolayer.

To determine whether PGE_2 contributed to gp120-induced synapse loss we examined the effects of gp120 in the absence and presence of AH6809, an antagonist for prostaglandin 1 and 2 receptors ($EP_{1\text{-}2}R$) (Woodward et al., 1995). Gp120-induced synapse loss was blocked completely by 10 µM AH6809 (Figure 2.6B). Thus, activation of $EP_{1\text{-}2}Rs$ by PGs is necessary for gp120-induced synapse loss. However, the inhibition of gp120-induced IL-1β expression by 10 µM AH6809 was incomplete (Figure 2.6C), suggesting that PGs might also act downstream of IL-1β to facilitate synapse loss (Figure 2.7B, green arrows). AH6809 alone had no effect on IL-1β mRNA levels (1.0 ± 0.08 fold change). This is consistent with a previous report showing synapse loss induced by the direct application of IL-1β requires PGE_2 production (Mishra et al., 2012). Furthermore, calcium imaging experiments showed that IL-1β-induced potentiation of NMDA receptors was not blocked by AH6809 (Figure 2.6D). These data indicate that the PG pathway downstream of IL-1β is separate from that mediating the potentiation of NMDA receptors (Figure 2.7B). Thus, activation of PG receptors is required for gp120-induced synapse loss (Figure 2.6B). These results suggest that, in addition to preventing synapse loss through 2-AG activation of CB_2R (Figure 2.5), JZL184 inhibition of PGE_2 production could also reduce IL-1β production (Figure 2.6C) and exert downstream actions such as an inhibition of PG-induced glutamate release.

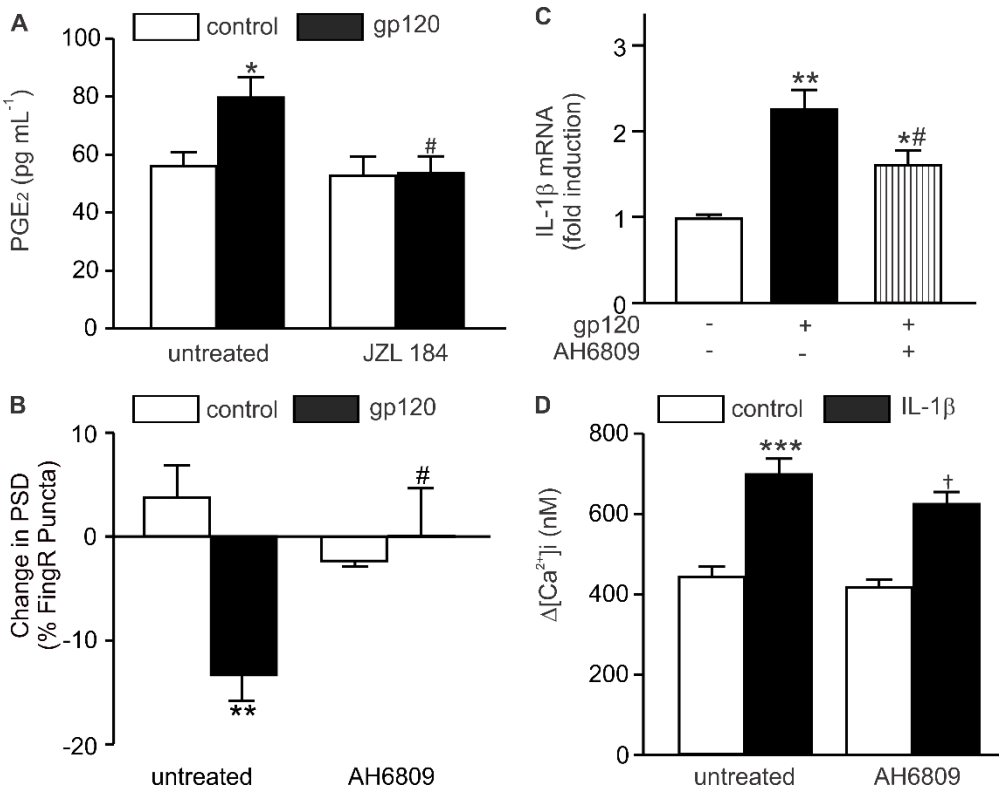

Figure 2.6 MGL inhibition blocks gp120-induced PGE_2 production. $EP_{1\text{-}2}R$ activation is required for synapse loss and IL-1β expression. (A) Bar graph shows changes in PGE_2 levels in culture media measured using ELISA. PGE_2 levels are shown for control conditions in the absence (n=14) or presence of 1 µM JZL184 (n=9) and after treatment with 600 pM gp120 for 4 h in the absence (n=17) or presence (n=14) of 1 µM JZL184. *p<0.05 relative to untreated control, #p<0.05 relative to the group only treated with gp120 (one-way ANOVA with Tukey's post-test). (B) Bar graph shows changes in the number of PSD95.FingR-eGFP puncta under control conditions in the absence (n=11) or presence (n=6) of 10 µM AH6809, an $EP_{1\text{-}2}R$ antagonist, or 24 h following treatment with 600 pM gp120 in the absence (n=9) or presence (n=9) AH6809. **p<0.01 relative to untreated control, #p<0.05 relative to the group treated with gp120 alone (one-way ANOVA with Tukey's post-test). (C) Bar graph summarizes changes of IL-1β mRNA expression in untreated cultures (n=10) and after 4 h treatment with 600 pM gp120 in the absence (n=11) or presence (n=10) of 10 µM AH6809. Data are expressed as fold induction relative to untreated group. *p<0.05, **p<0.01 relative to untreated group; #p<0.05 relative to the group treated with gp120 alone (one-way ANOVA with Tukey's post-test). (D) Bar graph shows $\Delta[Ca^{2+}]_i$ evoked by 10 µM NMDA for control cells in the absence (n=7) and presence (n=6) of 10 µM AH6809 and neurons treated with 3 ng mL^{-1} IL-1β for 4 h in the absence (n=11) and presence (n=8) of AH6809. ***p<0.001 relative to untreated control, †p<0.05 relative to AH6809 treated control (one-way ANOVA with Tukey's post-test).

IV. Discussion

Chronic neuroinflammation underlies the pathogenesis of HAND (Sodhi et al., 2004; Saylor et al., 2016). Infected immune cells release viral proteins and inflammatory factors which act on microglia, astrocytes, and neurons to produce the synaptodendritic damage that correlates with cognitive decline in HIV infected patients (Ellis et al., 2007). Here we used a simplified *in vitro* model to study the interaction of the eCB system with the neuroinflammatory response evoked by the HIV envelope protein. HIV gp120 induced synapse loss, a hallmark of HAND, by activating microglia to release IL-1β that then potentiated NMDA receptor function (Viviani et al., 2006; Kim et al., 2011). Inhibiting the metabolism of the eCB, 2-AG, attenuated gp120-induced synapse loss via activation of CB_2R and may have also protected synapses via reduced PG production. These pathways are summarized in Figure 2.7.

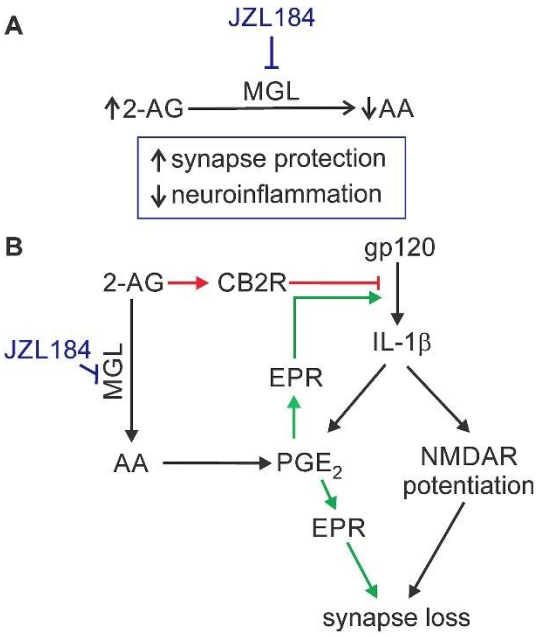

Figure 2.7 Summary scheme shows the hypothesized mechanism of the synapse protection induced by the inhibition of MGL. (A) Diagram illustrates the JZL184-induced increase in 2-AG that activates CB_2R-dependent synapse protection and the reduced AA production that decreases PGE_2-mediated synapse loss. (B) Scheme shows 2-AG and AA dependent pathways affected by JZL184 to reduce synapse loss. Solid arrows indicate flow of signaling pathways. Green lines highlight prostaglandin signaling and red lines highlight eCB signaling.

The suppression of gp120-induced synapse loss described here is the first report of a CB_2R-mediated effect of JZL184 on neuroinflammation induced synaptic damage. 2-AG is one of the most abundant eCBs in the brain and is a full agonist at both CB_1R and CB_2R (Gonsiorek et al., 2000). MGL is the primary enzyme responsible for 2-AG hydrolysis in brain, accounting for 85% of its metabolism (Blankman et al., 2007). Pharmacological and genetic inactivation of MGL has been shown to significantly increase brain 2-AG levels (Long et al., 2009; Grabner et al., 2016). Thus, the accumulation of 2-AG in the presence of JZL184 is expected. However, the relative contribution of increased 2-AG versus decreased AA following inhibition of MGL has varied in different models. In the mouse experimental autoimmune encephalitis model, inhibition of MGL reduced symptoms via a CB_1R/CB_2R mechanism (Brindisi et al., 2016). Blocking MGL suppresses LPS-induced neuroinflammation and loss of dopamine neurons in a model of Parkinson's disease by decreasing PG production with no evidence for enhanced eCB signaling (Nomura et al., 2011). Similarly, in transgenic mouse models of Alzheimer's disease JZL184 was neuroprotective but, without clear involvement of CB receptors (Chen et al., 2012; Piro et al., 2012). In mice, JZL184 increased brain 2-AG 8-fold and elicited an array of CB_1R-mediated behavioral effects (Long et al., 2009). The principal conclusion from the studies described in this report is that CB_2R activation following inhibition of MGL affords significant protection from synapse loss induced by gp120.

There are several aspects of gp120-induced synapse loss that might render it particularly susceptible to CB_2R activation. In a previous report, we showed that the $CB_{1/2}R$ agonist WIN55,212-2 blocked gp120-induced IL-1β production and synapse loss through activation of CB_2Rs on microglia (Kim et al., 2011). Perhaps gp120 activation of the CXCR4 pathway to trigger IL-1β release from microglia is particularly sensitive to inhibition by CB_2R activation. CB_2R agonists have been shown to inhibit chemokine CXCL12-induced and CXCR4-mediated chemotaxis of T lymphocytes (Ghosh et al., 2006). The neuroprotective effects of JZL184 in transgenic models of Alzheimer's disease appear to result from activation of peroxisome proliferator-activated receptor-γ and decreased PG activation of NF-κB resulting in reduced expression of β-secretase and decreased Aβ production, a pathway not expected to be regulated by CB receptors (Piro et al., 2012; Zhang et al., 2014). Responses in microglia evoked by LPS activation of the toll-like receptor 4 pathway are inhibited by CB_2R agonists (Romero-Sandoval et al., 2009; Oh et al., 2010; Merighi et al.; Ma et al., 2015; Malek et al., 2015) although, there are reports of non-receptor mediated effects of CBs (Puffenbarger et al., 2000; Tham et al., 2007) and

a lack of CB_2R effects in some studies (Kouchi, 2015). The failure of CB_2R to contribute to the anti-inflammatory effect of JZL184 *in vivo* may result from receptor desensitization following the prolonged treatment protocols used for *in vivo* studies (Nomura et al., 2011). Indeed, prolonged administration of JZL184 desensitizes CB_1R (Schlosburg et al., 2010). However, desensitization of the CB_2Rs that mediate the effect described here has not been explicitly shown, in part because the expression of CB_2Rs is upregulated by inflammatory stimuli (Benito et al., 2008). In acute models of peripheral inflammatory pain, JZL184 produces analgesia via CB_1 and CB_2 receptors (Guindon et al., 2011). Thus, JZL184 may reduce neuroinflammation by PG and/or eCB mechanisms depending on the specific inflammatory stimulus and duration of treatment.

In the brain, hydrolysis of 2-AG by MGL is the primary source of AA for conversion to PGs by cyclooxygenase (Nomura et al., 2011). PGE_2 production is required for IL-1β-evoked synapse loss (Mishra et al., 2012). Here, we tested whether decreased PG levels contributed to the synapse protective effects of JZL184. Activation of $EP_{1\text{-}2}Rs$ was necessary for gp120-induced synapse loss and JZL184 blocked gp120-induced PGE_2 production. Thus, it is likely that JZL184 suppression of PGE_2 production contributed to the protective effect. However, because AM630 completely blocked the synapse protection afforded by JZL184, we conclude that the reduction in PG levels produced by MGL inhibition was not the primary mechanism in this model. JZL184 did not suppress the basal level of PGE_2 present in unstimulated cultures, suggesting that sufficient PGE_2 from a source other than MGL was available to enable gp120-induced synapse loss. Furthermore, IL-1β potentiated NMDA receptors independent of $EP_{1\text{-}2}R$ activation, suggesting separate IL-1β actions on PG production and NMDA receptor signaling. A partial attenuation of gp120-evoked IL-1β production with the $EP_{1\text{-}2}R$ antagonist can be reconciled with its complete block of gp120-induced synapse loss by considering the PG regulation of synapse loss at two steps in the pathway activated by gp120. Activation of $EP_{1\text{-}2}Rs$ facilitates glial production of IL-1β and stimulates glutamate release resulting in biochemical potentiation of NMDARs and their direct activation, respectively (Mishra et al., 2012). Thus, we cannot rule out a contribution resulting from decreased PGE_2 synthesis. The CB_2R- and $EP_{1\text{-}2}R$-depedence of JZL184 inhibition of IL-1β production were both partial effects, consistent with the idea that the inhibition of MGL has dual actions via CB_2 receptor signaling and decreased PGE_2 production.

HIV-1 gp120 evoked synapse loss via a multi-step process (Figure 7) involving

multiple cell types. The primary effects of JZL184 appear to be on glia where activation of CB_2R or reduced PGE_2-dependent activation of $EP_{1\text{-}2}Rs$ inhibits the release of IL-1β. In a previous study we found that IL-1β induced PGE_2 production was required for synapse loss, presumably via an $EP_{1\text{-}2}R$ mediated increase in presynaptic glutamate release (Mishra et al., 2012). If we consider a role for presynaptic glutamate release in gp120-induced synapse loss, then we might expect a CB_1R-mediated component to JZL184-mediated synapse protection because 2-AG mediates a robust inhibition of excitatory synaptic transmission (Straiker et al., 2009; Roloff et al., 2010). However, neither rimonabant nor LY320135 affected JZL184-mediated protection, suggesting that the elevation in 2-AG might be localized to a microdomain with preferential access to microglia independent of presynaptic terminals.

Cannabinoid receptor agonists have beneficial effects in models of HAND (Kim et al., 2011; Avraham et al., 2014; Purohit et al., 2014). However, drugs that directly activate cannabinoid receptors might cause receptor desensitization during long-term treatment, diminishing the neuroprotective efficacy of the endocannabinoid system. Agonists with actions on CB_1 receptors or those with low selectivity may have abuse liability. Alternatively, inhibition of MGL only potentiates endogenously produced 2-AG so that receptor activation is dependent on a stimulus. High doses of JZL184 produced extensive CB_1 receptor activation (Long et al., 2009). However, prolonged, low-dose JZL184 treatment elicited an anti-inflammatory effect without producing CB_1 receptor tolerance or cannabinoid dependence (Kinsey et al., 2013). Furthermore, because brain AA production is primarily dependent on MGL, in contrast to the gut, drugs that inhibit MGL can reduce brain PG levels without the gastrointestinal side effects produced by nonsteroidal anti-inflammatory drugs (Scheiman, 2016). Thus, drugs that inhibit MGL show promise for reducing neuroinflammation in HAND.

Dendritic damage and loss of synaptic connections correlate with cognitive decline in HAND patients. Synapse loss induced by HIV proteins occurs early and via a different signaling pathway from that leading to neuronal death (Kim et al., 2008b), suggesting that synapse loss might be a mechanism to reduce excitotoxicity (Hargus and Thayer, 2013). Indeed, synapse loss is reversible (Shin et al., 2012) and rescue of synapses lost following exposure to the neuroinflammatory HIV protein Tat restored cognitive function (Raybuck et al., 2017). Chronic inhibition of MGL in amyloid precursor protein transgenic mice induced recovery of synaptic spines and improvement of spatial learning and memory

function (Chen et al., 2012). Perhaps the synapse loss induced by the neuroinflammatory component of neurodegenerative diseases is readily reversible. It will be interesting to determine whether, in addition to protecting synapses from loss induced by HIV proteins, MGL inhibition by drugs such as JZL184 can rescue synapses when given after loss has already occurred.

This report shows for the first time that pharmacological inhibition of MGL can afford neuroprotection via activation of CB_2 receptors on brain microglia. This mechanism differs from other reports in which the reduced neuroinflammation produced by JZL184 was primarily mediated via reduced PG signaling. The mechanism of protection afforded by MGL inhibitors may depend on the specific cell types involved in the neuroinflammatory response, the concentration and duration of drug treatment and the unique signaling pathways recruited in response to various inflammatory stimuli. This is the first report showing inhibition of MGL affords neuroprotection in a model of HAND, suggesting that the chronic neuroinflammation that underlies this disorder may be particularly susceptible to modulation of the eCB system.

Chapter Three:

HIV gp120-induced neuroinflammation potentiates NMDA receptors to overcome basal suppression of inhibitory synapses by p38 MAPK.

Xinwen Zhang[1], Matthew V. Green[2], and Stanley A. Thayer[1,2]*

[1]Department of Pharmacology and [2]Graduate Program in Neuroscience, University of Minnesota Medical School Minneapolis, MN

Content adapted from published article: Zhang X, Green MV, Thayer SA (2019) HIV gp120-induced neuroinflammation potentiates NMDA receptors to overcome basal suppression of inhibitory synapses by p38 MAPK. J Neurochem. 148(4):499-515

Contributions: XZ and SAT designed the study; XZ and MVG performed experiments and collected data; XZ and SAT analyzed data and wrote the manuscript; SAT provided reagents and conceptual advice.

I. Introduction

HIV-associated neurocognitive disorder (HAND) affects about half of the over 36 million people infected (Saylor et al., 2016). Although broad application of combination antiretroviral therapy (cART) has dramatically reduced the number of patients that progress to AIDS, cART does not eradicate HIV from the brain (Ellis et al., 2007; Saylor et al., 2016). Thus, the prevalence of HAND remains high, in part because of the increased lifespan of HIV infected individuals (Eggers et al., 2017). Currently there is no effective treatment for HAND.

Chronic neuroinflammation is a major component of HAND pathogenesis (Chen et al., 2014; Gill and Kolson, 2014; Walsh et al., 2014; Hong and Banks, 2015). HIV-infected macrophages and microglia release viral proteins and cytokines eliciting an inflammatory response that disturbs neuronal network activity and causes progressive loss of cognitive function (Ellis et al., 2007). In response to excess excitatory drive produced by HIV-associated neuroinflammation, neurons decrease the number of excitatory synapses (Bellizzi et al., 2006; Kim et al., 2008b; Green et al., 2018; Guha et al., 2018). Loss of excitatory synapses correlates with cognitive decline in HAND (Ellis et al., 2007). Normal network activity requires balanced excitatory and inhibitory neurotransmission (Pozo and Goda, 2010). Changes in inhibitory signaling are also associated with excitotoxicity and neuroinflammation.

Neurons exposed to the inflammatory cytokine interleukin-1β (IL-1β) increase surface expression of γ-aminobutyric acid type A receptors ($GABA_ARs$) (Serantes et al., 2006), suggesting that inhibitory neurotransmission can be influenced by inflammatory pathways. Excessive upregulation of GABAergic signaling in response to inflammatory and excitotoxic stress impairs cognitive function. For example, in models of stroke, excess GABAergic tone impairs network recovery (Orfila et al., 2017) and in schizophrenia patients, increased synaptic α2 subunit-containing $GABA_A$ receptors are associated with cognitive dysfunction (Impagnatiello et al., 1998; Lewis et al., 2004; Guidotti et al., 2005). Upregulation of GABAergic synaptic markers also occurs following prolonged exposure to HIV neurotoxins, suggesting that excess inhibitory signaling may be involved in HAND as well (Fitting et al., 2013; Hargus and Thayer, 2013). At present, how GABA-mediated inhibition is regulated during HIV-induced neuroinflammation is not known.

HAND pathogenesis occurs primarily through an indirect mechanism mediated by the release of toxic agents, such as the HIV envelope protein gp120. HIV gp120 is shed by infected cells (Kaul et al., 2001), elicits neurotoxicity at picomolar concentrations

(Meucci and Miller, 1996; Kim et al., 2011; Zhou et al., 2017), and has been detected in the brains of patients with HAND (Jones et al., 2000). HIV gp120 evokes synaptic and behavioral deficits *in vivo* that mimic significant aspects of HAND (Toggas et al., 1994; Thaney et al., 2018). In this study, we used an *in vitro* model to study changes in inhibitory synapses during exposure to the neuroinflammatory stimulus HIV gp120. The envelope protein evoked the release of IL-1β from microglia. The resulting stimulation of IL-1 receptors on neurons activates a Src and NMDA receptor pathway that increases the number of inhibitory synapses. This pathway overcame a basal suppression of inhibitory synapse number mediated by p38 MAPK. Recognizing that these two pathways regulate inhibitory synapse number, and that there is crosstalk between these pathways, provides insight into the neuronal response to inflammation and may guide the development of therapeutics targeting inhibitory signaling in HAND.

II. Materials and Methods

Materials

Materials were obtained from the following sources: IL-1β (catalog number: 501-RL-010) and IL-1 receptor antagonist (IL-1ra) (catalog number: 1545-RA-025) were from R&D Systems (Minneapolis, MN, USA); 3-(4-chlorophenyl) 1-(1,1-dimethylethyl)-1H-pyrazolo[3,4-d]pyrimidin-4-amine (PP2) (catalog number: 1407), 1-Phenyl-1H-pyrazolo[3,4-d]pyrimidin-4-amine (PP3) (catalog number: 2794), 3-Chloro-4-fluoro-N-[4-[[2-(phenylcarbonyl)hydrazino]carbonyl]benzyl]benzenesulfonamide (TCN201) (catalog number: 4154), cycloheximide, 4-[5-(4-Fluorophenyl)-2-[4-(methylsulfonyl)phenyl]-1H-imidazol-4-yl]pyridine (SB203580) (catalog number: 1202), *trans*-4-[4-(4-Fluorophenyl)-5-(2-methoxy-4-pyrimidinyl)-1*H*-imidazol-1-yl]cyclohexanol (SB239063) (catalog number: 1962), 6-Cyano-7-nitroquinoxaline-2,3-dione disodium (CNQX) (catalog number: 1045), bicuculline methiodide, and tetrodotoxin (TTX) (catalog number: 1069) were from Tocris Bioscience (Bristol, UK); 4-Ethyl-2(p-methoxyphenyl)-5-(4'-pyridyl)-IH-imidazole (SB202474) was from Millipore Sigma (catalog number: 559387; St. Louis, MO, USA). Dulbecco's modified Eagle's medium (DMEM) (catalog number: 31053), Hanks' balanced salt solution (catalog number: 14175), fetal bovine serum (catalog number: 26140), horse serum (catalog number: 16050) and penicillin/streptomycin (catalog number: 15140) were from ThermoFisher Scientific (Carlsbad, CA, USA). The expression vector for GPHN.FingR-eGFP, pCAG-GPHN.FingR-eGFP, was generated by Don Arnold’s laboratory and obtained from Addgene (catalog number: 46296; Cambridge, MA, USA).

The expression vector for synapsin driven tdTomato was generated by inserting tdTomato from pLVX-tdTomato-N1 (catalog number: 632563; Clontech-Takara Bio, Mountain View, CA, USA) into the pSyn backbone of pSyn-PSD95-GFP provided by Kirill Martemyanov (Scripps Research Institute, Jupiter, FL, USA). The plasmid for RapR-p38 expression (pCMV5-Flag-RapR-p38) was generated in Klaus Hahn's laboratory and obtained from Addgene (catalog number: 25935). HIV-1 $gp120_{IIIB}$ was from the National Institutes of Health (NIH) AIDS Reagent Program, Division of AIDS, National Institute of Allergy and Infectious Diseases, NIH (catalog number:11784).

Cell culture

All animal care and experimental procedures were performed following the Guide for the Care and Use of Laboratory Animals published by the U.S. National Institutes of Health. Ethical approval was granted by the Institutional Animal Care and Use Committee of the University of Minnesota (protocol 1612-34372A). Primary hippocampal cultures were derived from fetal Sprague Dawley rats (RRID:MGI:5651135, Charles River, Wilmington, MA, USA) as described previously (Zhang and Thayer, 2018). Rats were euthanized by CO_2 inhalation then hippocampi from embryonic day 17 fetuses were dissected and placed in Ca^{2+} and Mg^{2+} free Hanks' balanced salt solution (HBSS). Hippocampi were dissociated by trituration with flame-narrowed Pasteur pipettes of decreasing aperture in DMEM supplemented with 10% fetal bovine serum and penicillin/streptomycin (100 U mL^{-1} and 100 mg mL^{-1}, respectively). Cells were plated onto Matrigel-coated (150 µL, 0.2 mg mL^{-1}, BD Biosciences, Billerica, MA, USA) glass-bottomed Petri dishes. Cultures were kept in a humidified atmosphere of 10% CO_2 and 90% air (pH 7.4) at 37 ^{O}C. Culture media was exchanged on day 1 and 8 *in vitro* with DMEM supplemented with 10% horse serum and penicillin/streptomycin. All cultures were maintained for 12-16 days *in vitro* prior to use in experiments. These cultures contain 24 ± 4% neurons, 55 ± 4% astrocytes and 13 ± 6% microglia (Zhang and Thayer, 2018).

Transfection

Cultures were transfected using a previously described calcium phosphate procedure (Zhang and Thayer, 2018). After 11- or 12-days *in vitro,* culture media was exchanged with DMEM containing 1 mM kynurenic acid, 10 mM $MgCl_2$, and 5 mM HEPES. A DNA/calcium phosphate precipitate containing 0.5 µg of total plasmid DNA per well was allowed to form at room temperature for 1.5 h, then added dropwise to the cells. After a

1 h incubation, cells were washed twice with DMEM supplemented with 10 mM $MgCl_2$ and 5 mM HEPES and conditioned media saved at the beginning of the procedure was returned to the cells. Experiments were started 2-3 days after transfection.

Confocal imaging and image processing

Confocal imaging and image processing were performed as previously described (Zhang and Thayer, 2018). Petri dishes containing transfected cells were placed in an incubator (LCI, Seoul, Korea; 37 °C and 10% CO_2) on the stage of an inverted laser scanning confocal microscope (Nikon A1, Melville, NY, USA) and imaged with a 60 x (1.4 numerical aperture) oil-immersion objective. Optical sections spanning 9 µm (1 µm per step) in the z-dimension were collected and combined into a maximum z-projection. GFP was excited at 488 nm and emission collected from 500 to 550 nm. TdTomato was excited at 561 nm and emission collected from 570 nm to 620 nm. After imaging, cells were returned to the cell culture incubator and the coordinates of the computer-controlled stage saved to allow repeated imaging of the same cell at later time points.

An algorithm written in MetaMorph 7 (RRID:SCR_002368, San Jose, CA, USA) was used to count the GFP puncta in an unbiased manner (Waataja et al., 2008). A threshold 0.25 times the standard deviation above the image mean was applied to the red image creating a 1-bit image. This binary image was used as a mask via a logical AND function with the green channel maximum z-projection. A top-hat filter (80 pixels) was applied to the masked green image. A threshold set 1.5 standard deviations above the mean intensity inside the mask was then applied to the contrast enhanced image. Punctate structures between 12 and 80 pixels (0.13-0.86 μm^2) were counted as postsynaptic densities. Changes in the number of GPHN.FingR-GFP puncta from 2-3 microscopic fields from a single dish were averaged and considered an individual sample (n =1).

Electrophysiology

Electrodes were pulled using a horizontal micropipette puller (P-87; Sutter Instruments) from glass capillaries (Narishige). Pipette resistance was 3–5 MΩ. Miniature inhibitory postsynaptic currents (mIPSCs) were recorded with the following extracellular solution (in mM): 140 NaCl, 5 KCl, 9 CaCl, 6 MgCl, 5 glucose, and 10 HEPES, pH adjusted to 7.4 with NaOH. The intracellular recording solution was composed of (in mM): 140 KCl, 0.2 EGTA, 10 HEPES, 10 glucose, 5 MgATP, and 0.3 NaGTP, pH adjusted to 7.2 with

KOH. Whole-cell voltages were amplified with an AxoPatch 200B (Molecular Devices), low-pass filtered at 2 kHz, and digitized at 10 kHz with a Digidata 1322A digitizer and pClamp software (Molecular Devices). Cells with series resistance over 25 MΩ were excluded from analysis. For mIPSCs recordings cells were voltage clamped at -70 mV in the presence of 3 µM CNQX, 50 µM APV, and 100 nM TTX. Data were analyzed with miniAnalysis software (Synaptosoft) using a threshold of 15 pA.

Statistics

All data are presented as mean ± SEM. Data distributions were determined using the D'Agostino-Pearson normality test and homogeneity of variances determined using Bartlett's test; all statistical tests were performed on normally distributed data of equal variance. Student's *t*-test (unpaired two-tailed) was used for statistical analysis in two-group comparison. For comparison among multiple groups, one-way or two-way ANOVAs were performed with Tukey's post hoc test. Time course data were analyzed with a two-way repeated measures ANOVA. Statistical significance was defined as $p<0.05$. Sample sizes were not statistically predetermined but conform to similar studies. A test for outliers was not performed in this study. For imaging inhibitory synapses, the change in puncta from 2-3 fields from a single dish were averaged and considered as n=1. Imaging experiments included data from at least 8 dishes from 3-5 different cell culture platings. Gephyrin puncta were counted using an objective image processing algorithm that obviated the need to blind the experimenter. No other blinding methods were employed in this study. All statistical analyses were performed using Prism, GraphPad 7 (La Jolla, CA 92037 USA).

III. Results

HIV gp120IIIB increases the number of inhibitory synapses

The number of inhibitory synapses between hippocampal neurons in culture was determined by counting puncta produced by expression of a fluorescent antibody-like protein in live cells. Rat hippocampal cultures were transfected with plasmids that express a red fluorescent protein (tdTomato) to resolve cell morphology and a recombinant intrabody (GPHN.FingR-eGFP) that binds to gephyrin, a scaffolding protein located at the postsynaptic terminal of inhibitory synapses (Tyagarajan and Fritschy, 2014) (Figure 3.1A). Previous studies have shown that GPHN.FingR-eGFP expressed in rat neurons labels synaptic structures as indicated by co-localization of intrabody enhanced green fluorescent protein (EGFP) puncta with endogenous gephyrin (Gross et al., 2013). To quantify the number of inhibitory synapses, an image processing algorithm was used to count fluorescent puncta meeting size and intensity criteria that were in contact with a binary mask created from the tdTomato image (Figure 3.1A). Functional analysis revealed that the number of labeled gephyrin puncta correlates with the frequency of mIPSCs (Figure 3.1B) indicating that fluorescent puncta identify functional synapses. To determine whether gp120 influences the number of inhibitory synapses, transfected neurons were imaged before (0 h) and 4 and 24 h after treatment with 600 pM gp120. Treatment with gp120 for 24 h increased the number of intrabody-labeled gephyrin puncta by 18 ± 5% compared to untreated control (Figure 3.1C, D). The number of inhibitory synapses was unchanged after 4 h exposure to gp120, indicating that the increase occurred in a time-dependent manner. To determine if gp120 affected neuronal survival, we calculated the percentage of neurons that retained tdTomato fluorescence at the 24 h time point for the experimental cohorts included in Figure 3.1D. In the untreated control group, 84 ± 4 % of neurons survived; in gp120 treated group, 89 ± 9 % of the neurons survived, indicating that treatment with gp120 did not elicit significant neuronal death (Unpaired two-tailed *t*-test; $t_{(8)}$=0.48, p=0.65, n=5). This result is consistent with a previous cell survival study from our lab using a propidium iodide uptake assay that found 600 pM gp120 did not induce significant neuronal death until after exposure for 48 h (Kim et al., 2011). To determine if the effects of gp120 required intact tertiary structure and also to exclude a possible contribution from endotoxin contamination in the gp120 stock, transfected neurons were imaged before (0 h) and 24 h after treatment with 600 pM gp120 or heat-inactivated gp120 (HI-gp120, 95 °C for 1 h). Treatment with HI-gp120 did not increase the number of inhibitory synapses (Figure 3.1E).

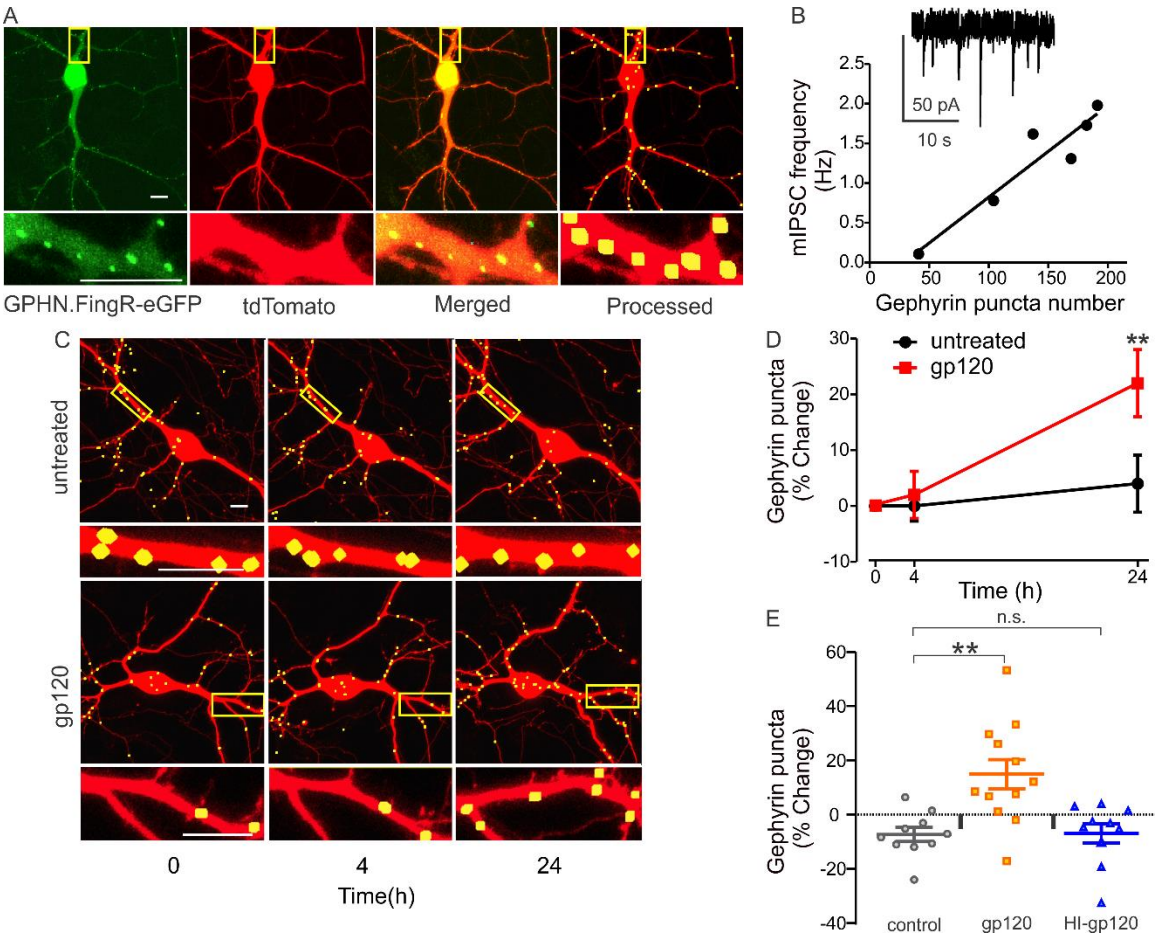

Figure 3.1 gp120 increases the number of inhibitory synapses. (A) Representative confocal images of a neuron expressing GPHN.FingR-eGFP and tdTomato were acquired and processed as described in Methods. Identified gephyrin puncta (yellow) were dilated and overlaid on the tdTomato maximum projection (Processed) for display purposes. Insets are enlarged images of the boxed regions. Scale bars represent 10 µm. (B) The number of gephyrin puncta correlates with the frequency of mIPSCs ($r_{(4)}$=0.95, p=0.004, n=6; data from 2 independent cell preparations). (C) Representative processed confocal images and (D) plot showing time-dependent increase in the number of gephyrin labelled inhibitory synapses following treatment with gp120 (600 pM) (two-way repeated measures ANOVA; $F_{(2, 26)}$= 6.61, p=0.005, n=14; data from 5 independent cell preparations). (E) Treatment with 600 pM gp120 for 24 h increased the number of gephyrin labelled inhibitory synapses. Heat-inactivated gp120 (HI-gp120) did not affect the number of inhibitory synapses. (One-way ANOVA; $F_{(2,29)}$=9.43, p=0.0007, n=10 for control and HI-gp120 group; n=12 for gp120 treated group; data from 3 independent cell preparations). Insets are enlarged images of the boxed regions. Scale bars represent 10 µm. Data are expressed as mean ± SEM. Two-way repeated measures ANOVA or one-way ANOVA was followed with Tukey's post hoc test, **p<0.01, compared to control group (n=number of individual dishes in each group).

HIV gp120 activates CXCR4 to release IL-1β from microglia to upregulate inhibitory synapses

The IIIB strain of the HIV-1 envelope protein gp120 binds to its co-receptor C-X-C chemokine receptor type 4 (CXCR4) and CD4 to initiate viral entry. The interaction of gp120 with CXCR4 activates microglia to release inflammatory cytokines that affect neurons (Viviani et al., 2006; Kim et al., 2011; Zhang and Thayer, 2018). To determine whether this receptor was involved in the gp120-induced increase in the number of intrabody-labeled gephyrin puncta, we co-treated neuronal cultures with the CXCR4 antagonist AMD3100 (1 μM) and gp120. AMD3100 prevented the increase in gephyrin puncta evoked by 24 h treatment with gp120 (Figure 3.2A). CXCR4 is expressed in microglia, astrocytes, and neurons (Bonavia et al., 2003), which are all present in our primary hippocampal cultures. To test whether microglia were necessary for the effects of gp120, we eliminated microglia from the culture by treating with Leucine-Methyl-Ester (LME) (25 mM for 1 h followed by DMEM wash, or DMEM for 1 h followed by DMEM wash for control) 24 h prior to treating with gp120. LME treatment reduced the number of microglia by 95% compared to DMEM wash controls, as determined by immunocytochemistry with the Ox-42 antibody. Elimination of microglia prior to treatment with gp120 prevented the increase in intrabody-labeled gephyrin puncta compared to DMEM wash controls (Figure 3.2B).

The interaction of gp120 with CXCR4 on microglia can evoke the release of inflammatory cytokines such as IL-1β. IL-1β increases the amplitude of evoked IPSCs (Hellstrom et al., 2005) and surface expression of functional GABAARs (Serantes et al., 2006). Here we examined the role of IL-1β in the gp120-induced up-regulation of inhibitory synapses. Treatment with IL-1β (3 ng/mL) for 24 h significantly increased the number of intrabody-labeled gephyrin puncta by 24 ± 4 % compared to control (Figure 3.2C). Thus, IL-1β mimics the effects of gp120 on the number of inhibitory synapses. To determine whether the gp120-induced increase in inhibition is mediated by IL-1β, cultures were co-treated with 1 μg/ml IL-1 receptor antagonist (IL-1ra) and gp120 (600 pM). IL-1ra prevented the gp120-induced increase in the number of intrabody labeled gephyrin puncta (Figure 3.2D). Collectively, these results indicate that gp120 activates CXCR4 on microglia to stimulate a neuroinflammatory pathway to release IL-1β that acts on its receptor to alter the number of inhibitory synapses.

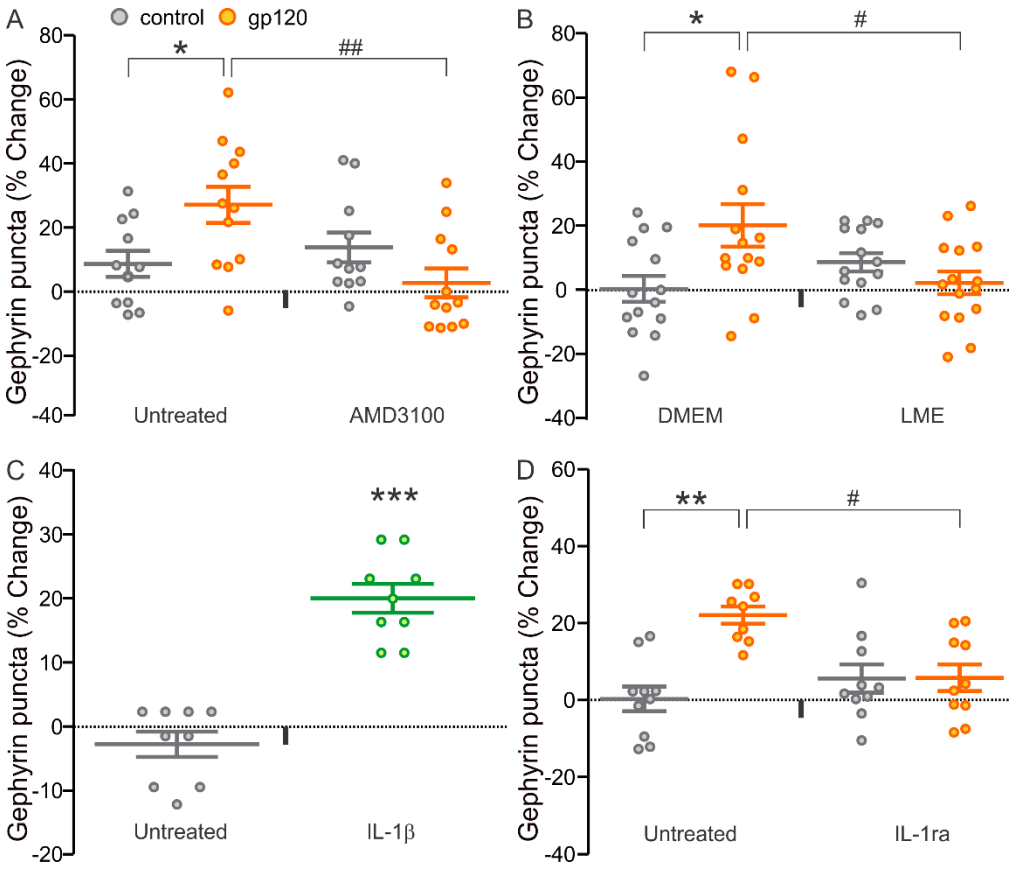

Figure 3.2 gp120-evoked release of IL-1β from microglia upregulates the number of inhibitory synapses. (A) CXCR4 antagonist, AMD3100 (1 µM), inhibits gp120-induced (600 pM) increases in the number of intrabody-labeled gephyrin puncta (24 h) relative to initial puncta count (0 h) (two-way ANOVA; $F_{(1,42)}$=9.45, p=0.004, n=11 for control; n=12 for gp120 treated groups; data from 4 independent cell preparations). (B) Removal of microglia by 1 h treatment with 25 mM LME blocks gp120-induced increases in the number of inhibitory synapses (two-way ANOVA; $F_{(1,53)}$=6.10, p=0.02; data from 5 independent cell preparations) compared to DMEM wash (n=14). (C) IL-1β (3 ng/mL for 24 h) alone increases the number of inhibitory synapses (Unpaired two-tailed *t*-test; $t_{(16)}$=4.8, p=0.0002, n=9; data from 3 independent cell preparations). (D) IL-1ra (1 µg/mL) blocks the gp120-induced increase in the number of inhibitory synapses (two-way ANOVA; $F_{(1,36)}$=8.03, p=0.008, n=10; data from 4 independent cell preparations). Data are expressed as mean ± SEM. Two-way ANOVAs were followed by Tukey's post hoc test, *p<0.05, **p<0.01, ***p<.001 compared to untreated control. $^{\#}$ p<0.05, $^{\#\#}$p<0.01, compared to gp120 alone (untreated) (n=number of individual dishes in each group).

Basal p38 MAPK activity suppresses the number of inhibitory synapses

IL-1 receptor activation was previously shown to couple to the p38 mitogen-activated protein kinase (p38 MAPK) pathway to inhibit long-term potentiation (Kelly et al., 2003) and upregulation of this pathway is also reported to induce synaptic changes associated with neurodegenerative disease (Sama and Norris, 2013). Therefore, we tested whether inhibition of p38 affected the number of inhibitory synapses. Treatment with SB203,580 (10 μM), a selective p38 MAPK inhibitor, alone induced an increase in gephyrin puncta (Figure 3.3A, B). This increase was not observed with the inactive analog SB202474 (10 μM) (Figure 3.3C), and was also observed with a second p38 inhibitor, SB239063 (10 μM) (Figure 3.3D). These data suggest that p38 tonically suppresses GABAergic neurotransmission by decreasing the number of inhibitory synapses. To further explore the role of p38, we employed a genetic approach. RapR-p38 is a genetically modified p38 kinase that acts as a dominant negative when expressed in the presence of wild type p38. RapR-p38 is activated by rapamycin, enabling regulation of p38 activity independent of its upstream physiological signaling pathway (Karginov et al., 2010). In cells expressing RapR-p38, tdTomato and GPHN.FingR-eGFP, rapamycin treatment reduced the number of inhibitory synapses by 19 ± 3% compared to those not treated with rapamycin (Figure 3.3E). Thus, activation of p38 is sufficient to suppress the formation of new inhibitory synapses under basal conditions.

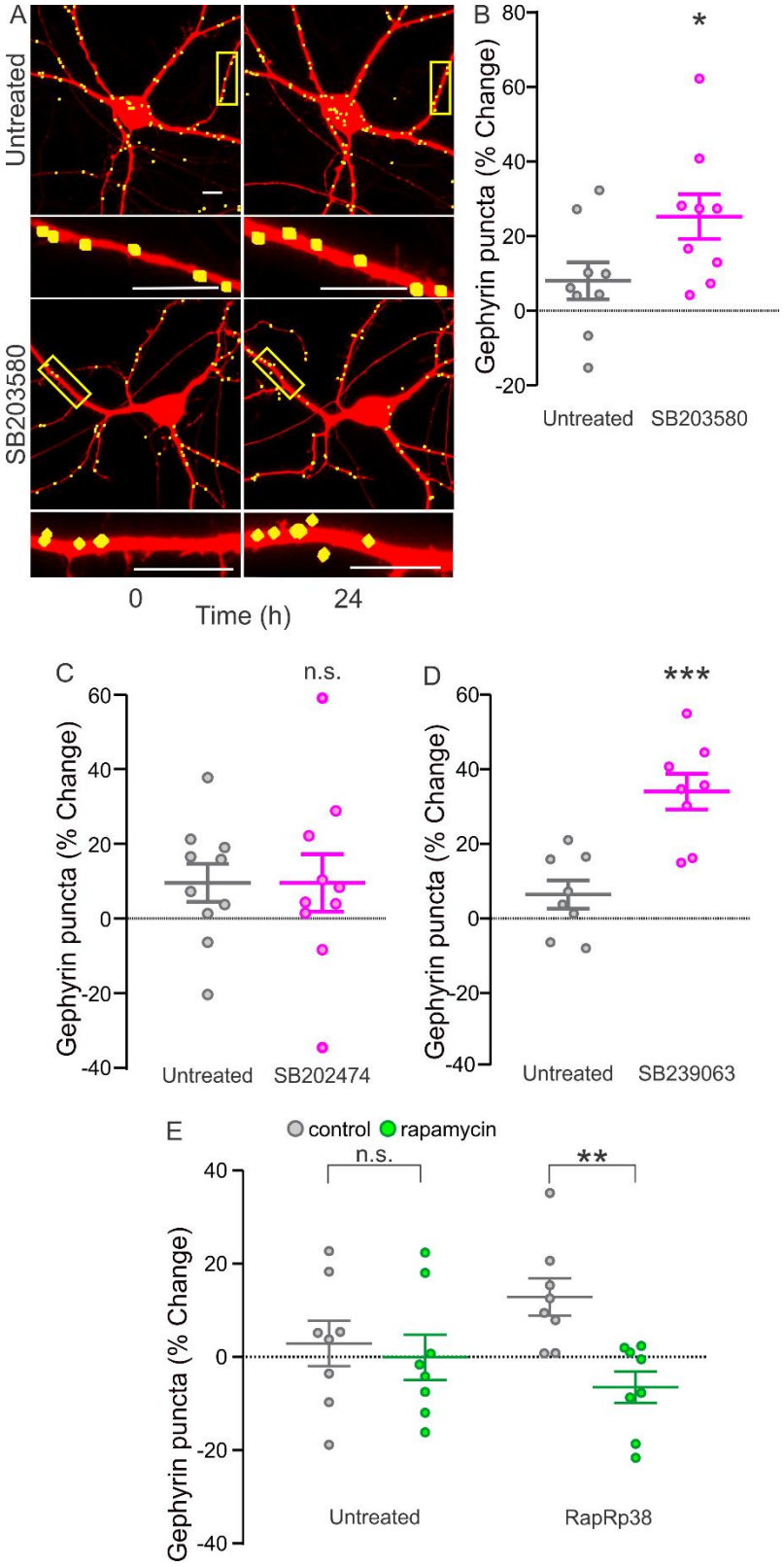

Figure 3.3 p38 MAPK mediates basal suppression of the number of inhibitory synapses. (A) Representative processed confocal images and (B) bar graph showing the p38 antagonist SB203,580 (10 µM) alone increases the number of intrabody-labeled

gephyrin puncta (24 h) relative to untreated (Unpaired two-tailed *t*-test; $t_{(16)}$=2.21, p=0.04, n=9; data from 3 independent cell preparations). (C) SB202474 (10 µM), an inactive analog of SB203580, does not affect the gp120-induced (600 pM) increase in the number of intrabody-labeled gephyrin puncta (24 h)(Unpaired two-tailed t-test; $t_{(18)}$=0.004, p= 1, n=10; data from 3 independent cell preparations). (D) The number of intrabody-labeled gephyrin puncta is increased by 24 h treatment with SB239063 (10 µM), a p38 MAPK inhibitor (Unpaired two-tailed t-test; $t_{(14)}$=4.95, p=0.0002, n=8; data from 3 independent cell preparations). (E) Treatment with rapamycin (200 nM) decreases the number of inhibitory synapses in cells expressing RapRp38 (Unpaired two-tailed t-test, $t_{(14)}$=3.71, p=0.002; data from 3 independent cell preparations) but not untreated cells (Unpaired two-tailed t-test, $t_{(14)}$=0.43, p=0.7; data from 3 independent cell preparations) (n=8). Data are expressed as mean ± SEM, *p<0.05, **p<0.01, ***p<.001 compared to control (n=number of individual dishes in each group).

HIV gp120 activates Src and GluN2A-containing NMDARs to increase the number of inhibitory synapses

IL-1β stimulates phosphorylation of NMDARs by Src family kinases (SFKs) (Viviani et al., 2003; Viviani et al., 2006). Over activation of NMDARs leads to an increase in the number of inhibitory synapses following exposure to the HIV protein Tat (Hargus and Thayer, 2013). Thus, to determine the downstream mechanism for the gp120-induced increase in inhibitory synapses, we used the selective SFK inhibitor, PP2, to determine whether the gp120-induced increase in inhibitory postsynaptic sites is mediated by SFKs. PP2 (10 μM), but not the inactive analog PP3 (10 μM), prevented the gp120-induced increase in intrabody-labeled gephyrin puncta (24 h) (Figure 3.4A, B, C). The SFKs Src and Fyn have been shown to regulate inhibitory synaptic transmission (Ohnishi et al., 2011). To determine the specific SFK responsible for the gp120-induced increase in inhibitory synapses and to compliment the pharmacological approach with a genetic method, cultures were co-transfected with expression plasmids for tdTomato and gephyrin intrabody with or without plasmids that encode dominant-negative Src (DN-Src) or dominant-negative Fyn (DN-Fyn) (Mariotti et al., 2001). Gp120 treatment increased the number of intrabody labeled gephyrin puncta in both untreated neurons and neurons expressing DN-Fyn (Fig. 4D). However, in neurons expressing DN-Src, gp120 failed to induce a significant increase in inhibitory synapses (Figure 3.4D). These data suggest that Src mediates the gp120-induced increase in the number of inhibitory synapses.

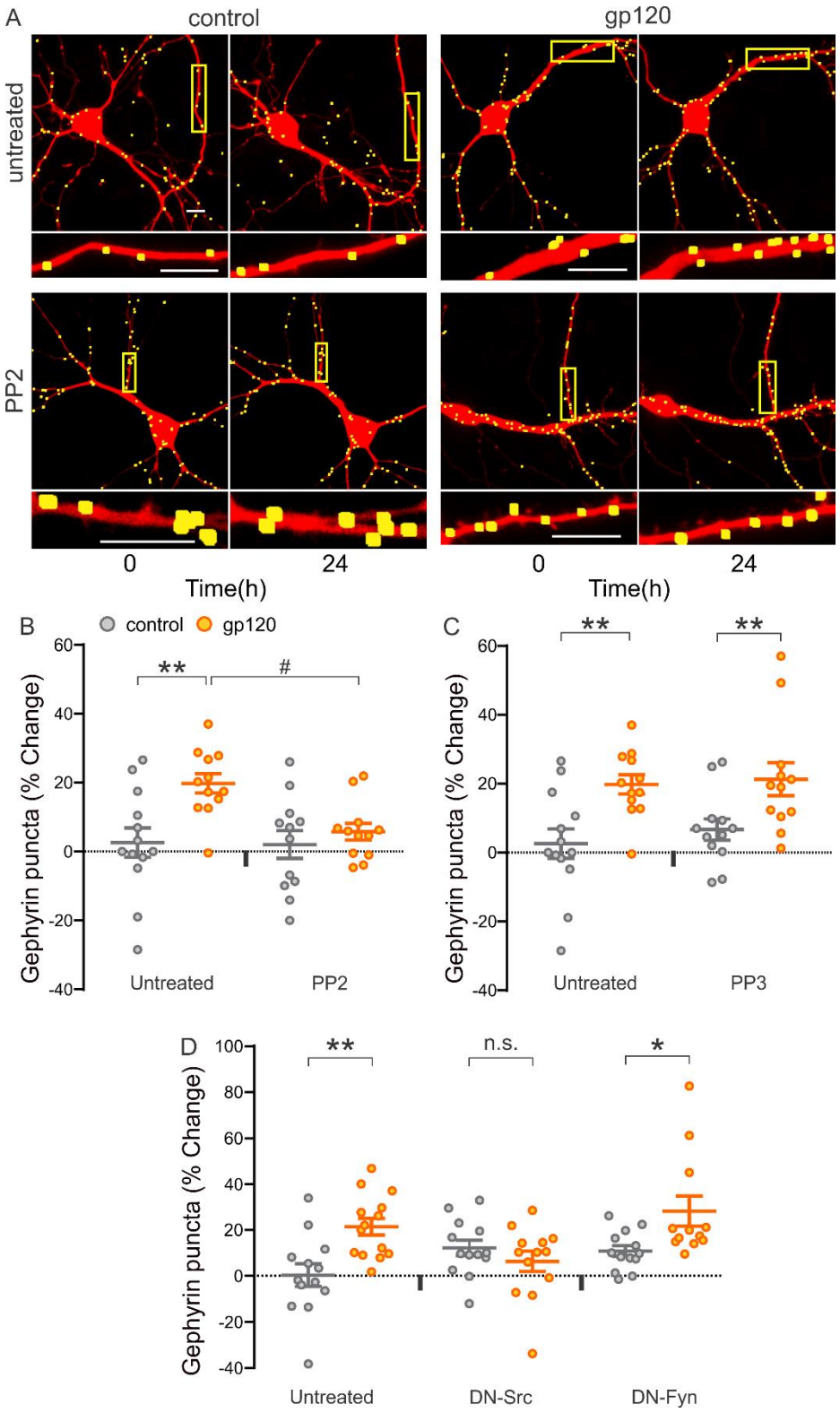

Figure 3.4 HIV gp120-induced upregulation of the number of inhibitory synapses requires Src. (A) Representative confocal images and (B) bar graph showing that the Src family kinase inhibitor PP2 (10 μM) reduced gp120-induced increase in the number of intrabody-labeled gephyrin puncta (two-way ANOVA; $F_{(1,45)}$=5.10, p=0.03, n=13 for

untreated control; n=12 for other groups; data from 5 independent cell preparations). (C) PP3 (10 μM), an inactive analog of PP2, does not affect the gp120-induced (600 pM) increase in the number of inhibitory synapses (two-way ANOVA; $F(1, 43)=0.012$, $p=0.9$, n=13 for untreated control; n=12 for untreated gp120 group; n=12 for PP3 control group; n=10 for PP3 gp120 group; data from 5 independent cell preparations). (D) gp120 induces an increase in the number of intrabody-labeled gephyrin puncta in untreated cultures ($t_{(25)}=3.47$, $p=0.002$, n=13 for untreated control; n=14 for untreated gp120 group) and cultures expressing dominant-negative Fyn ($t_{(23)}=2.58$, $p=0.02$, n=13 for Fyn control group; n=12 for Fyn gp120 treated group), but in cultures expressing dominant-negative Src the gp120-induced response was blocked (Unpaired two-tailed *t*-test; $t_{(24)}=1.04$, $p=0.3$, n=13; data from 6 independent cell preparations). Two-way ANOVAs were followed by Tukey's post hoc test, $^{*}p<0.05$, $^{**}p<0.01$ compared to control. $^{\#}$ $p<0.05$ compared to gp120 alone (untreated) (n=number of individual dishes in each group).

Src phosphorylates NMDARs increasing their activity (Kohr and Seeburg, 1996). Thus, we tested whether NMDA receptors mediate the gp120-induced increase in inhibition. In previous work, we found that synaptic changes induced by HIV proteins were mediated by GluN2A-containing NMDARs (Hargus and Thayer, 2013; Shin and Thayer, 2013). TCN201 (10 μM), an inhibitor of GluN2A-containing NMDARs, prevented the gp120-induced increase in intrabody-labeled gephyrin puncta (24 h) (Figure 3.5A). Increases in the number of inhibitory synapses could result from potentiated $GABA_AR$ function, insertion of intracellular $GABA_ARs$, or gene expression and production of new receptors (Kneussel and Hausrat, 2016). To determine whether the gp120-induced increase in inhibition requires gene expression, we pre-treated the culture with the protein synthesis inhibitor, cycloheximide (CHX) (10 μM). CHX prevented the gp120-induced increase in intrabody labeled puncta (Figure 3.5B). These data indicate that translation following activation of Src and GluN2A-containing NMDARs is required for the gp120-induced increases in intrabody labeled gephyrin puncta.

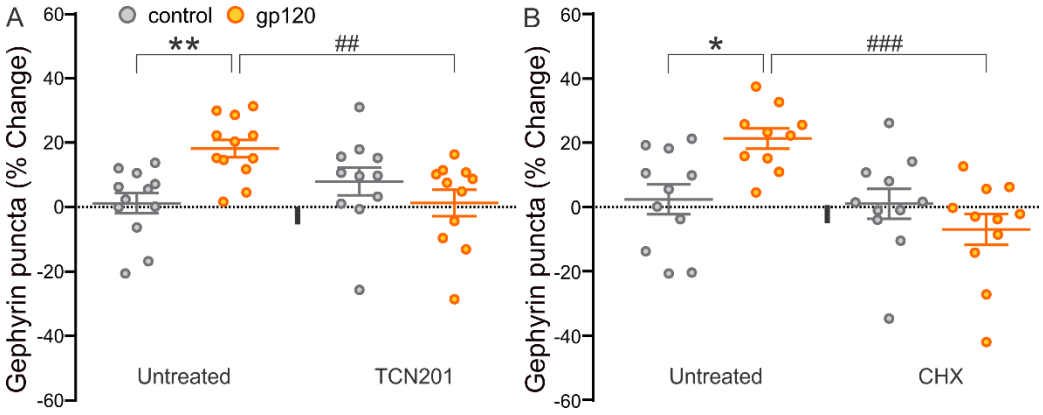

Figure 3.5 Upregulation of the number of inhibitory synapses requires GluN2A-containing NMDARs and protein synthesis. (A) TCN201 (10 µM), an antagonist for GluN2A-containing NMDARs blocks the gp120-induced increase in the number of intrabody-labeled gephyrin puncta (two-way ANOVA; $F_{(1,42)}$=10.93, p=0.002, n=12 for untreated groups; n=11 for TCN201 treated groups; data from 4 independent cell preparations). (B) The protein synthesis inhibitor cycloheximide (CHX) (10 µM) blocks the gp120-induced increase in the number of inhibitory synapses (two-way ANOVA, $F_{(1,39)}$=9.29, p=0.004, n=11 for untreated control; n=10 for untreated gp120 group; n=11 for CHX treated groups; data from 4 independent cell preparations). Data are expressed as mean ± SEM. Two-way ANOVAs were followed by Tukey's post hoc test, *p<0.05, **p<0.01 compared to control. $^{\#\#}$p<0.01, $^{\#\#\#}$p<0.001 compared to gp120 alone (untreated) (n=number of individual dishes in each group).

IV. Discussion

Elevated inhibitory signaling is associated with many neurodegenerative conditions (Fernandez et al., 2007; Hines et al., 2012; Wu et al., 2014). In this study, we examined how inhibitory synapses are affected in an *in vitro* model of HIV-associated neuroinflammation. Using an imaging-based approach to quantify GABAergic synapses in living neural networks, we found that gp120, a potent neurotoxin that *in vivo* mimics significant aspects of HAND (Toggas et al., 1994), increased the number of inhibitory synapses between hippocampal neurons. The effects of gp120 were mediated by the release of the inflammatory cytokine IL-1β from microglia, consistent with previous studies (Louboutin et al., 2010; Kim et al., 2011), and suggesting that the synaptic changes we observed are broadly relevant to neuroinflammatory conditions. Stimulation of IL-1 receptors activated a Src-NMDAR pathway to increase GABAergic synapses. This pathway reversed a tonic p38 MAPK-mediated suppression of inhibitory synapse number, suggesting that during neurotoxic challenge this upregulation overcomes a basal regulatory process. This novel dual mechanism of control provides insights into the regulation of inhibitory synapses at rest and during neuroinflammation that may identify approaches to improve cognitive function in HAND.

This study is based on a synaptic imaging approach. The method uses a recombinant antibody-like protein (intrabody) linked to EGFP, which binds to the post-synaptic scaffolding protein gephyrin and forms fluorescent clusters around inhibitory synapses. Intrabodies do not induce the formation of new inhibitory synapses as may occur with EGFP gephyrin fusion proteins previously used (Hargus and Thayer, 2013). Electrophysiological analysis demonstrated that the labeled puncta number correlates with mIPSC frequency, confirming that intrabody labelled sites represent functional inhibitory synapses. The principal advantage of the live-cell synaptic imaging approach is synapse counts from the same region of interest can be imaged before and after treatment enabling synapse count, which varies considerably between cells, to be normalized to its pre-treatment value. While we have not performed *in vivo* validation for the specific synaptic changes described in this report, the loss of excitatory synapses induced by HIV proteins using this same cell culture model was replicated *in vivo* in experiments in which pharmacological rescue of synapses also reversed cognitive impairment (Raybuck et al., 2017). Thus, synaptic changes observed in this mixed glial and neuronal culture have effectively predicted similar outcomes *in vivo*.

HIV gp120 has been detected in the brains of HIV-infected patients with dementia using immunohistochemistry (Jones et al., 2000). We are not aware of a quantitative measure of gp120 levels in brain or cerebrospinal fluid (CSF) of HIV patients. However, high levels of anti-gp120 antibody have been detected in the CSF compared to serum in HIV patients with cognitive deficits, suggesting accumulation of gp120 in the CSF (Trujillo et al., 1996). The levels of gp120 in the plasma, serum, and other tissues from HIV patients range from 0.3 to 92 ng/ml depending on the tissue (Oh et al., 1992; Santosuosso et al., 2009; Rychert et al., 2010). Thus, the 600 pM (72 ng/ml) concentration of gp120 used in this study is comparable to that found in the tissues of HIV infected individuals.

HIV gp120 activated CXCR4 to evoke the release of IL-1β from microglia. This observation is consistent with the tropism of the IIIB strain of gp120 which binds to CXCR4 (Moore et al., 1997; Islam et al., 2013). Recombinant $gp120_{IIIB}$ has previously been demonstrated to induce release of inflammatory cytokines including IL-1β from human monocytes (Clouse et al., 1991). HIV_{IIIB} is a widely studied laboratory strain that was not isolated from the CNS of HAND patients. However, CCR5 tropic gp120 has been found in HIV-infected brain and induces an inflammatory response similar to the $gp120_{IIIB}$-evoked response described here, including release of IL-1β in both rodent brain and cultured human microglia (Ashraf et al., 2014; Walsh et al., 2014). Thus, the IL-1β dependent increase of inhibitory synapses evoked by the CXCR4 preferring gp120 used here would also be predicted to result from exposure to CCR5 preferring strains. Furthermore, neuronal injury resulting from expression of $gp120_{IIIB}$ is prevented in CCR5 knockout mice, suggesting an indirect pathologic role for CCR5 in CXCR4-initiated neuroinflammation (Maung et al., 2014).

HIV neurotoxicity is indirect resulting from the release of viral proteins and inflammatory cytokines from infected microglia and macrophages (Ellis et al., 2007; Saylor et al., 2016). For productive infection, HIV gp120 interacts with a chemokine receptor (CXCR4 or CCR5) and CD4 to gain cell entry (Deng et al., 1996; Berger et al., 1999). Rodent models like the cell culture studied here, cannot be infected by HIV because they lack CD4 expression. However, gp120 can bind to and interact with chemokine receptors in the absence of CD4 (Hesselgesser et al., 1997; Kaul and Lipton, 1999). The $gp120_{IIIB}$ used in this study binds to rodent CXCR4 and elicits the release of inflammatory cytokines (Clouse et al., 1991; Brelot et al., 1997; Bagetta et al., 1999; Bezzi et al., 2001). Thus, results of this study are particularly relevant to gp120 shed from infected cells that then acts on additional non-infected cells. We have previously shown that treatment of the

same neuron-glia co-cultures used here with 600 pM gp120 increased expression of IL-1β mRNA and release of IL-1β protein (Kim et al., 2011; Zhang and Thayer, 2018). The concentration of IL-1β released into the cell culture media was 70 pg/mL which likely underestimates the local concentration in the culture monolayer and is lower than the concentration employed in this study to increase the number of inhibitory synapses. Treating the culture with threonine-lysine-proline, which blocks activation of microglia, inhibits gp120 evoked IL-1β release, suggesting that microglia are the primary source for IL-1β (Kim et al. 2011). The gp120-evoked release of IL-1β replicates one of the neuroinflammatory mechanisms thought to mediate HAND and is consistent with studies from other laboratories showing that the highly potent effects that result from prolonged exposure to low concentrations (picomolar) of the envelope protein are indirect (Meucci and Miller, 1996; Viviani et al., 2006; Medders et al., 2010; Kim et al., 2011; Yang et al., 2013). Upregulation of inhibitory synapses was blocked selectively by expression of dominant negative Src in neurons, suggesting that key steps in the downstream regulatory pathways are located within neurons. Neurons express IL-1Rs (Vezzani et al., 2011) but astrocytes also exhibit IL-1 receptor signaling (Ravizza and Vezzani, 2006) and could contribute to the effects described here. gp120-induced potentiation of NMDA receptor function and subsequent loss of excitatory synapses are also mediated by an IL-1β induced pathway (Zhang and Thayer, 2018), consistent with the key role of IL-1β in HIV gp120-induced neuronal injury. IL-1β mRNA and protein expression levels are increased significantly in the brain tissues of HIV positive patients (Persidsky and Gendelman, 1997; Xing et al., 2009; Walsh et al., 2014). In HIV-1 encephalitis patients, the expression of IL-1β is signicantly higher compared to HIV seropositive or seronegative patients without HIV-1 encephalitis (Zhao et al., 2001). A slightly modified form of recombinant human IL-1ra is currently being tested in a clinical trial for HAND (ClinicalTrials.gov Identifier: NCT02527460). The signaling pathway activated by gp120 and described here might reveal additional targets relevant to HAND pharmacotherapy.

The gp120-evoked increase in the number of inhibitory synapses appears to be mediated by a homeostatic plasticity mechanism to counteract excessive excitation (Pozo and Goda, 2010; Green et al., 2018). We did not detect significant cell death during a 24 h exposure to gp120 although, others have described a 23-55 % loss of neurons during a 24-72 exposure to gp120 concentrations ranging from 200 pM to 100 nM (Medders et al., 2010; Avdoshina et al., 2016; Liu et al., 2016). Our results suggest that there is an early adaptive, possibly protective, response that is initiated by the same potentiation of

NMDARs that triggers the cell death process. HIV gp120 potentiated NMDAR function via activation of the tyrosine kinase Src, a process known to sensitize the NMDAR to activation by glutamate (Viviani et al., 2006; Krogh et al., 2014; Green and Thayer, 2016; Zhang and Thayer, 2018). In hypothalamic neurons, IL-1 receptors couple to Src via MyD88-dependent production of ceramide (Davis et al., 2006) and in hippocampal neurons this pathway impairs spine structural remodeling (Tong et al., 2018). IL-1β is pro-convulsive and is thought to mediate some of the seizure promoting effects of inflammation (Rijkers et al., 2009). We have shown previously that following exposure to agents that potentiate NMDARs via Src activation, the synaptic network undergoes a series of adaptive changes over the next 18-24 h (Kim et al., 2008a; Kim et al., 2011; Green and Thayer, 2016; Zhang and Thayer, 2018). These adaptive mechanisms, including loss of excitatory synapses, appear to be part of a homeostatic plasticity mechanism that is not part of the neuronal death process (Shin et al., 2012; Raybuck et al., 2017; Green et al., 2018). We posit that the gp120-induced increase in inhibitory synapses is part of a coping mechanism that occurs during 24 h treatment with agents that potentiate NMDARs. Activation of GluN2A-containing NMDARs appears to regulate synaptic plasticity and be neuroprotective (Liu et al., 2007; Baez et al., 2018), whereas activation of GluN2B-containing NMDARs is associated with neuronal death pathways (Taghibiglou et al., 2009; Tu et al., 2010). The increase in inhibitory synapses was dependent on activation of GluN2A-containing NMDARs and protein synthesis, consistent with previous reports showing that activation of synaptic NMDARs triggers expression of pro-survival genes (Bading, 2017) and the idea that increased synaptic inhibition attenuates excitotoxicity. Thus, synaptic changes may be a mechanism to cope with over activation of NMDARs (Green et al., 2018). This study supports the idea that activation of potentiated GluN2A-containing NMDARs increases inhibitory synapse number as an adaptive mechanism to counteract excess excitation and promote neuronal survival.

Gp120-induced neuroinflammation and subsequent activation of IL-1Rs increases the formation of inhibitory synapses, an adaptive process that might improve neuronal survival at the cost of impaired function. Increased inhibitory tone suppresses long-term potentiation (LTP) in the hippocampus (Arima-Yoshida et al., 2011; Schreurs et al., 2017). Enhanced GABAergic inhibitory signaling is associated with cognitive deficits in many neurodegenerative conditions. For example, excess GABA release from reactive astrocytes impairs memory in mouse models of Alzheimer's disease (Jo et al., 2014) and increased synaptic α2-containing GABA receptors are associated with memory

dysfunction in schizophrenia (Lewis et al., 2004). Excessive inhibition of GABA transporters, a target of some antiepileptic drugs, produces cognitive deficits (Cavanna et al., 2010). Reversing the synaptic adaptations that occur under neuroinflammatory and excitotoxic conditions by recovering lost excitatory synapses and reducing upregulated inhibitory synapses may provide a novel strategy to improve cognitive function (Ryan et al., 2015; Calvo-Flores Guzman et al., 2018). However, if this form of synaptic scaling is a coping mechanism to improve neuronal survival, then it will be important to consider the potential adverse consequences of attenuating this protective mechanism when designing pharmacotherapies.

Inhibition of p38 MAPK in naïve cultures increased the number of inhibitory synapses and activating a mutant form of p38 expressed in hippocampal neurons decreased the number of inhibitory synapses. This is consistent with previous work in rat and mouse hippocampal neurons showing that p38 activated phosphatidylinositol 3-kinase, protein phosphatase 1, and dynamin GTPase to reduce trafficking of $GABA_A$Rs to the cell surface (Pribiag and Stellwagen, 2013). These results indicate that there is basal activation of a p38 MAPK pathway in hippocampal neurons that constrains the number of inhibitory synapses. Medders et al (Medders et al., 2010) conducted an extensive analysis of p38 MAPK activation in a similar mixed neuron-glia co-culture. Consistent with our results they found p38 activated in neurons under basal conditions. They also found that gp120 activated p38 in microglia, possibly as a step in the secretory process. We did not address the role of p38 in microglia although, such a role is not inconsistent with our finding that microglial activation is upstream of the neuronal response. Activation of IL-1Rs stimulates p38 MAPK in hippocampal neurons (Tong et al., 2012). Thus, both p38 MAPK and Src-NMDAR pathways are upregulated and coordinately regulate the number of inhibitory synapses in the presence of gp120. The Src-NMDAR pathway is the dominant signal at the synapse in this condition. It appears that normal homeostatic balance between the two pathways is disrupted under neuroinflammatory conditions.

This report shows for the first time that gp120 increases the number of inhibitory synapses through a neuroinflammatory mechanism initiated by IL-1β. The number of inhibitory synapses is coordinately regulated by both p38 MAPK and Src-NMDAR pathways with the Src-NMDAR pathway dominating under inflammatory conditions. Identifying the mechanisms that control the number of inhibitory synapses provides a better understanding of the pathogenesis of HAND and may guide the development of therapeutics targeting inhibitory signaling during neuroinflammation.

Chapter Four:

Presynaptic GluN2B-Containing NMDARs Regulate Spontaneous Glutamate Release to Control Synaptogenesis

Xinwen Zhang, Stanley A. Thayer*

Department of Pharmacology, University of Minnesota Medical School Minneapolis, MN

Content adapted from manuscript submitted to Journal of Neurophysiology September 2019.

Contributions: XZ and SAT designed the study; XZ performed experiments and collected data; XZ and SAT analyzed data and wrote the manuscript; SAT provided reagents and conceptual advice.

I. Introduction

Synaptic transmission is important for fast information transfer, maintenance of homeostatic network activity, and the development of new synaptic connections (Abbott and Regehr, 2004; Fong et al., 2015; Kavalali, 2015). Evoked neurotransmitter release is the major form of synaptic transmission and occurs when presynaptic action potentials (APs) depolarize the nerve terminal activating voltage-gated Ca^{2+} channels to trigger Ca^{2+}-dependent synchronized-release of neurotransmitter. Spontaneous neurotransmission is independent of presynaptic APs and occurs in an asynchronous manner when a single synaptic vesicle releases its contents from the nerve terminal (Schneggenburger and Rosenmund, 2015). Emerging evidence suggests that spontaneous neurotransmission plays an important role in synaptogenesis (Huntwork and Littleton, 2007; Choi et al., 2014; Ramirez et al., 2017). However, the specific mechanism regulating the spontaneous release of neurotransmitter and how it relates to synapse formation is still not clearly understood.

NMDA receptors (NMDARs) regulate both presynaptic glutamate release and postsynaptic Ca^{2+} influx during spontaneous neurotransmission (Reese and Kavalali, 2016; Abrahamsson et al., 2017). Presynaptic GluN2B-containing NMDARs regulate spontaneous glutamate release in a manner insensitive to Ca^{2+} or Mg^{2+}. Distinct populations of post-synaptic NMDARs are activated by evoked versus spontaneous glutamate release (Atasoy et al., 2008; Reese and Kavalali, 2016), suggesting the two release processes play distinct roles in neuronal networks. Recent work has shown that the frequency of spontaneous glutamate release regulates postsynaptic strength (Crawford et al., 2017). Antagonists for NMDARs stimulate synaptogenesis under certain conditions. For example, blocking GluN2B-containing NMDARs induces recovery in the number of glutamatergic synapses following synapse loss caused by excitotoxic proteins (Shin et al., 2012; Raybuck et al., 2017). The NMDAR antagonist ketamine also induces rapid synaptogenesis in animal models of depression (Ohgi et al., 2015). It is not clear whether the synaptogenic actions of antagonists for GluN2B-containing NMDARs result from inhibition of spontaneous neurotransmitter release.

In this paper, we address the question of whether activation of presynaptic GluN2B-containing NMDARs regulate spontaneous glutamate release and if so, whether their blockade triggers new synapse formation. A genetically encoded ratiometric calcium indicator, GCaMP-6s-R, enabled us to examine both the frequency and amplitude of spontaneous spine calcium transients (SSCTs). Treatment with an antagonist selective

for GluN2B-NMDARs, Ro 25-6981, decreased the frequency but not amplitude of SSCTs, indicating presynaptic regulation of spontaneous neurotransmitter release. Treatment with Ro 25-6981 in the presence of TTX increased in the number of synapses, indicating that SSCTs regulated by presynaptic GluN2B-NMDARs control synapse formation.

II. Materials and Methods

Materials

Materials were obtained from the following sources: (4*R*,6*S*,8*S*,10*Z*,12*R*,14*R*,16*E*,18*R*,19*R*,20*S*,21*S*)-11,19,21-Trihydroxy-4,6,8,12,14,18,20-heptamethyl-22-[(2*S*,2'*R*,5*S*,5'*S*)-octahydro-5'-[(1*R*)-1-hydroxyethyl]-2,5'-dimethyl[2,2'-bifuran]-5-yl]-9-oxo-10,16-docosadienoic acid (ionomycin free acid) (catalog number: 2092); Carbonyl cyanide 4-(trifluoromethoxy)phenylhydrazone (FCCP) (catalog number: 0453); (6a*R*,11a*S*,11b*R*)-*rel*-10-Acetyl-2,6,6a,7,11a,11b-hexahydro-7,7-dimethyl-9*H*-pyrrolo[1',2':2,3]isoindolo[4,5,6-*cd*]indol-9-one (cyclopiazonic acid) (catalog number: 1235); (αR,βS)-α-(4-Hydroxyphenyl)-β-methyl-4-(phenylmethyl)-1-piperidinepropanol maleate (Ro 25-6981 maleate) (catalog number: 1594); D-(-)-2-Amino-5-phosphonopentanoic acid (APV) (catalog number: 0106); tetrodotoxin (TTX) (catalog number: 1069) were from Tocris Bioscience (Bristol, UK). Dulbecco's modified Eagle's medium (DMEM) (catalog number: 31053), Hanks' balanced salt solution (catalog number: 14175), fetal bovine serum (catalog number: 26140), horse serum (catalog number: 16050), and penicillin/streptomycin (catalog number: 15140) came from ThermoFisher Scientific (Carlsbad, CA, USA). The expression plasmid for pCAG-PSD95.FingR-eGFP was generated by Don Arnold's laboratory and obtained from Addgene (catalog number: 46296; Cambridge, MA, USA). The expression plasmid pSyn-tdTomato was generated as previously described (Zhang and Thayer, 2018). The expression plasmid pCaMKII-GCaMP-6s-R was generated by inserting GCaMP-6s-R from pCAG-GCaMP-6s-R kindly provided by Dr Jung-Hwa Cho (University of Southern California, Los Angeles, CA, USA) into the CaMKII backbone of pAAV-CaMKIIa-hChR2(H134R)-EYFP, a gift from Dr. Karl Deisseroth (Addgene, catalog number: 26969).

Primary Hippocampal Culture

All animal care and experimental procedures were carried out according to the Guide for the Care and Use of Laboratory Animals published by the U.S. National Institutes of Health. Ethical approval was granted by the Institutional Animal Care and Use

Committee of the University of Minnesota (protocol 1612-34372A). Primary hippocampal cultures were prepared from fetal Sprague–Dawley rats (RRID:MGI:5651135, Charles River, Wilmington, MA, USA) as previously described (Zhang and Thayer, 2018). All cultures were maintained for 11-14 DIV prior to use in experiments. These cultures contain 24 ± 4% neurons, 55 ± 4% astrocytes, and 13 ± 6% microglia as previously described (Zhang and Thayer, 2018).

Transfection

Cultures were transfected using a previously described calcium phosphate procedure (Zhang and Thayer, 2018). Transfection was performed on DIV 11 or 12. Experiments were started 2–4 days post transfection.

Live Cell Synaptic Imaging and Image Processing

Live cell imaging of synapses was performed as described previously (Zhang and Thayer, 2018). An algorithm written in MetaMorph 7 (RRID:SCR_002368, San Jose, CA, USA) was used to count the number of GFP puncta in an unbiased manner (Waataja et al., 2008; Zhang et al., 2019).

Ca^{2+} Imaging

Ca^{2+} imaging was performed on cells 14-15 DIV and 2-4 days after transfection with pCamKII-GCaMP-6s-R. This tandem construct encodes the Ca^{2+}-sensitive green-fluorescent reporter GCaMP-6s and the calcium-insensitive red fluorescent-protein mCherry linked by a rigid α-helix (Cho et al., 2017). Thus, the ratio of detected green and red fluorescence directly relates to $[Ca^{2+}]_i$. Cover-glasses containing transfected cells were transferred to a recording chamber, placed on the stage of an inverted microscope (Olympus IX71, Melville, NY, USA), and imaged with a 60x oil immersion objective (1.4 numerical aperture). Image series were collected at 10 Hz using a Photometrics Cascade 512B EMCCD camera (Roper Scientific, Tucson, AZ, USA) controlled with MetaMorph software (San Jose, CA, USA). 10 frames were collected on the red channel before and after each 2 min green channel image series. Excitation was provided by two LEDs (Thorlabs, Newton, NJ, USA) combined with a 505 nm dichroic mirror and directed through the epifluorescence port with a collimating lens (Thorlabs, Newton, NJ, USA). The green channel was excited at 490 nm, reflected off a 524 nm dichroic, and emission collected at 507 nm (40 nm band pass). The red channel was excited at 565 nm, reflected off a 640

nm dichroic, and emission collected at 610 nm (60 nm band pass) (Chroma, Vermont, U.S.A). All recordings were conducted at room temperature (21 °C) with the same LED power settings. During experimental recordings, cells were superfused with 1 μM TTX supplemented-Mg^{2+} free artificial cerebrospinal fluid (ACSF) at a rate of 1-2 ml/min for 2 min followed by 1 μM TTX supplemented-Mg^{2+} free ACSF containing drugs or supplemented with Mg^{2+} for 2 min. After background subtraction, the red and green image intensities were converted to green/red ratios and further converted to intracellular Ca^{2+} concentration ($[Ca^{2+}]_i$).

To detect SSCTs, green/red ratios were calculated for regions of interests (ROI) encompassing spontaneous activity during the recording. An SSCT was defined by an increase in the green/red ratio greater than two standard deviations above the average ratio from the previous 2 s and the slope calculated over both previous and current 200 ms windows were greater than 0.15 /s. These criteria allow consideration of baseline changes resulting from bleaching or field drift. All detected peaks were counted to calculate frequency (event/min) and the amplitude further converted to Ca^{2+} concentration.

Calibration of GCaMP-6s-R

Calibration of GCaMP-6s-R expressed in rat hippocampal neurons was performed 48 h after transfection (Fig. 1A). Neurons were sequentially superfused with normal artificial cerebrospinal fluid (ACSF), Ca^{2+}-free ACSF + 1 mM EGTA, Ca^{2+}-free ACSF + 1 mM EGTA supplemented with ionomycin cocktail, 5 mM Ca^{2+} ACSF, and 5 mM Ca^{2+} ACSF supplemented with ionomycin cocktail. The ionomycin cocktail includes ionomycin (Ca^{2+} ionophore, 5 μM), FCCP (uncoupler of mitochondrial oxidative phosphorylation that eliminates the driving force for mitochondria Ca^{2+} uptake, 1 μM) (Baron et al., 2003), and cyclopiazonic acid (SERCA type Ca^{2+}-ATPase inhibitor that blocks Ca^{2+} uptake to sarcoplasmic and endoplasmic reticulum Ca^{2+} stores, 10 μM) (Ghosh et al., 2011; Cho et al., 2017). After background subtraction, the green (GCaMP-6s) and red (mCherry) image pairs were converted to $[Ca^{2+}]_i$ using the formula $[Ca^{2+}]_i = K_d\beta(R - R_{min})/(R_{max} - R)$ (Grynkiewicz et al., 1985). The dissociation constant (K_d) for GCaMP-6s-R was 258 nM (Cho et al., 2017). β is the ratio of fluorescence intensity acquired with mCherry excitation and emission wavelengths measured in Ca^{2+}-free ACSF supplemented with ionomycin cocktail to that measured in 5 mM Ca^{2+} ACSF supplemented with ionomycin cocktail. R is green/red fluorescence intensity ratio. R_{min}, R_{max}, and β were determined in a series of calibration recordings like that shown in Figure 1A. Values for R_{min}, R_{max}, and β were 0.064

± 0.004, 0.72 ± 0.03 and 0.98 ± 0.11, respectively. These calibration constants were applied to all experimental recordings.

Statistics

The distributions of data were determined using D'Agostino-Pearson normality test and homogeneity of variances determined using Bartlett's test; all statistical tests were performed on data of normal distribution with equal variance. For statistical analysis in two-group comparisons, unpaired two-tailed Student's *t*-test was used. For comparison among multiple groups, one-way ANOVA were performed with Tukey's post hoc test. Statistical significance was defined as $p < 0.05$. Sample sizes were not statistically predetermined but conform to similar studies. A test for outliers was performed in Microsoft Excel 2010 (Redmond, WA, USA). Data points that are more than 1.5 times interquartile ranges below the first quartile or above the third quartile were considered as outliers and removed. For imaging of SSCTs, spike amplitude or frequency from all the active spines in the field were averaged and considered as n = 1. For imaging excitatory synapses, the change in PSD95.FingR-eGFP puncta from two to three fields from one dish were averaged as n = 1. Each experiment included data from at least 7 dishes from three to six different platings. PSD95 puncta were counted using an automated image processing algorithm that obviated the need to blind experimenters. No other blinding methods were applied. All data are presented as mean ± SEM. Statistical analyses except for the test for outliers were performed using Prism, GraphPad 7 (La Jolla, CA 92037 USA).

III. Results

Ratiometric GCaMP-6s-R detects NMDAR-mediated SSCTs.

The genetically encoded ratiometric calcium indicator GCaMP-6s-R was used to detect SSCTs. Cells were bathed in Mg^{2+}-free ACSF containing 1 µM TTX to block evoked neurotransmitter release. Dendritic structures were imaged as described in Methods and shown in Figure 1B. Individual dendritic spines were identified in the mCherry image and regions of interest (ROIs) selected manually. Figure 4.1C shows traces from 8 ROIs that exhibited SSCTs and identified in Figure 4.1B by matching colored arrows. In control recordings the SSCT amplitude increased slightly in the second 2 min epoch relative to the first although this trend was not statistically significant (Figure 4.1D). The SSCT frequency was also similar in the first relative to the second epoch (Figure 4.1E control). Superfusion with ACSF containing the NMDAR antagonist APV (50 µM) or ACSF

containing 1 mM Mg^{2+} completely blocked the SSCTs (Figure 4.1C and E), indicating that the detected events are mediated by NMDARs.

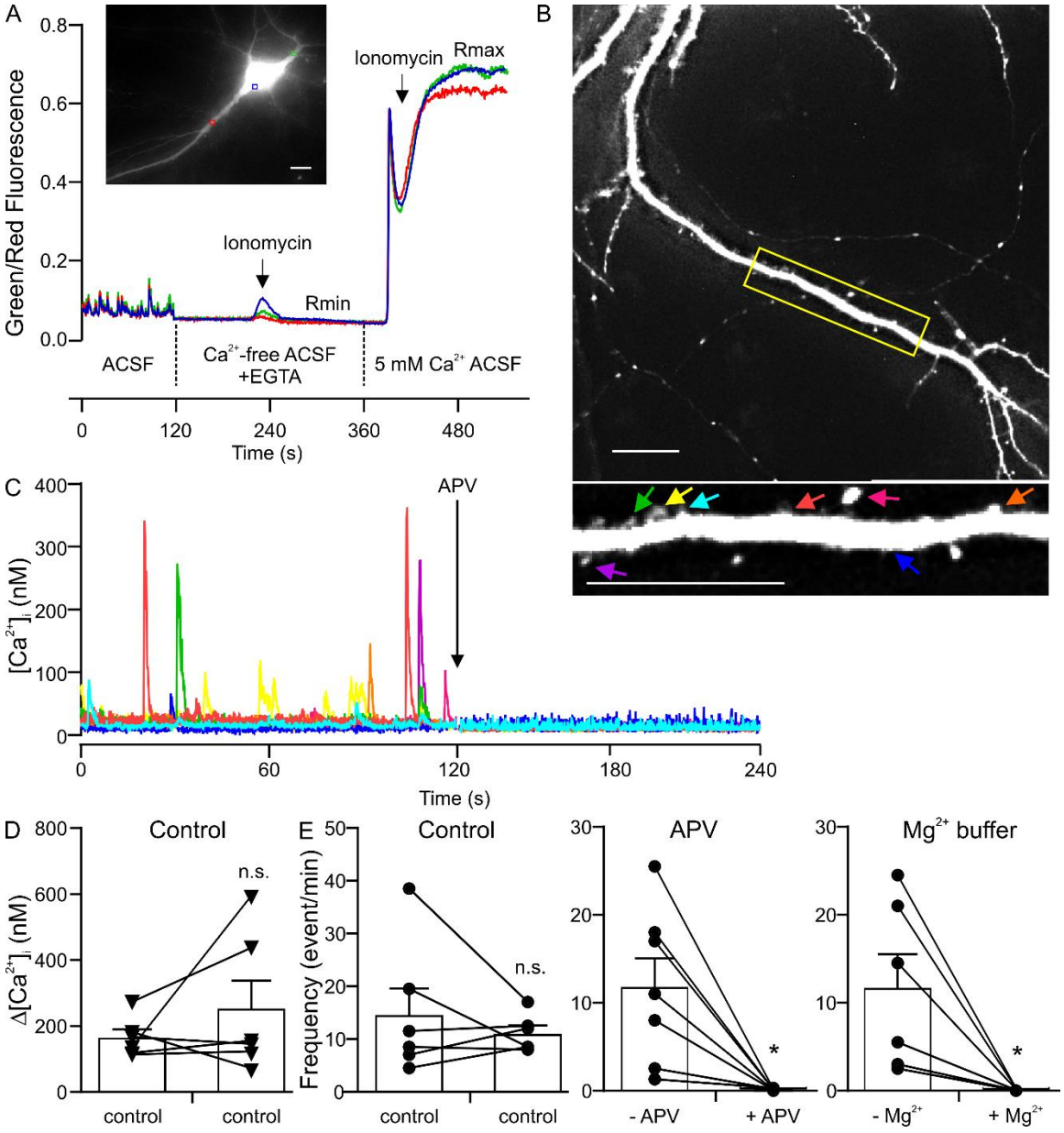

Figure 4.1 Ratiometric GCaMP-6s-R detects NMDAR-mediated SSCTs. (A) Representative traces show calibration of ratiometric GCaMP-6s-R. Hippocampal neurons were bathed in modified ACSF as indicated. Ionomycin cocktail (final concentrations: 5 µM ionomycin, 1 µM FCCP and 10 µM cyclopiazonic acid) was applied directly to a static bath at the times indicated by the arrows. R_{min} and R_{max} were determined from the lowest and highest $[Ca^{2+}]_i$, respectively. Inset shows ROIs color coded to match traces overlaid on red channel image. (B) Representative red channel image of a neuron expressing GCaMP-6s-R. Inset is enlarged image of the boxed region. Arrows placed over active spines for analysis are color-coded to corresponding traces in C. Scale bars represent 10 µm. (C) Representative traces indicating amplitude and frequency changes of SSCTs before and after perfusion with 50 µM APV (arrow) for the spines labeled in Figure 1B. (D) Bar graph and trend lines indicating changes in amplitude of SSCTs for the same field perfused with control ACSF (paired two-tailed *t*-test; $t_{(5)} = 1.1$, $p = 0.33$, $n = 6$; data from three independent culture preparations). (E) Bar graphs and trend lines indicating changes

in the frequency of SSCTs before and after perfusion with control ACSF (paired two-tailed *t*-test; $t_{(5)} = 0.91$, $p = 0.41$, $n = 6$; data from three independent culture preparations), and ACSF containing 50 µM APV (paired two-tailed *t*-test; $t_{(6)} = 3.5$, $p = 0.013$, $n = 7$; data from three independent culture preparations) or supplemented with 1 mM Mg^{2+} (paired two-tailed *t*-test; $t_{(5)} = 3.0$, $p = 0.03$, $n = 6$; data from three independent culture preparations). Data are expressed as mean ± SEM. *$p < 0.05$, **$p < 0.01$, compared with the same fields before treatments (paired two-tailed Student's *t*-test, *n* = number of individual dishes in each group).

SSCTs are regulated by GluN2B-containing NMDARs

To determine the subtype of NMDARs controlling SSCTs, Ro 25-6981, a potent and selective antagonist of GluN2B-containing NMDARs was added to the extracellular solution (Mg^{2+}-free ACSF containing 1 µM TTX) (Fischer et al., 1997). SSCTs for the same dendritic structure were imaged and analyzed for changes in frequency and amplitude before and after treatment with 0.1 µM Ro 25-6981. Representative traces for ROIs of all active spines in an individual field are shown in Figure 4.2A. Event frequency and amplitude of SSCTs calculated for 7 recordings are shown before and after application of 0.1 µM Ro 25-6981 (Figure 4.2B-C). Ro 25-6981 (0.1 µM) significantly decreased the event frequency by 49 ± 10% but did not significantly affect the amplitude (net change in $[Ca^{2+}]_i$) of the SSCTs. A change in event frequency without affecting amplitude is consistent with a presynaptic site of action. To further test this possibility, the concentration-response relationship for Ro 25-6981 was determined using the same approach. Various concentrations of Ro 25-6981 (0, 0.1, 1, 10 µM) were applied to neurons exhibiting SSCTs and changes in frequency and amplitude determined. Ro 25-6981 produced a concentration dependent inhibition of SSCT frequency with an IC_{50} of 0.21 µM, in good agreement with the reported IC_{50} of 0.4 µM for Ro 25-6981 inhibition of glutamate neurotoxicity (Fischer et al., 1997). Ro 25-6981 at the highest concentration (10 µM) blocked 88 % of the spontaneous SSCT events, suggesting that presynaptic GluN2B NMDARs regulate these events. Ro 25-6981 did not significantly affect the amplitude of SSCTs at any concentration tested (Figure 4.2D). These results are consistent with presynaptic inhibition of glutamate release in the absence of postsynaptic action.

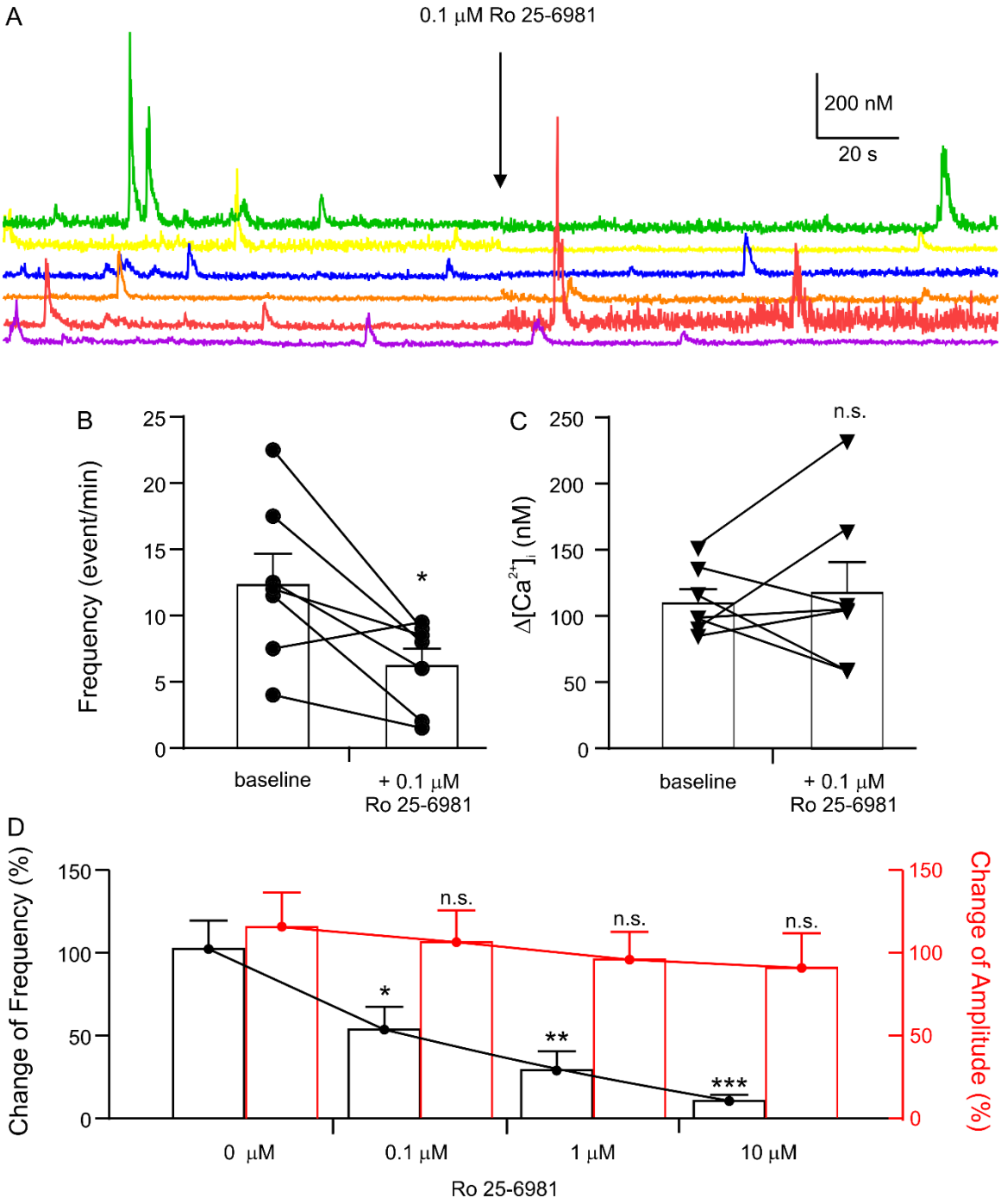

Figure 4.2 Ro 25-6981 reduces the frequency but not amplitude of SSCTs. (A) Representative traces showing SSCTs before and after perfusion of 0.1 μM Ro 25-6981. (B-C) Bar graphs and trend lines indicating reduced frequency (B) (paired two-tailed *t*-test; $t_{(6)}$ = 3.1, *p* = 0.021, *n* = 7; data from six independent culture preparations) but not amplitude (C) (paired two-tailed *t*-test; $t_{(6)}$ = 0.39, *p* = 0.71, *n* = 7; data from six independent culture preparations) of SSCTs by treatment with 0.1 μM Ro 25-6981. (D) Bar graphs indicating dose-dependent change in the frequency (One-way ANOVA; $F_{(3,24)}$ = 10.42, *p* = 0.0001, *n* = 7 for each group; data from six independent culture preparations) but not amplitude (One-way ANOVA; $F_{(3,24)}$ = 0.52, *p* = 0.68, *n* = 7 for each group; data from six

independent culture preparations) of SSCTs after treatment with the indicated concentrations of Ro 25-6981. Data are expressed as mean ± SEM. Unpaired two-tailed Student's *t*-test or One-way ANOVA followed by Tukey's *post hoc* test, **p* < 0.05, ***p* < 0.01, ****p* < .001 compared with control (0 µM Ro 25-6981 treatment) (*n* = number of individual dishes in each group).

Inhibition of presynaptic GluN2B-containing NMDARs increases the number of synaptic connections when evoked release is blocked

Previous studies from our lab have demonstrated that blocking GluN2B-containing NMDARs with the selective antagonist ifenprodil induces recovery of synaptic connections lost during exposure to a neurotoxic protein (Shin et al., 2012; Raybuck et al., 2017). Furthermore, Crawford et al. (2017) have shown that blocking spontaneous glutamate release when evoked release is also blocked will increase synaptic strength. Because Ro 25-6981 inhibited spontaneous glutamate release (Figure 4.2), we examined whether this drug might stimulate synaptogenesis under conditions in which evoked neurotransmitter release is blocked. To detect changes in the number of synapses, cells were transfected with expression plasmids for an eGFP-tagged recombinant antibody-like protein (PSD95.FingR-eGFP) to selectively label the post-synaptic density of excitatory synapses and a red fluorescent protein (tdTomato) to fill the cell structure. The number of labeled synapses was determined using an algorithm that counted fluorescent puncta that met size and intensity thresholds and were in contact with a mask derived from the tdTomato image (Waataja et al., 2008). PSD95.FingR-eGFP was previously shown to label functional synapses (Zhang and Thayer, 2018) enabling this live-cell imaging-based assay to track the number of synapses on the same neuron over time. The number of synaptic connections in untreated cultures (control) and cultures treated with 1 µM TTX did not change significantly over 24 h (Figure 4.3A-B). Treatment with the combination of 1 µM TTX and 10 µM Ro 25-6981 for 24 h increased the number of synapses by 15 ± 6 % which was significantly different compared to control which decreased by 6 ± 5 % (Figure 4.3A-B). In a separate cohort of cells, treatment with 10 µM Ro 25-6981 alone did not increase the number of synapses (Figure 4.3C). These data indicate that blocking presynaptic GluN2B-containing NMDARs when evoked neurotransmitter release is also blocked stimulates new synapse formation.

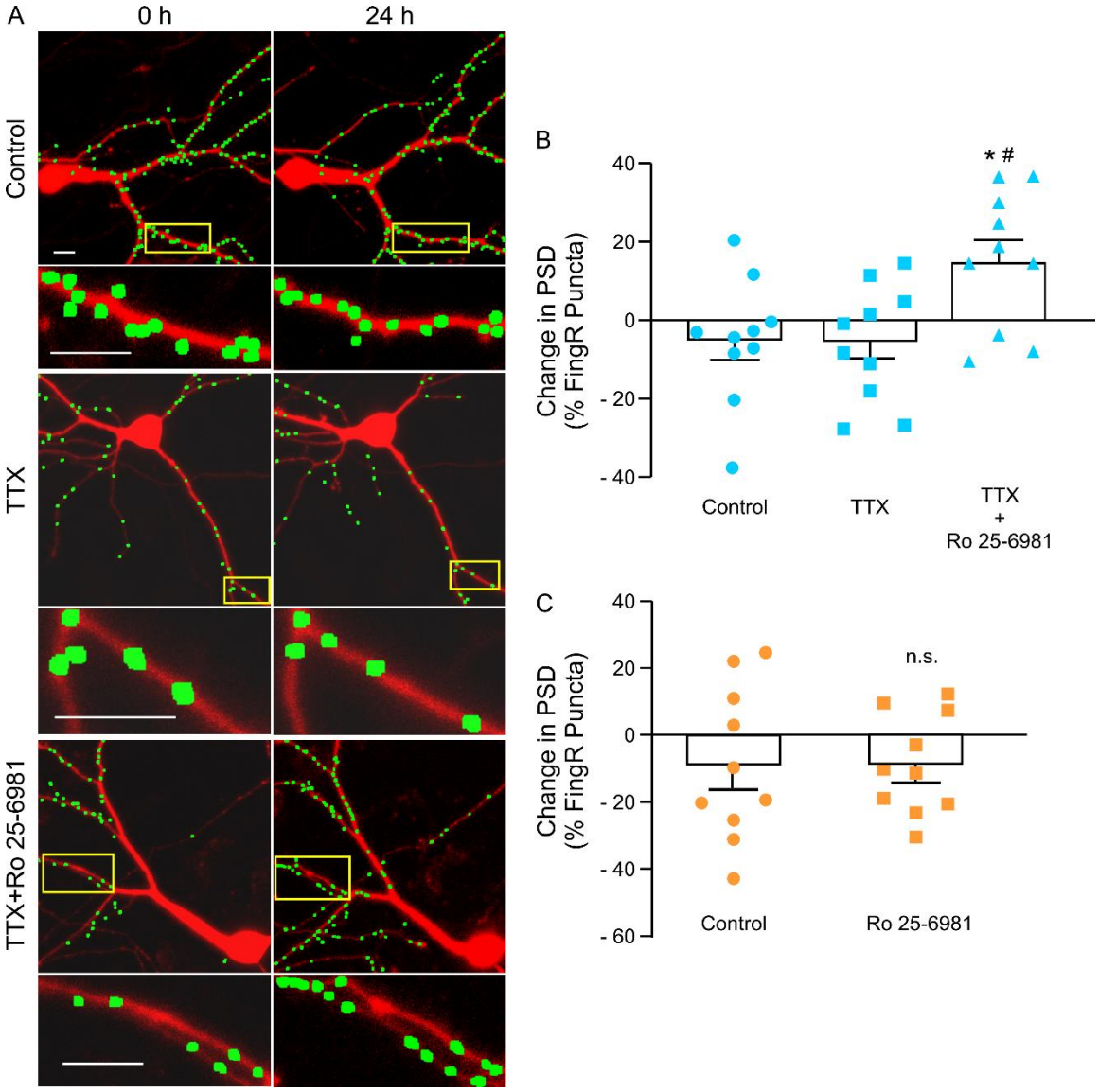

Figure 4.3 Treatment with Ro 25-6981 in the presence of TTX increased the number of excitatory synapses. (A) Representative processed confocal images showing neurons before (0 h) and after no treatment (control) or treatment with either 1 µM TTX or both TTX and 10 µM Ro 25-6981 for 24 h. The images are processed as described in Materials and Methods. Identified PSD95 puncta (green) are dilated and overlaid on the tdTomato maximum projection images for display purposes. Insets are enlarged images of the boxed regions. Scale bars represent 10 µm. (B) Treatment with 10 µM Ro 25-6981 in the presence of 1 µM TTX increased the number of intrabody-labeled PSD95 puncta (One-way ANOVA; $F_{(2,27)}$ = 5.5, p = 0.01, n = 10 for each group; data from three independent culture preparations). (C) Treatment with 10 µM Ro 25-6981 alone does not influence the number of PSD95 puncta (unpaired two-tailed t-test; $t_{(20)}$ = 0.18, p = 0.86, n = 11; data from three independent culture preparations). Data are expressed as mean ± SEM. Unpaired two-tailed Student's t-test or One-way ANOVA followed by Tukey's *post hoc* test, *p < 0.05 compared with control; #p < 0.05 compared with TTX treated group (n = number of individual dishes in each group).

IV. Discussion

Spontaneous neurotransmission regulates synaptic strength and during development controls synapse formation (Crawford et al., 2017; Ramirez et al., 2017; Andreae and Burrone, 2018). Ro 25-6981, an antagonist for GluN2B-containing NMDARs, reduces spontaneous and evoked glutamate release in visual cortex, although via different signaling mechanisms (Abrahamsson et al., 2017). In this study, we examined the role of GluN2B-containing NMDARs in regulating SSCTs and synaptogenesis. We found that presynaptic GluN2B-containing NMDARs regulate the spontaneous release of glutamate, and that blocking these receptors initiates the formation of new synapses.

This imaging-based study used state of the art genetically encoded fluorescent reporter proteins to quantify SSCTs and the number of synapses. The structure of GCaMP-6s-R links the Ca^{2+} indicator GCaMP-6s to Ca^{2+}-insensitive mCherry (Cho et al., 2017). Thus, the ratio of green to red fluorescence intensity is related to $[Ca^{2+}]_i$ in a manner that is independent of the expression level of the indicator and thickness of the sample. This indicator enabled accurate quantification of the amplitude of SSCTs providing a method to show that Ro 25-6891 affected the frequency of spontaneous events but not the amplitude of the $[Ca^{2+}]_i$ transients. This presynaptic role for GluN2B-containing NMDARs is consistent with studies in visual cortex (Abrahamsson et al., 2017) and the lack of postsynaptic effects of Ro 25-6891 in hippocampal cultures may result from the developmental switch from GluN2B- to GluN2A-containing NMDARs in the postsynaptic density (Stocca et al., 2008). We used a recombinant antibody-like protein, PSD95.FingR-eGFP, to label post-synaptic density protein PSD95 as a method to track changes in the number of functional excitatory synapses in live cells (Gross et al., 2013; Zhang and Thayer, 2018). This method allowed visualization of synaptic sites before and after treatments that blocked evoked and spontaneous glutamate release. Only when evoked and spontaneous glutamate were both inhibited did a significant increase in synaptic number occur.

The observation that new synapses form when glutamatergic synaptic transmission is inhibited is consistent with a form of homeostatic scaling (Keck et al., 2017). Modulation of spontaneous glutamate release has been implicated in this form of plasticity (Kavalali, 2015) and is consistent with studies that found selective block of spontaneous neurotransmission induced potentiation of glutamatergic synaptic strength (Nosyreva et al., 2013; Crawford et al., 2017; Ramirez et al., 2017). However, our results differ from these studies in that only when evoked glutamate release was blocked with

TTX did Ro 25-6891 stimulate new synapse formation. This difference may be due to different mechanisms strengthening existing synapses versus stimulating the formation of new connections. Blocking evoked neurotransmission with TTX will induce upscaling under certain conditions (Hargus and Thayer, 2013), although the 24 h treatment used in this study did not induce synapse formation. Spontaneous neurotransmitter release plays a different role in maintaining synaptic homeostasis in established networks from its role in building new networks. During development spontaneous neurotransmitter release enhances the elaboration of dendritic arbors and is required for the development of normal axon terminals (Andreae et al., 2012; Andreae and Burrone, 2015). These roles are contrary to the results described here and in other studies of mature neurons (Li et al., 2010; Autry et al., 2011; Kavalali and Monteggia, 2012; Nosyreva et al., 2014). Clearly, there are multiple mechanisms to maintain synaptic homeostasis with distinct processes participating under various conditions.

The possibility that impaired spontaneous synaptic transmission is necessary for stimulating new synapse formation by antagonists of GluN2B-containing NMDARs may be important in certain disease states. Decreased synapse density correlates with symptom severity in depressed human subjects and with cognitive decline in several neurodegenerative diseases (Ellis et al., 2007; Serrano-Pozo et al., 2011; Holmes et al., 2019). In animal models, antagonists for GluN2B-containing NMDARs increase spine density and reverse cognitive impairment and depression-like behaviors (Miller et al., 2014; Raybuck et al., 2017). Blocking spontaneous neurotransmission may underlie the synaptic potentiation and fast antidepressant effects produced by ketamine (Autry et al., 2011; Nosyreva et al., 2013). In a mouse model of HIV-associated neurocognitive disorder, the synapse loss and cognitive impairment induced by the HIV protein Tat was reversed by ifenprodil, an antagonist for GluN2B-containing NMDARs (Shin et al., 2012; Raybuck et al., 2017). Interestingly, in the absence of neuropsychiatric impairment, antagonists for GluN2B-containing NMDARs do not stimulate synapse formation or improve cognition (Raybuck et al. 2017). Thus, the synaptogenic actions of antagonists for GluN2B-containing NMDARs are enhanced when evoked synaptic transmission is impaired. Perhaps an enhanced role of spontaneous neurotransmitter release under this condition accounts for this state-dependent pharmacology.

In summary, we have shown that inhibition of presynaptic GluN2B-containing NMDARs, under conditions where evoked glutamate release is blocked, stimulates new synapse formation in an established synaptic network. We speculate that targeted

inhibition of these presynaptic receptors when neuropathology impairs normal evoked neurotransmission, might restore synaptic density.

Chapter Five: Concluding Remarks

I. Summary of current studies

The studies described in this dissertation expand our understanding of gp120-induced changes in excitatory and inhibitory synapses using primary cultured hippocampal cells and demonstrated that modulation of the eCB system and NMDAR subtypes have therapeutic potentials for protecting neuronal function in HAND. HIV gp120-caused excitatory synapse loss has previously been described (Kim et al., 2011). In the second chapter, I further demonstrated that gp120-induced activation of microglia and release of IL-1β potentiates NMDAR-mediated Ca^{2+} influx leading to loss of excitatory synapses. Inhibition of MGL of the eCB system was previously shown to enhance 2-AG levels decreasing neuroinflammation (Nomura et al., 2011; Kerr et al., 2013). I showed that pharmacological inhibition of MGL using the selective inhibitor JZL184 blocked gp120-induced release of IL-1β and loss of excitatory synapses. Blocking MGL suppress gp120-mediated neuroinflammation through both activation of CB2Rs and decreased production of PGE_2 (Zhang and Thayer, 2018).

Excitatory synapse loss induced by HIV neurotoxins occurs through pathways distinct from those leading to neuronal death (Kim et al., 2008b); we previously speculated that this type of functional loss can be part of an overactivated coping mechanism to maintain network homeostasis (Kim et al., 2008b; Shin et al., 2012; Shin and Thayer, 2013). Balance between excitatory and inhibitory synapses is also part of neuronal homeostasis (Liu, 2004; Turrigiano, 2012) and is important for maintaining normal cognitive function (Nelson and Valakh, 2015; Zorrilla de San Martin et al., 2018). Few studies have focused on HIV neurotoxin-induced changes in inhibitory synapses (Fitting et al., 2013; Hargus and Thayer, 2013; Green and Thayer, 2019). In chapter three, I discovered that gp120 increased the number of inhibitory synapses through microglial activation and subsequent release of IL-1β. GluN2A NMDARs mediate the change and overcome the p38 MAPK regulated suppression of inhibitory synapse density.

The work in chapter three and previous studies indicate that GluN2A-containing NMDARs are involved in HIV neurotoxin-induced loss of excitatory and increase in inhibitory synapse number (Shin et al., 2012; Hargus and Thayer, 2013; Zhang et al., 2019). This led me to investigate the role of subtypes of NMDARs in synaptogenesis. In chapter four, I discovered that presynaptic GluN2B-containing NMDARs regulates spontaneous release of glutamate and that inhibition of these presynaptic NMDARs

induces synaptogenesis. This work provides new insights on targeting NMDAR subtypes for development of neuroprotective agents.

II. Advantages and limitations of current study

In the second and third chapter, I utilized a live cell imaging-based assay to track the number of excitatory and inhibitory synapses in cultured hippocampal neurons during treatments. This technique was established and demonstrated to label functional synapses by previous work from our lab (Kim et al., 2008b; Kim et al., 2011; Shin et al., 2012; Hargus and Thayer, 2013). In the current studies, I updated the assay by incorporating a fluorescent recombinant antibody-like protein (intrabody) to bind to and label the endogenous excitatory and inhibitory post-synaptic scaffolding proteins PSD95 and gephyrin, instead of using fusion proteins that introduce exogenous production of these proteins (Gross et al., 2013). This technique has several advantages. First, it allows the experiments to be performed on living neurons. To investigate changes in the number of excitatory and inhibitory post-synaptic densities, cultures or tissues are usually fixed to allow immunolabeling of relevant proteins (Ellis et al., 2007); comparisons need to be made between different neurons receiving different treatments. Our assay allows direct comparison of the same cell before and after treatments. Additionally, an automated algorithm to count the number of labeled excitatory and inhibitory synapses was applied in our assay. This allows experimenters to be blinded during the data analysis. Third, the use of intrabody avoided potential increase of synapse number driven by expression of exogenous fusion proteins and was demonstrated to label functional excitatory and inhibitory synapses by immunocytochemistry and electrophysiological assays (Gross et al., 2013; Zhang and Thayer, 2018; Zhang et al., 2019). Thus, this assay is a powerful tool to understand the signaling pathways that modulate synaptic changes.

In the fourth chapter, I developed a spine calcium imaging assay that employs a ratiometric genetically-encoded Ca^{2+} indicator, GCaMP-6s-R. Compared to traditionally used non-ratiometric genetically-encoded Ca^{2+} indicators such as GCaMP-6s, this indicator allows detecting both amplitude and frequency changes in spine calcium transients before and after treatments. Imaging of NMDAR-mediated spontaneous spine calcium transients gives a direct visualization of release events occurring at individual spines providing both spatial and temporal information not acquired with conventional electrophysiology methods.

These studies, however, have limitations. Primary hippocampal cultures provide a simple and easily accessible system to probe and explore detailed signaling pathways for gp120-induced synaptic changes. The simple system does not incorporate properties of whole animal models or signaling unique to the human species. Thus, the findings need to be confirmed *in vivo*. In fact, previous studies from our lab have confirmed successful translation of *in vitro* work to *in vivo* (Raybuck et al., 2017). Furthermore, the current study focuses on gp120 and uses 600 pM of the protein for treatments. This concentration, although consistent with what is used in other studies (Meucci and Miller, 1996; Viviani et al., 2001; Viviani et al., 2006; Medders et al., 2010), may not mimic the real concentration of gp120 in brains of HAND patients which is currently not known. Thus, although the current study of gp120-induced release of IL-1β model largely mimics neuroinflammation in HIV patients (Xing et al., 2009; Walsh et al., 2014), more studies are needed to confirm the clinical relevance of the model.

III. Future directions and therapeutic potential of targeting the eCB system and NMDARs

More work is needed to fully discover the complete mechanisms for synaptodendritic damage-induced by HIV viral proteins and pro-inflammatory factors. Current studies uncovered changes in number of excitatory and inhibitory synapses as part of a potential homeostatic plasticity mechanism to counterbalance enhanced excitation. Whether other forms of coping mechanisms such as synaptic scaling to regulate the strength of individual synapses and regulation of intrinsic excitability are involved, and how these processes are coordinately controlled leading to loss of cognitive function need to be further investigated. Whether increases in inhibitory synapses correlate with cognitive dysfunction remains unclear and its clinical relevance needs to be established in human and animal models. Additionally, if loss of excitatory synapses is part of a survival mechanism for neurons, whether blocking this process and inducing recovery renders neurons more vulnerable to death need to be cautiously studied for developing therapeutic strategies. Whether there is a threshold for homeostatic adjustment of synapses, which is sufficient to counteract excessive excitation and support neuronal survival but also avoids loss of network function-associated with synapse loss, is important for future research.

Inhibition of MGL enhances CB2R activation and decreases PGE_2 production suggesting eCB system as a target to reduce neuroinflammation in HIV patients. Inhibition

of MGL was specifically associated with protection of excitatory synapses in the current studies, and this same drug treatment induced excitatory synapses recovery improving cognitive function in an Alzheimer's disease animal model (Chen et al., 2012). In fact, increased expression of CB2Rs in HIV-infected individuals (Benito et al., 2005; Cosenza-Nashat et al., 2011) and elevated PGE_2 levels in HIV-infected animal models (Blanchard et al., 2015) are reported; these reports further support the therapeutic potential of MGL inhibition. A highly potent, orally available MGL inhibitor, ABX-1431, is currently being investigated in a phase II trial for treatment of Tourette Syndrome suggesting this class of drugs is well-tolerated (ClinicalTrials.gov Identifier: NCT03625453). Furthermore, this type of drug provides "on-demand" neuroprotection and enhances the function of endogenous 2-AG, and thus, likely produces fewer psychoactive side effects compared to conventional cannabinoid receptor agonists. Despite that, potential side effects still needed to be cautiously studied.

Inhibition of GluN2A NMDARs blocks the loss of excitatory and the increase of inhibitory synapses; blocking GluN2B NMDARs induces regeneration of excitatory synapses. These studies suggest subtype specific differences in NMDARs that influences their potential roles in HAND. Current studies provide an initial insight to the function of presynaptic GluN2B NMDARs in synaptogenesis. Whether this is the underlying mechanism for GluN2B inhibitor-mediated synapse recovery under HIV neurotoxin-treated conditions needs to be investigated. The accurate pre-and post-synaptic locations of GluN2B and GluN2A NMDARs in hippocampus and their therapeutic roles need to be studied and confirmed in whole animal models and humans eventually.

In conclusion, studies in this dissertation expanded our mechanistic understanding of synaptic changes-induced by HIV gp120 and provides novel views for modulation of synaptic changes in HAND highlighting the eCB system and NMDAR subtypes as promising future directions for the development of neuroprotective agents.

Chapter Six: Bibliography

Abbott LF, Regehr WG (2004) Synaptic computation. Nature 431:796-803.

Abrahamsson T, Chou CYC, Li SY, Mancino A, Costa RP, Brock JA, Nuro E, Buchanan KA, Elgar D, Blackman AV, Tudor-Jones A, Oyrer J, Farmer WT, Murai KK, Sjostrom PJ (2017) Differential Regulation of Evoked and Spontaneous Release by Presynaptic NMDA Receptors. Neuron 96:839-855 e835.

Adle-Biassette H, Chretien F, Wingertsmann L, Hery C, Ereau T, Scaravilli F, Tardieu M, Gray F (1999) Neuronal apoptosis does not correlate with dementia in HIV infection but is related to microglial activation and axonal damage. Neuropathol Appl Neurobiol 25:123-133.

Albert SM, Martin EM (2014) HIV and the neuropsychology of everyday life. Neurology 82:2046-2047.

Alter G, Heckerman D, Schneidewind A, Fadda L, Kadie CM, Carlson JM, Oniangue-Ndza C, Martin M, Li B, Khakoo SI, Carrington M, Allen TM, Altfeld M (2011) HIV-1 adaptation to NK-cell-mediated immune pressure. Nature 476:96-100.

Andreae LC, Burrone J (2015) Spontaneous Neurotransmitter Release Shapes Dendritic Arbors via Long-Range Activation of NMDA Receptors. Cell Rep 10:873-882.

Andreae LC, Burrone J (2018) The role of spontaneous neurotransmission in synapse and circuit development. J Neurosci Res 96:354-359.

Andreae LC, Fredj NB, Burrone J (2012) Independent vesicle pools underlie different modes of release during neuronal development. J Neurosci 32:1867-1874.

Anthony IC, Ramage SN, Carnie FW, Simmonds P, Bell JE (2005) Influence of HAART on HIV-related CNS disease and neuroinflammation. J Neuropathol Exp Neurol 64:529-536.

Antinori A et al. (2007) Updated research nosology for HIV-associated neurocognitive disorders. Neurology 69:1789-1799.

Appay V, Sauce D (2008) Immune activation and inflammation in HIV-1 infection: causes and consequences. The Journal of pathology 214:231-241.

Arima-Yoshida F, Watabe AM, Manabe T (2011) The mechanisms of the strong inhibitory modulation of long-term potentiation in the rat dentate gyrus. Eur J Neurosci 33:1637-1646.

Arrildt KT, Joseph SB, Swanstrom R (2012) The HIV-1 env protein: a coat of many colors. Curr HIV/AIDS Rep 9:52-63.

Ashraf T, Jiang W, Hoque MT, Henderson J, Wu C, Bendayan R (2014) Role of anti-inflammatory compounds in human immunodeficiency virus-1 glycoprotein120-mediated brain inflammation. J Neuroinflammation 11:91.

Atasoy D, Ertunc M, Moulder KL, Blackwell J, Chung C, Su J, Kavalali ET (2008) Spontaneous and Evoked Glutamate Release Activates Two Populations of NMDA Receptors with Limited Overlap. J Neurosci 28:10151-10166.

Autry AE, Adachi M, Nosyreva E, Na ES, Los MF, Cheng P-f, Kavalali ET, Monteggia LM (2011) NMDA receptor blockade at rest triggers rapid behavioural antidepressant responses. Nature 475:91-95.

Avdoshina V, Taraballi F, Dedoni S, Corbo C, Paige M, Saygideger Kont Y, Uren A, Tasciotti E, Mocchetti I (2016) Identification of a binding site of the human immunodeficiency virus envelope protein gp120 to neuronal-specific tubulin. Journal of neurochemistry 137:287-298.

Avraham HK, Jiang S, Fu Y, Rockenstein E, Makriyannis A, Zvonok A, Masliah E, Avraham S (2014) The cannabinoid CB(2) receptor agonist AM1241 enhances neurogenesis in GFAP/Gp120 transgenic mice displaying deficits in neurogenesis. Br J Pharmacol 171:468-479.

Bading H (2017) Therapeutic targeting of the pathological triad of extrasynaptic NMDA receptor signaling in neurodegenerations. J Exp Med 214:569-578.

Baez MV, Cercato MC, Jerusalinsky DA (2018) NMDA Receptor Subunits Change after Synaptic Plasticity Induction and Learning and Memory Acquisition. Neural Plast 2018:5093048.

Bagetta G, Corasaniti MT, Berliocchi L, Nistico R, Giammarioli AM, Malorni W, Aloe L, Finazzi-Agro A (1999) Involvement of interleukin-1beta in the mechanism of human immunodeficiency virus type 1 (HIV-1) recombinant protein gp120-induced apoptosis in the neocortex of rat. Neuroscience 89:1051-1066.

Baier T, Neuwirth E (2007) Excel :: COM :: $$\mathsf{R}$$. Computational Statistics 22:91-108.

Baldewicz TT, Leserman J, Silva SG, Petitto JM, Golden RN, Perkins DO, Barroso J, Evans DL (2004) Changes in neuropsychological functioning with progression of HIV-1 infection: results of an 8-year longitudinal investigation. AIDS Behav 8:345-355.

Baron KT, Wang GJ, Padua RA, Campbell C, Thayer SA (2003) NMDA-evoked consumption and recovery of mitochondrially targeted aequorin suggests

increased Ca2+ uptake by a subset of mitochondria in hippocampal neurons. Brain Res 993:124-132.

Bellizzi MJ, Lu SM, Gelbard HA (2006) Protecting the synapse: evidence for a rational strategy to treat HIV-1 associated neurologic disease. J Neuroimmune Pharmacol 1:20-31.

Benito C, Tolon RM, Pazos MR, Nunez E, Castillo AI, Romero J (2008) Cannabinoid CB2 receptors in human brain inflammation. Br J Pharmacol 153:277-285.

Benito C, Kim W-K, Chavarria I, Hillard CJ, Mackie K, Tolon RM, Williams K, Romero J (2005) A Glial Endogenous Cannabinoid System Is Upregulated in the Brains of Macaques with Simian Immunodeficiency Virus-Induced Encephalitis. J Neurosci 25:2530-2536.

Berger EA, Murphy PM, Farber JM (1999) Chemokine receptors as HIV-1 coreceptors: roles in viral entry, tropism, and disease. Annual review of immunology 17:657-700.

Bezzi P, Domercq M, Brambilla L, Galli R, Schols D, De Clercq E, Vescovi A, Bagetta G, Kollias G, Meldolesi J, Volterra A (2001) CXCR4-activated astrocyte glutamate release via TNFa: amplification by microglia triggers neurotoxicity. Nature neuroscience 4:702-710.

Blanchard HC, Taha AY, Rapoport SI, Yuan ZX (2015) Low-dose aspirin (acetylsalicylate) prevents increases in brain PGE2, 15-epi-lipoxin A4 and 8-isoprostane concentrations in 9 month-old HIV-1 transgenic rats, a model for HIV-1 associated neurocognitive disorders. Prostaglandins Leukot Essent Fatty Acids 96:25-30.

Blankman JL, Cravatt BF (2013) Chemical probes of endocannabinoid metabolism. Pharmacological reviews 65:849-871.

Blankman JL, Simon GM, Cravatt BF (2007) A comprehensive profile of brain enzymes that hydrolyze the endocannabinoid 2-arachidonoylglycerol. Chem Biol 14:1347-1356.

Bliss TV, Collingridge GL (1993) A synaptic model of memory: long-term potentiation in the hippocampus. Nature 361:31-39.

Bollinger RC, Brookmeyer RS, Mehendale SM, Paranjape RS, Shepherd ME, Gadkari DA, Quinn TC (1997) Risk factors and clinical presentation of acute primary HIV infection in India. Jama 278:2085-2089.

Bonavia R, Bajetto A, Barbero S, Pirani P, Florio T, Schettini G (2003) Chemokines and their receptors in the CNS: expression of CXCL12/SDF-1 and CXCR4 and their role in astrocyte proliferation. Toxicol Lett 139:181-189.

Brack-Werner R (1999) Astrocytes: HIV cellular reservoirs and important participants in neuropathogenesis. AIDS 13:1-22.

Brelot A, Heveker N, Pleskoff O, Sol N, Alizon M (1997) Role of the first and third extracellular domains of CXCR-4 in human immunodeficiency virus coreceptor activity. J Virol 71:4744-4751.

Brindisi M et al. (2016) Development and Pharmacological Characterization of Selective Blockers of 2-Arachidonoyl Glycerol Degradation with Efficacy in Rodent Models of Multiple Sclerosis and Pain. J Med Chem 59:2612-2632.

Busillo JM, Benovic JL (2007) Regulation of CXCR4 signaling. Biochimica et biophysica acta 1768:952-963.

Cabral GA, Griffin-Thomas L (2009) Emerging role of the cannabinoid receptor CB2 in immune regulation: therapeutic prospects for neuroinflammation. Expert Rev Mol Med 11:e3.

Calvo-Flores Guzman B, Vinnakota C, Govindpani K, Waldvogel HJ, Faull RLM, Kwakowsky A (2018) The GABAergic system as a therapeutic target for Alzheimer's disease. Journal of neurochemistry.

Cavanna AE, Ali F, Rickards HE, McCorry D (2010) Behavioral and cognitive effects of anti-epileptic drugs. Discov Med 9:138-144.

Chen B (2019) Molecular Mechanism of HIV-1 Entry. Trends Microbiol.

Chen MF, Gill AJ, Kolson DL (2014) Neuropathogenesis of HIV-associated neurocognitive disorders: roles for immune activation, HIV blipping and viral tropism. Curr Opin HIV AIDS 9:559-564.

Chen R, Zhang J, Wu Y, Wang D, Feng G, Tang YP, Teng Z, Chen C (2012) Monoacylglycerol lipase is a therapeutic target for Alzheimer's disease. Cell Rep 2:1329-1339.

Cho JH, Swanson CJ, Chen J, Li A, Lippert LG, Boye SE, Rose K, Sivaramakrishnan S, Chuong CM, Chow RH (2017) The GCaMP-R Family of Genetically Encoded Ratiometric Calcium Indicators. ACS Chem Biol 12:1066-1074.

Choi BJ, Imlach WL, Jiao W, Wolfram V, Wu Y, Grbic M, Cela C, Baines RA, Nitabach MN, McCabe BD (2014) Miniature neurotransmission regulates Drosophila synaptic structural maturation. Neuron 82:618-634.

Churchill MJ, Gorry PR, Cowley D, Lal L, Sonza S, Purcell DF, Thompson KA, Gabuzda D, McArthur JC, Pardo CA, Wesselingh SL (2006) Use of laser capture microdissection to detect integrated HIV-1 DNA in macrophages and astrocytes from autopsy brain tissues. J Neurovirol 12:146-152.

Clinton SM, Meador-Woodruff JH (2004) Abnormalities of the NMDA Receptor and Associated Intracellular Molecules in the Thalamus in Schizophrenia and Bipolar Disorder. Neuropsychopharmacology 29:1353-1362.

Clouse KA, Cosentino LM, Wein KA, Pyle SW, Robbins PB, Hochstein HD, Natarajan V, Farrar WL (1991) The HIV-1 gp120 envelope protein has the intrinsic capacity to stimulate monokine secretion. The journal of Immunology 147:2892-2901.

Cohen MS et al. (2011) Prevention of HIV-1 infection with early antiretroviral therapy. The New England journal of medicine 365:493-505.

Cooley LA, Lewin SR (2003) HIV-1 cell entry and advances in viral entry inhibitor therapy. Journal of clinical virology : the official publication of the Pan American Society for Clinical Virology 26:121-132.

Corlew R, Brasier DJ, Feldman DE, Philpot BD (2008) Presynaptic NMDA receptors: newly appreciated roles in cortical synaptic function and plasticity. Neuroscientist 14:609-625.

Cosenza-Nashat MA, Bauman A, Zhao ML, Morgello S, Suh HS, Lee SC (2011) Cannabinoid receptor expression in HIV encephalitis and HIV-associated neuropathologic comorbidities. Neuropathol Appl Neurobiol 37:464-483.

Crawford DC, Ramirez DM, Trauterman B, Monteggia LM, Kavalali ET (2017) Selective molecular impairment of spontaneous neurotransmission modulates synaptic efficacy. Nat Commun 8:14436.

Crowe S, Zhu T, Muller WA (2003) The contribution of monocyte infection and trafficking to viral persistence, and maintenance of the viral reservoir in HIV infection. J Leukoc Biol 74:635-641.

Crowe SM, Carlin JB, Stewart KI, Lucas CR, Hoy JF (1991) Predictive value of CD4 lymphocyte numbers for the development of opportunistic infections and malignancies in HIV-infected persons. J Acquir Immune Defic Syndr 4:770-776.

Cull-Candy S, Brickley S, Farrant M (2001) NMDA receptor subunits: diversity, development and disease. Curr Opin Neurobiol 11:327-335.

D'Amour J A, Froemke RC (2015) Inhibitory and excitatory spike-timing-dependent plasticity in the auditory cortex. Neuron 86:514-528.

Davis CN, Tabarean I, Gaidarova S, Behrens MM, Bartfai T (2006) IL-1beta induces a MyD88-dependent and ceramide-mediated activation of Src in anterior hypothalamic neurons. Journal of neurochemistry 98:1379-1389.

Dawson VL, Dawson TM, Uhl GR, Snyder SH (1993) Human immunodeficiency virus type 1 coat protein neurotoxicity mediated by nitric oxide in primary cortical cultures. Proc Natl Acad Sci U S A 90:3256-3259.

Decloedt EH, Freeman C, Howells F, Casson-Crook M, Lesosky M, Koutsilieri E, Lovestone S, Maartens G, Joska JA (2016) Moderate to severe HIV-associated neurocognitive impairment: A randomized placebo-controlled trial of lithium. Medicine (Baltimore) 95:e5401.

Deng H, Liu R, Ellmeier W, Choe S, Unutmaz D, Burkhart M, Di Marzio P, Marmon S, Sutton RE, Hill CM, Davis CB, Peiper SC, Schall TJ, Littman DR, Landau NR (1996) Identification of a major co-receptor for primary isolates of HIV-1. Nature 381:661-666.

Dhopeshwarkar A, Mackie K (2016) Functional Selectivity of CB2 Cannabinoid Receptor Ligands at a Canonical and Noncanonical Pathway. J Pharmacol Exp Ther 358:342-351.

Di Marzo V, Stella N, Zimmer A (2015) Endocannabinoid signalling and the deteriorating brain. Nat Rev Neurosci 16:30-42.

Diana MA, Marty A (2004) Endocannabinoid-mediated short-term synaptic plasticity: depolarization-induced suppression of inhibition (DSI) and depolarization-induced suppression of excitation (DSE). Br J Pharmacol 142:9-19.

Dickson DW, Mattiace LA, Kure K, Hutchins K, Lyman WD, Brosnan CF (1991) Biology of disease: microglia in human disease, with an emphasis on acquired immune deficiency syndrome. Lab Invest 64:135-156.

Eggers C, Arendt G, Hahn K, Husstedt IW, Maschke M, Neuen-Jacob E, Obermann M, Rosenkranz T, Schielke E, Straube E (2017) HIV-1-associated neurocognitive disorder: epidemiology, pathogenesis, diagnosis, and treatment. J Neurol 264:1715-1727.

Elemans M, Boelen L, Rasmussen M, Buus S, Asquith B (2017) HIV-1 adaptation to NK cell-mediated immune pressure. PLoS pathogens 13:e1006361.

Ellis R, Langford D, Masliah E (2007) HIV and antiretroviral therapy in the brain: neuronal injury and repair. Nat Rev Neurosci 8:33-44.

Ellis RJ, Calero P, Stockin MD (2009) HIV infection and the central nervous system: a primer. Neuropsychol Rev 19:144-151.

Ellis RJ, Deutsch R, Heaton RK, Marcotte TD, McCutchan JA, Nelson JA, Abramson I, Thal LJ, Atkinson JH, Wallace MR, Grant I (1997) Neurocognitive impairment is an independent risk factor for death in HIV infection. San Diego HIV Neurobehavioral Research Center Group. Arch Neurol 54:416-424.

Ellis RJ, Letendre S, Vaida F, Haubrich R, Heaton RK, Sacktor N, Clifford DB, Best BM, May S, Umlauf A, Cherner M, Sanders C, Ballard C, Simpson DM, Jay C, McCutchan JA (2014) Randomized trial of central nervous system-targeted antiretrovirals for HIV-associated neurocognitive disorder. Clin Infect Dis 58:1015-1022.

Epstein L, Gendelman H (1993) Human immunodeficiency virus type 1 infection of the nervous system: pathogenic mechanisms. Annals of neurology 33:429-436.

Etherton MR, Lyons JL, Ard KL (2015) HIV-associated Neurocognitive Disorders and Antiretroviral Therapy: Current Concepts and Controversies. Current infectious disease reports 17:485.

Everall IP, Bell C, Mallory M, Langford D, Adame A, Rockestein E, Masliah E (2002) Lithium ameliorates HIV-gp120-mediated neurotoxicity. Mol Cell Neurosci 21:493-501.

Everall IP, Heaton RK, Marcotte TD, Ellis RJ, McCutchan JA, Atkinson JH, Grant I, Mallory M, Masliah E (1999) Cortical synaptic density is reduced in mild to moderate human immunodeficiency virus neurocognitive disorder. HNRC Group. HIV Neurobehavioral Research Center. Brain Pathol 9:209-217.

Felder CC, Joyce KE, Briley EM, Glass M, Mackie KP, Fahey KJ, Cullinan GJ, Hunden DC, Johnson DW, Chaney MO, Koppel GA, Brownstein M (1998) Ly320135, a Novel Cannabinoid Cb1 Receptor Antagonist, Unmasks Coupling of the Cb1 Receptor to Stimulation of Camp Accumulation. Journal of Pharmacology & Experimental Therapeutics 284:291-297.

Ferguson MR, Rojo DR, von Lindern JJ, O'Brien WA (2002) HIV-1 replication cycle. Clinics in laboratory medicine 22:611-635.

Fernandez F, Morishita W, Zuniga E, Nguyen J, Blank M, Malenka RC, Garner CC (2007) Pharmacotherapy for cognitive impairment in a mouse model of Down syndrome. Nature neuroscience 10:411-413.

Festa L, Gutoskey CJ, Graziano A, Waterhouse BD, Meucci O (2015) Induction of Interleukin-1beta by Human Immunodeficiency Virus-1 Viral Proteins Leads to Increased Levels of Neuronal Ferritin Heavy Chain, Synaptic Injury, and Deficits in Flexible Attention. J Neurosci 35:10550-10561.

Fine SM, Angel RA, Perry SW, Epstein LG, Rothstein JD, Dewhurst S, Gelbard HA (1996) Tumor necrosis factor alpha inhibits glutamate uptake by primary human astrocytes - implications for pathogenesis of hiv-1 dementia. Journal of Biological Chemistry 271:15303-15306.

Finzi D, Hermankova M, Pierson T, Carruth LM, Buck C, Chaisson RE, Quinn TC, Chadwick K, Margolick J, Brookmeyer R, Gallant J, Markowitz M, Ho DD, Richman DD, Siliciano RF (1997) Identification of a Reservoir For Hiv-1 in Patients On Highly Active Antiretroviral Therapy. Science (New York, NY) 278:1295-1300.

Fischer-Smith T, Bell C, Croul S, Lewis M, Rappaport J (2008) Monocyte/macrophage trafficking in acquired immunodeficiency syndrome encephalitis: lessons from human and nonhuman primate studies. J Neurovirol 14:318-326.

Fischer G, Mutel V, Trube G, Malherbe P, Kew JNC, Mohacsi E, Heitz MP, Kemp JA (1997) Ro 25–6981, a Highly Potent and Selective Blocker of N-Methyl-D-aspartate Receptors Containing the NR2B Subunit. Characterization in Vitro. Journal of Pharmacology and Experimental Therapeutics 283:1285-1292.

Fitting S, Ignatowska-Jankowska BM, Bull C, Skoff RP, Lichtman AH, Wise LE, Fox MA, Su J, Medina AE, Krahe TE, Knapp PE, Guido W, Hauser KF (2013) Synaptic dysfunction in the hippocampus accompanies learning and memory deficits in human immunodeficiency virus type-1 Tat transgenic mice. Biol Psychiatry 73:443-453.

Flores CE, Nikonenko I, Mendez P, Fritschy JM, Tyagarajan SK, Muller D (2015) Activity-dependent inhibitory synapse remodeling through gephyrin phosphorylation. Proc Natl Acad Sci U S A 112:E65-72.

Fong MF, Newman JP, Potter SM, Wenner P (2015) Upward synaptic scaling is dependent on neurotransmission rather than spiking. Nat Commun 6:6339.

Fontana G, Valenti L, Raiteri M (1997) Gp120 Can Revert Antagonism At the Glycine Site of Nmda Receptors Mediating Gaba Release From Cultured Hippocampal Neurons. Journal of Neuroscience Research 49:732-738.

Freed EO (2001) HIV-1 replication. Somat Cell Mol Genet 26:13-33.

Freund TF, Katona I, Piomelli D (2003) Role of endogenous cannabinoids in synaptic signaling. Physiological Reviews 83:1017-1066.

Gao R, Penzes P (2015) Common mechanisms of excitatory and inhibitory imbalance in schizophrenia and autism spectrum disorders. Curr Mol Med 15:146-167.

Gelbard HA, Dzenko KA, DiLoreto D, del Cerro C, del Cerro M, Epstein LG (1993) Neurotoxic effects of tumor necrosis factor alpha in primary human neuronal cultures are mediated by activation of the glutamate AMPA receptor subtype: implications for AIDS neuropathogenesis. Dev Neurosci 15:417-422.

Gelman BB (2015) Neuropathology of HAND With Suppressive Antiretroviral Therapy: Encephalitis and Neurodegeneration Reconsidered. Curr HIV/AIDS Rep 12:272-279.

Ghosh B, Li Y, Thayer SA (2011) Inhibition of the plasma membrane Ca2+ pump by CD44 receptor activation of tyrosine kinases increases the action potential afterhyperpolarization in sensory neurons. J Neurosci 31:2361-2370.

Ghosh S, Preet A, Groopman JE, Ganju RK (2006) Cannabinoid receptor CB2 modulates the CXCL12/CXCR4-mediated chemotaxis of T lymphocytes. Mol Immunol 43:2169-2179.

Gill AJ, Kolson DL (2014) Chronic inflammation and the role for cofactors (hepatitis C, drug abuse, antiretroviral drug toxicity, aging) in HAND persistence. Curr HIV/AIDS Rep 11:325-335.

Gonsiorek W, Lunn C, Fan XD, Narula S, Lundell D, Hipkin RW (2000) Endocannabinoid 2-arachidonyl glycerol is a full agonist through human type 2 cannabinoid receptor: Antagonism by anandamide. Molecular pharmacology 57:1045-1050.

Gonzalez-Islas C, Wenner P (2006) Spontaneous network activity in the embryonic spinal cord regulates AMPAergic and GABAergic synaptic strength. Neuron 49:563-575.

Gonzalez-Scarano F, Martin-Garcia J (2005) The neuropathogenesis of AIDS. Nat Rev Immunol 5:69-81.

Gorantla S, Makarov E, Roy D, Finke-Dwyer J, Murrin L, Gendelman H, Poluektova L (2010) Immunoregulation of a CB2 Receptor Agonist in a Murine Model of NeuroAIDS. Journal of Neuroimmune Pharmacology 5:456-468.

Grabner GF, Eichmann TO, Wagner B, Gao Y, Farzi A, Taschler U, Radner FP, Schweiger M, Lass A, Holzer P, Zinser E, Tschop MH, Yi CX, Zimmermann R (2016) Deletion of Monoglyceride Lipase in Astrocytes Attenuates Lipopolysaccharide-induced Neuroinflammation. J Biol Chem 291:913-923.

Grant I et al. (2014) Asymptomatic HIV-associated neurocognitive impairment increases risk for symptomatic decline. Neurology 82:2055-2062.

Green MV, Thayer SA (2016) NMDARs Adapt to Neurotoxic HIV Protein Tat downstream of a GluN2A-Ubiquitin Ligase Signaling Pathway. J Neurosci 36:12640-12649.

Green MV, Thayer SA (2019) HIV gp120 upregulates tonic inhibition through alpha5-containing GABAARs. Neuropharmacology 149:161-168.

Green MV, Raybuck JD, Zhang X, Wu MM, Thayer SA (2018) Scaling Synapses in the Presence of HIV. Neurochem Res.

Gross GG, Junge JA, Mora RJ, Kwon HB, Olson CA, Takahashi TT, Liman ER, Ellis-Davies GC, McGee AW, Sabatini BL, Roberts RW, Arnold DB (2013) Recombinant probes for visualizing endogenous synaptic proteins in living neurons. Neuron 78:971-985.

Grynkiewicz G, Poenie M, Tsien RY (1985) A new generation of Ca^{2+} indicators with greatly improved fluorescence properties. Journal of Biological Chemistry 260:3440-3450.

Guggenhuber S, Monory K, Lutz B, Klugmann M (2010) AAV vector-mediated overexpression of CB1 cannabinoid receptor in pyramidal neurons of the hippocampus protects against seizure-induced excitoxicity. PLoS One 5:e15707.

Guha D, Wagner MCE, Ayyavoo V (2018) Human immunodeficiency virus type 1 (HIV-1)-mediated neuroinflammation dysregulates neurogranin and induces synaptodendritic injury. J Neuroinflammation 15:126.

Guidotti A, Auta J, Davis JM, Dong E, Grayson DR, Veldic M, Zhang X, Costa E (2005) GABAergic dysfunction in schizophrenia: new treatment strategies on the horizon. Psychopharmacology (Berl) 180:191-205.

Guindon J, Guijarro A, Piomelli D, Hohmann AG (2011) Peripheral antinociceptive effects of inhibitors of monoacylglycerol lipase in a rat model of inflammatory pain. Br J Pharmacol 163:1464-1478.

Hahn J, Wang X, Margeta M (2015) Astrocytes increase the activity of synaptic GluN2B NMDA receptors. Front Cell Neurosci 9:117.

Hargus NJ, Thayer SA (2013) Human immunodeficiency virus-1 Tat protein increases the number of inhibitory synapses between hippocampal neurons in culture. J Neurosci 33:17908-17920.

Heaton RK, Velin RA, McCutchan JA, Gulevich SJ, Atkinson JH, Wallace MR, Godfrey HP, Kirson DA, Grant I (1994) Neuropsychological impairment in human

immunodeficiency virus-infection: implications for employment. HNRC Group. HIV Neurobehavioral Research Center. Psychosom Med 56:8-17.

Heaton RK, Marcotte TD, Mindt MR, Sadek J, Moore DJ, Bentley H, McCutchan JA, Reicks C, Grant I (2004) The impact of HIV-associated neuropsychological impairment on everyday functioning. J Int Neuropsychol Soc 10:317-331.

Heaton RK et al. (2010) HIV-associated neurocognitive disorders persist in the era of potent antiretroviral therapy: CHARTER Study. Neurology 75:2087-2096.

Hellstrom IC, Danik M, Luheshi GN, Williams S (2005) Chronic LPS exposure produces changes in intrinsic membrane properties and a sustained IL-beta-dependent increase in GABAergic inhibition in hippocampal CA1 pyramidal neurons. Hippocampus 15:656-664.

Heneka MT et al. (2015) Neuroinflammation in Alzheimer's disease. The Lancet Neurology 14:388-405.

Hesselgesser J, Halks-Miller M, DelVecchio V, Peiper SC, Hoxie J, Kolson DL, Taub D, Horuk R (1997) CD4-independent association between HIV-1 gp120 and CXCR4: functional chemokine receptors are expressed in human neurons. Curr Biol 7:112-121.

Hines RM, Davies PA, Moss SJ, Maguire J (2012) Functional regulation of GABAA receptors in nervous system pathologies. Curr Opin Neurobiol 22:552-558.

Hiratani N, Fukai T (2017) Detailed Dendritic Excitatory/Inhibitory Balance through Heterosynaptic Spike-Timing-Dependent Plasticity. J Neurosci 37:12106-12122.

Holmes SE, Scheinost D, Finnema SJ, Naganawa M, Davis MT, DellaGioia N, Nabulsi N, Matuskey D, Angarita GA, Pietrzak RH, Duman RS, Sanacora G, Krystal JH, Carson RE, Esterlis I (2019) Lower synaptic density is associated with depression severity and network alterations. Nat Commun 10:1529.

Hong S, Banks WA (2015) Role of the immune system in HIV-associated neuroinflammation and neurocognitive implications. Brain, behavior, and immunity 45:1-12.

Howlett AC, Barth F, Bonner TI, Cabral G, Casellas P, Devane WA, Felder CC, Herkenham M, Mackie K, Martin BR, Mechoulam R, Pertwee RG (2002) International Union of Pharmacology. XXVII. Classification of cannabinoid receptors [Review]. Pharmacological reviews 54:161-202.

Hu S, Sheng WS, Rock RB (2013) CB2 receptor agonists protect human dopaminergic neurons against damage from HIV-1 gp120. PLoS One 8:e77577.

Huntwork S, Littleton JT (2007) A complexin fusion clamp regulates spontaneous neurotransmitter release and synaptic growth. Nature neuroscience 10:1235-1237.

Impagnatiello F, Guidotti AR, Pesold C, Dwivedi Y, Caruncho H, Pisu MG, Uzunov DP, Smalheiser NR, Davis JM, Pandey GN, Pappas GD, Tueting P, Sharma RP, Costa E (1998) A decrease of reelin expression as a putative vulnerability factor in schizophrenia. Proc Natl Acad Sci U S A 95:15718-15723.

Iskander S, Walsh KA, Hammond RR (2004) Human CNS cultures exposed to HIV-1 gp120 reproduce dendritic injuries of HIV-1-associated dementia. J Neuroinflammation 1:7.

Islam S, Hoque SA, Adnan N, Tanaka A, Jinno-Oue A, Hoshino H (2013) X4-tropic human immunodeficiency virus IIIB utilizes CXCR4 as coreceptor, as distinct from R5X4-tropic viruses. Microbiol Immunol 57:437-444.

Jiang J, Quan Y, Ganesh T, Pouliot WA, Dudek FE, Dingledine R (2013) Inhibition of the prostaglandin receptor EP2 following status epilepticus reduces delayed mortality and brain inflammation. Proc Natl Acad Sci U S A 110:3591-3596.

Jo S et al. (2014) GABA from reactive astrocytes impairs memory in mouse models of Alzheimer's disease. Nature medicine 20:886-896.

Johansson JU, Woodling NS, Wang Q, Panchal M, Liang X, Trueba-Saiz A, Brown HD, Mhatre SD, Loui T, Andreasson KI (2015) Prostaglandin signaling suppresses beneficial microglial function in Alzheimer's disease models. J Clin Invest 125:350-364.

Johansson JU, Pradhan S, Lokteva LA, Woodling NS, Ko N, Brown HD, Wang Q, Loh C, Cekanaviciute E, Buckwalter M, Manning-Bog AB, Andreasson KI (2013) Suppression of inflammation with conditional deletion of the prostaglandin E2 EP2 receptor in macrophages and brain microglia. J Neurosci 33:16016-16032.

Johnson JW, Glasgow NG, Povysheva NV (2015) Recent insights into the mode of action of memantine and ketamine. Curr Opin Pharmacol 20:54-63.

Johnson LF, Mossong J, Dorrington RE, Schomaker M, Hoffmann CJ, Keiser O, Fox MP, Wood R, Prozesky H, Giddy J, Garone DB, Cornell M, Egger M, Boulle A (2013) Life expectancies of South African adults starting antiretroviral treatment: collaborative analysis of cohort studies. PLoS medicine 10:e1001418.

Jones MV, Bell JE, Nath A (2000) Immunolocalization of HIV envelope gp120 in HIV encephalitis with dementia. AIDS 14:2709-2713.

Joska JA, Westgarth-Taylor J, Myer L, Hoare J, Thomas KG, Combrinck M, Paul RH, Stein DJ, Flisher AJ (2011) Characterization of HIV-Associated Neurocognitive Disorders among individuals starting antiretroviral therapy in South Africa. AIDS Behav 15:1197-1203.

Kano M, Ohno-Shosaku T, Maejima T (2002) Retrograde signaling at central synapses via endogenous cannabinoids. Molecular Psychiatry 7:234-235.

Karginov AV, Ding F, Kota P, Dokholyan NV, Hahn KM (2010) Engineered allosteric activation of kinases in living cells. Nat Biotechnol 28:743-747.

Kaul M, Lipton SA (1999) Chemokines and activated macrophages in HIV gp120-induced neuronal apoptosis. Proc Natl Acad Sci U S A 96:8212-8216.

Kaul M, Garden GA, Lipton SA (2001) Pathways to neuronal injury and apoptosis in HIV-associated dementia. Nature 410:988-994.

Kavalali ET (2015) The mechanisms and functions of spontaneous neurotransmitter release. Nat Rev Neurosci 16:5-16.

Kavalali ET, Monteggia LM (2012) Synaptic mechanisms underlying rapid antidepressant action of ketamine. Am J Psychiatry 169:1150-1156.

Keck T, Hubener M, Bonhoeffer T (2017) Interactions between synaptic homeostatic mechanisms: an attempt to reconcile BCM theory, synaptic scaling, and changing excitation/inhibition balance. Curr Opin Neurobiol 43:87-93.

Kelly A, Vereker E, Nolan Y, Brady M, Barry C, Loscher CE, Mills KH, Lynch MA (2003) Activation of p38 plays a pivotal role in the inhibitory effect of lipopolysaccharide and interleukin-1 beta on long term potentiation in rat dentate gyrus. J Biol Chem 278:19453-19462.

Kerr DM, Harhen B, Okine BN, Egan LJ, Finn DP, Roche M (2013) The monoacylglycerol lipase inhibitor JZL184 attenuates LPS-induced increases in cytokine expression in the rat frontal cortex and plasma: differential mechanisms of action. Br J Pharmacol 169:808-819.

Kerza-Kwiatecki AP, Amini S (1999) CNS as an HIV-1 reservoir; BBB and drug delivery. J Neurovirol 5:113-114.

Kim HJ, Waataja JJ, Thayer SA (2008a) Cannabinoids inhibit network-driven synapse loss between hippocampal neurons in culture. J Pharmacol Exp Ther 325:850-858.

Kim HJ, Martemyanov KA, Thayer SA (2008b) Human immunodeficiency virus protein Tat induces synapse loss via a reversible process that is distinct from cell death. J Neurosci 28:12604-12613.

Kim HJ, Shin AH, Thayer SA (2011) Activation of cannabinoid type 2 receptors inhibits HIV-1 envelope glycoprotein gp120-induced synapse loss. Molecular pharmacology 80:357-366.

Kinsey SG, Wise LE, Ramesh D, Abdullah R, Selley DE, Cravatt BF, Lichtman AH (2013) Repeated Low Dose Administration of the Monoacylglycerol Lipase Inhibitor JZL184 Retains CB1 Receptor Mediated Antinociceptive and Gastroprotective Effects. J Pharmacol Exp Ther 345:492-501.

Kirov SA, Sorra KE, Harris KM (1999) Slices have more synapses than perfusion-fixed hippocampus from both young and mature rats. J Neurosci 19:2876-2886.

Klegeris A, Bissonnette CJ, McGeer PL (2003) Reduction of human monocytic cell neurotoxicity and cytokine secretion by ligands of the cannabinoid-type CB2 receptor. British Journal of Pharmacology 139:775-786.

Kneussel M, Hausrat TJ (2016) Postsynaptic Neurotransmitter Receptor Reserve Pools for Synaptic Potentiation. Trends in neurosciences 39:170-182.

Kohr G, Seeburg PH (1996) Subtype-specific regulation of recombinant NMDA receptor-channels by protein tyrosine kinases of the src family. J Physiol 492 (Pt 2):445-452.

Kouchi Z (2015) Monoacylglycerol lipase promotes Fcgamma receptor-mediated phagocytosis in microglia but does not regulate LPS-induced upregulation of inflammatory cytokines. Biochem Biophys Res Commun 464:603-610.

Kovalevich J, Langford D (2012) Neuronal toxicity in HIV CNS disease. Future Virol 7:687-698.

Krogh KA, Wydeven N, Wickman K, Thayer SA (2014) HIV-1 protein Tat produces biphasic changes in NMDA-evoked increases in intracellular Ca2+ concentration via activation of Src kinase and nitric oxide signaling pathways. Journal of neurochemistry 130:642-656.

Laga M, Icenogle JP, Marsella R, Manoka AT, Nzila N, Ryder RW, Vermund SH, Heyward WL, Nelson A, Reeves WC (1992) Genital papillomavirus infection and cervical dysplasia--opportunistic complications of HIV infection. International journal of cancer 50:45-48.

Lambotte O, Deiva K, Tardieu M (2003) HIV-1 persistence, viral reservoir, and the central nervous system in the HAART era. Brain Pathol 13:95-103.

Lavreys L, Thompson ML, Martin HL, Jr., Mandaliya K, Ndinya-Achola JO, Bwayo JJ, Kreiss J (2000) Primary human immunodeficiency virus type 1 infection: clinical manifestations among women in Mombasa, Kenya. Clin Infect Dis 30:486-490.

Lawrence CB, Allan SM, Rothwell NJ (1998) Interleukin-1-Beta and the Interleukin-1 Receptor Antagonist Act in the Striatum to Modify Excitotoxic Brain Damage in the Rat. European Journal of Neuroscience 10:1188-1195.

Letendre S (2011) Central nervous system complications in HIV disease: HIV-associated neurocognitive disorder. Topics in antiviral medicine 19:137-142.

Letendre S, Marquie-Beck J, Capparelli E, Best B, Clifford D, Collier AC, Gelman BB, McArthur JC, McCutchan JA, Morgello S, Simpson D, Grant I, Ellis RJ (2008) Validation of the CNS Penetration-Effectiveness rank for quantifying antiretroviral penetration into the central nervous system. Arch Neurol 65:65-70.

Letendre SL, Woods SP, Ellis RJ, Atkinson JH, Masliah E, van den Brande G, Durelle J, Grant I, Everall I (2006) Lithium improves HIV-associated neurocognitive impairment. Aids 20:1885-1888.

Lewis DA, Volk DW, Hashimoto T (2004) Selective alterations in prefrontal cortical GABA neurotransmission in schizophrenia: a novel target for the treatment of working memory dysfunction. Psychopharmacology (Berl) 174:143-150.

Li N, Lee B, Liu RJ, Banasr M, Dwyer JM, Iwata M, Li XY, Aghajanian G, Duman RS (2010) mTOR-dependent synapse formation underlies the rapid antidepressant effects of NMDA antagonists. Science (New York, NY) 329:959-964.

Li W, Li G, Steiner J, Nath A (2009) Role of Tat Protein in HIV Neuropathogenesis. Neurotox Res 16:205-220.

Lin Y, Bloodgood BL, Hauser JL, Lapan AD, Koon AC, Kim TK, Hu LS, Malik AN, Greenberg ME (2008) Activity-dependent regulation of inhibitory synapse development by Npas4. Nature 455:1198-1204.

Liu G (2004) Local structural balance and functional interaction of excitatory and inhibitory synapses in hippocampal dendrites. Nature neuroscience 7:373-379.

Liu Y, Wong TP, Aarts M, Rooyakkers A, Liu L, Lai TW, Wu DC, Lu J, Tymianski M, Craig AM, Wang YT (2007) NMDA Receptor Subunits Have Differential Roles in Mediating Excitotoxic Neuronal Death Both In Vitro and In Vivo. J Neurosci 27:2846-2857.

Liu Z, Zang Y, Qiao L, Liu K, Ouyang Y, Zhang Y, Chen D (2016) ASPP2 involvement in p53-mediated HIV-1 envelope glycoprotein gp120 neurotoxicity in mice cerebrocortical neurons. Sci Rep 6:33378.

Long JZ, Li W, Booker L, Burston JJ, Kinsey SG, Schlosburg JE, Pavon FJ, Serrano AM, Selley DE, Parsons LH, Lichtman AH, Cravatt BF (2009) Selective blockade of 2-arachidonoylglycerol hydrolysis produces cannabinoid behavioral effects. Nat Chem Biol 5:37-44.

Louboutin JP, Reyes BA, Agrawal L, Van Bockstaele EJ, Strayer DS (2010) HIV-1 gp120-induced neuroinflammation: relationship to neuron loss and protection by rSV40-delivered antioxidant enzymes. Exp Neurol 221:231-245.

Ma L, Jia J, Liu X, Bai F, Wang Q, Xiong L (2015) Activation of murine microglial N9 cells is attenuated through cannabinoid receptor CB2 signaling. Biochem Biophys Res Commun 458:92-97.

Maartens G, Celum C, Lewin SR (2014) HIV infection: epidemiology, pathogenesis, treatment, and prevention. Lancet (London, England) 384:258-271.

Malek N, Popiolek-Barczyk K, Mika J, Przewlocka B, Starowicz K (2015) Anandamide, Acting via CB2 Receptors, Alleviates LPS-Induced Neuroinflammation in Rat Primary Microglial Cultures. Neural Plast 2015:130639.

Malhotra AK, Pinals DA, Weingartner H, Sirocco K, Missar CD, Pickar D, Breier A (1996) NMDA receptor function and human cognition: the effects of ketamine in healthy volunteers. Neuropsychopharmacology 14:301-307.

Marder E, Goaillard JM (2006) Variability, compensation and homeostasis in neuron and network function. Nat Rev Neurosci 7:563-574.

Mariotti A, Kedeshian PA, Dans M, Curatola AM, Gagnoux-Palacios L, Giancotti FG (2001) EGF-R signaling through Fyn kinase disrupts the function of integrin alpha6beta4 at hemidesmosomes: role in epithelial cell migration and carcinoma invasion. J Cell Biol 155:447-458.

Marlink R, Kanki P, Thior I, Travers K, Eisen G, Siby T, Traore I, Hsieh CC, Dia MC, Gueye EH, et al (1994) Reduced rate of disease development after HIV-2 infection as compared to HIV-1. Science (New York, NY) 265:1587-1590.

Marra CM, Zhao Y, Clifford DB, Letendre S, Evans S, Henry K, Ellis RJ, Rodriguez B, Coombs RW, Schifitto G, McArthur JC, Robertson K (2009) Impact of combination antiretroviral therapy on cerebrospinal fluid HIV RNA and neurocognitive performance. AIDS 23:1359-1366.

Marsicano G, Goodenough S, Monory K, Hermann H, Eder M, Cannich A, Azad SC, Cascio MG, Gutierrez SO, van der Stelt M, Lopez-Rodriguez ML, Casanova E, Schutz G, Zieglgansberger W, Di Marzo V, Behl C, Lutz B (2003) CB1 Cannabinoid Receptors and On-Demand Defense Against Excitotoxicity. Science (New York, NY) 302:84-88.

Maschke M, Kastrup O, Esser S, Ross B, Hengge U, Hufnagel A (2000) Incidence and prevalence of neurological disorders associated with HIV since the introduction of highly active antiretroviral therapy (HAART). J Neurol Neurosurg Psychiatry 69:376-380.

Masliah E, Heaton RK, Marcotte TD, Ellis RJ, Wiley CA, Mallory M, Achim CL, McCutchan JA, Nelson JA, Atkinson JH, Grant I (1997) Dendritic injury is a pathological substrate for human immunodeficiency virus-related cognitive disorders. HNRC Group. The HIV Neurobehavioral Research Center. Ann Neurol 42:963-972.

Maung R, Hoefer MM, Sanchez AB, Sejbuk NE, Medders KE, Desai MK, Catalan IC, Dowling CC, de Rozieres CM, Garden GA, Russo R, Roberts AJ, Williams R, Kaul M (2014) CCR5 knockout prevents neuronal injury and behavioral impairment induced in a transgenic mouse model by a CXCR4-using HIV-1 glycoprotein 120. J Immunol 193:1895-1910.

McArthur JC, Brew BJ, Nath A (2005) Neurological complications of HIV infection. The Lancet Neurology 4:543-555.

McArthur JC, Steiner J, Sacktor N, Nath A (2010) Human Immunodeficiency Virus-Associated Neurocognitive Disorders Mind the Gap. Ann Neurol 67:699-714.

Medders KE, Sejbuk NE, Maung R, Desai MK, Kaul M (2010) Activation of p38 MAPK is required in monocytic and neuronal cells for HIV glycoprotein 120-induced neurotoxicity. J Immunol 185:4883-4895.

Mellors JW, Munoz A, Giorgi JV, Margolick JB, Tassoni CJ, Gupta P, Kingsley LA, Todd JA, Saah AJ, Detels R, Phair JP, Rinaldo CR, Jr. (1997) Plasma viral load and CD4+ lymphocytes as prognostic markers of HIV-1 infection. Annals of internal medicine 126:946-954.

Mennicken F, Maki R, de Souza EB, Quirion R (1999) Chemokines and chemokine receptors in the CNS: a possible role in neuroinflammation and patterning. Trends in pharmacological sciences 20:73-78.

Merighi S, Gessi S, Varani K, Simioni C, Fazzi D, Mirandola P, Borea PA (2012) Cannabinoid Cb(2) Receptor Modulates Microglial Cells Stimulated with

Lypopolysaccharide: Role of Erk-1/2 Kinase Signalling in Nitric Oxide Release. Br J Pharmacol 165:1773-1788.

Meucci O, Miller RJ (1996) Gp120-induced neurotoxicity in hippocampal pyramidal neuron cultures - protective action of tgf-beta-1. Journal of Neuroscience 16:4080-4088.

Miller OH, Yang L, Wang CC, Hargroder EA, Zhang Y, Delpire E, Hall BJ (2014) GluN2B-containing NMDA receptors regulate depression-like behavior and are critical for the rapid antidepressant actions of ketamine. Elife 3:e03581.

Mishra A, Kim HJ, Shin AH, Thayer SA (2012) Synapse loss induced by interleukin-1beta requires pre- and post-synaptic mechanisms. J Neuroimmune Pharmacol 7:571-578.

Monory K et al. (2006) The endocannabinoid system controls key epileptogenic circuits in the hippocampus. Neuron 51:455-466.

Monyer H, Burnashev N, Laurie DJ, Sakmann B, Seeburg PH (1994) Developmental and regional expression in the rat brain and functional properties of four NMDA receptors. Neuron 12:529-540.

Moore JP, Trkola A, Dragic T (1997) Co-receptors for HIV-1 entry. Curr Opin Immunol 9:551-562.

Muccioli GG, Labar G, Lambert DM (2008) CAY10499, a novel monoglyceride lipase inhibitor evidenced by an expeditious MGL assay. Chembiochem 9:2704-2710.

Nath A (1999) Pathobiology of human immunodeficiency virus dementia. Semin Neurol 19:113-127.

Nath A (2002) Human immunodeficiency virus (HIV) proteins in neuropathogenesis of HIV dementia. The Journal of infectious diseases 186 Suppl 2:S193-198.

Nelson SB, Valakh V (2015) Excitatory/Inhibitory Balance and Circuit Homeostasis in Autism Spectrum Disorders. Neuron 87:684-698.

Newcomer JW, Krystal JH (2001) NMDA receptor regulation of memory and behavior in humans. Hippocampus 11:529-542.

Nomura DK, Morrison BE, Blankman JL, Long JZ, Kinsey SG, Marcondes MC, Ward AM, Hahn YK, Lichtman AH, Conti B, Cravatt BF (2011) Endocannabinoid hydrolysis generates brain prostaglandins that promote neuroinflammation. Science (New York, NY) 334:809-813.

Nosyreva E, Autry AE, Kavalali ET, Monteggia LM (2014) Age dependence of the rapid antidepressant and synaptic effects of acute NMDA receptor blockade. Front Mol Neurosci 7:94.

Nosyreva E, Szabla K, Autry AE, Ryazanov AG, Monteggia LM, Kavalali ET (2013) Acute suppression of spontaneous neurotransmission drives synaptic potentiation. J Neurosci 33:6990-7002.

Nunez E, Benito C, Pazos MR, Barbachano A, Fajardo O, Gonzalez S, Tolon RM, Romero J (2004) Cannabinoid CB2 receptors are expressed by perivascular microglial cells in the human brain: an immunohistochemical study. Synapse 53:208-213.

Oh SK, Cruikshank WW, Raina J, Blanchard GC, Adler WH, Walker J, Kornfeld H (1992) Identification of HIV-1 envelope glycoprotein in the serum of AIDS and ARC patients. J Acquir Immune Defic Syndr 5:251-256.

Oh YT, Lee JY, Lee J, Lee JH, Kim JE, Ha J, Kang I (2010) Oleamide suppresses lipopolysaccharide-induced expression of iNOS and COX-2 through inhibition of NF-kappaB activation in BV2 murine microglial cells. Neurosci Lett 474:148-153.

Ohgi Y, Futamura T, Hashimoto K (2015) Glutamate Signaling in Synaptogenesis and NMDA Receptors as Potential Therapeutic Targets for Psychiatric Disorders. Curr Mol Med 15:206-221.

Ohnishi H, Murata Y, Okazawa H, Matozaki T (2011) Src family kinases: modulators of neurotransmitter receptor function and behavior. Trends in neurosciences 34:629-637.

Orfila JE, Grewal H, Dietz RM, Strnad F, Shimizu T, Moreno M, Schroeder C, Yonchek J, Rodgers KM, Dingman A, Bernard TJ, Quillinan N, Macklin WB, Traystman RJ, Herson PS (2017) Delayed inhibition of tonic inhibition enhances functional recovery following experimental ischemic stroke. J Cereb Blood Flow Metab:271678X17750761.

Osmond D, Charlebois E, Lang W, Shiboski S, Moss A (1994) Changes in AIDS survival time in two San Francisco cohorts of homosexual men, 1983 to 1993. Jama 271:1083-1087.

Pacher P, Batkai S, Kunos G (2006) The endocannabinoid system as an emerging target of pharmacotherapy. Pharmacological reviews 58:389-462.

Pan B, Wang W, Long JZ, Sun D, Hillard CJ, Cravatt BF, Liu QS (2009) Blockade of 2-arachidonoylglycerol hydrolysis by selective monoacylglycerol lipase inhibitor 4-nitrophenyl 4-(dibenzo[d][1,3]dioxol-5-yl(hydroxy)methyl)piperidine-1-carboxylate (JZL184) Enhances retrograde endocannabinoid signaling. J Pharmacol Exp Ther 331:591-597.

Papouin T, Ladepeche L, Ruel J, Sacchi S, Labasque M, Hanini M, Groc L, Pollegioni L, Mothet JP, Oliet SH (2012) Synaptic and extrasynaptic NMDA receptors are gated by different endogenous coagonists. Cell 150:633-646.

Persidsky Y, Gendelman HE (1997) Development of laboratory and animal model systems for HIV-1 encephalitis and its associated dementia. Journal of Leukocyte Biology 62:100-106.

Piro JR, Benjamin DI, Duerr JM, Pi Y, Gonzales C, Wood KM, Schwartz JW, Nomura DK, Samad TA (2012) A dysregulated endocannabinoid-eicosanoid network supports pathogenesis in a mouse model of Alzheimer's disease. Cell Rep 1:617-623.

Pozo K, Goda Y (2010) Unraveling mechanisms of homeostatic synaptic plasticity. Neuron 66:337-351.

Pribiag H, Stellwagen D (2013) TNF-alpha downregulates inhibitory neurotransmission through protein phosphatase 1-dependent trafficking of GABA(A) receptors. J Neurosci 33:15879-15893.

Price RW (1996) Neurological complications of HIV infection. Lancet (London, England) 348:445-452.

Puffenbarger RA, Boothe AC, Cabral GA (2000) Cannabinoids inhibit LPS-inducible cytokine mRNA expression in rat microglial cells. Glia 29:58-69.

Purohit V, Rapaka RS, Rutter J (2014) Cannabinoid receptor-2 and HIV-associated neurocognitive disorders. J Neuroimmune Pharmacol 9:447-453.

Ramarao MK, Murphy EA, Shen MW, Wang Y, Bushell KN, Huang N, Pan N, Williams C, Clark JD (2005) A fluorescence-based assay for fatty acid amide hydrolase compatible with high-throughput screening. Anal Biochem 343:143-151.

Ramirez DMO, Crawford DC, Chanaday NL, Trauterman B, Monteggia LM, Kavalali ET (2017) Loss of Doc2-Dependent Spontaneous Neurotransmission Augments Glutamatergic Synaptic Strength. J Neurosci 37:6224-6230.

Ravizza T, Vezzani A (2006) Status epilepticus induces time-dependent neuronal and astrocytic expression of interleukin-1 receptor type I in the rat limbic system. Neuroscience 137:301-308.

Raybuck JD, Hargus NJ, Thayer SA (2017) A GluN2B-Selective NMDAR Antagonist Reverses Synapse Loss and Cognitive Impairment Produced by the HIV-1 Protein Tat. J Neurosci 37:7837-7847.

Reese AL, Kavalali ET (2016) Single synapse evaluation of the postsynaptic NMDA receptors targeted by evoked and spontaneous neurotransmission. Elife 5.

Reger M, Welsh R, Razani J, Martin DJ, Boone KB (2002) A meta-analysis of the neuropsychological sequelae of HIV infection. J Int Neuropsychol Soc 8:410-424.

Resnick L, Berger JR, Shapshak P, Tourtellotte WW (1988) Early penetration of the blood-brain-barrier by HIV. Neurology 38:9-14.

Rijkers K, Majoie HJ, Hoogland G, Kenis G, De Baets M, Vles JS (2009) The role of interleukin-1 in seizures and epilepsy: a critical review. Exp Neurol 216:258-271.

Roloff AM, Thayer SA (2009) Modulation of excitatory synaptic transmission by Delta 9-tetrahydrocannabinol switches from agonist to antagonist depending on firing rate. Molecular pharmacology 75:892-900.

Roloff AM, Anderson GR, Martemyanov KA, Thayer SA (2010) Homer 1a Gates the Induction Mechanism for Endocannabinoid-Mediated Synaptic Plasticity. J Neurosci 30:3072-3081.

Romero-Sandoval EA, Horvath R, Landry RP, DeLeo JA (2009) Cannabinoid receptor type 2 activation induces a microglial anti-inflammatory phenotype and reduces migration via MKP induction and ERK dephosphorylation. Mol Pain 5:25.

Rossi S, Studer V, Moscatelli A, Motta C, Coghe G, Fenu G, Caillier S, Buttari F, Mori F, Barbieri F, Castelli M, De Chiara V, Monteleone F, Mancino R, Bernardi G, Baranzini SE, Marrosu MG, Oksenberg JR, Centonze D (2013) Opposite roles of NMDA receptors in relapsing and primary progressive multiple sclerosis. PLoS One 8:e67357.

Rouzer CA, Marnett LJ (2009) Cyclooxygenases: structural and functional insights. Journal of lipid research 50 Suppl:S29-34.

Ryan TJ, Roy DS, Pignatelli M, Arons A, Tonegawa S (2015) Memory. Engram cells retain memory under retrograde amnesia. Science (New York, NY) 348:1007-1013.

Rychert J, Strick D, Bazner S, Robinson J, Rosenberg E (2010) Detection of HIV gp120 in plasma during early HIV infection is associated with increased proinflammatory and immunoregulatory cytokines. AIDS Res Hum Retroviruses 26:1139-1145.

Sama DM, Norris CM (2013) Calcium dysregulation and neuroinflammation: Discrete and integrated mechanisms for age-related synaptic dysfunction. Ageing Res Rev.

Santosuosso M, Righi E, Lindstrom V, Leblanc PR, Poznansky MC (2009) HIV-1 envelope protein gp120 is present at high concentrations in secondary lymphoid organs of individuals with chronic HIV-1 infection. The Journal of infectious diseases 200:1050-1053.

Saylor D, Dickens AM, Sacktor N, Haughey N, Slusher B, Pletnikov M, Mankowski JL, Brown A, Volsky DJ, McArthur JC (2016) HIV-associated neurocognitive disorder - pathogenesis and prospects for treatment. Nat Rev Neurol 12:234-248.

Scheiman JM (2016) NSAID-induced Gastrointestinal Injury: A Focused Update for Clinicians. J Clin Gastroenterol 50:5-10.

Schifitto G, Navia BA, Yiannoutsos CT, Marra CM, Chang L, Ernst T, Jarvik JG, Miller EN, Singer EJ, Ellis RJ, Kolson DL, Simpson D, Nath A, Berger J, Shriver SL, Millar LL, Colquhoun D, Lenkinski R, Gonzalez RG, Lipton SA (2007) Memantine and HIV-associated cognitive impairment: a neuropsychological and proton magnetic resonance spectroscopy study. Aids 21:1877-1886.

Schlosburg JE, Blankman JL, Long JZ, Nomura DK, Pan B, Kinsey SG, Nguyen PT, Ramesh D, Booker L, Burston JJ, Thomas EA, Selley DE, Sim-Selley LJ, Liu QS, Lichtman AH, Cravatt BF (2010) Chronic monoacylglycerol lipase blockade causes functional antagonism of the endocannabinoid system. Nature neuroscience 13:1113-1119.

Schneggenburger R, Rosenmund C (2015) Molecular mechanisms governing Ca(2+) regulation of evoked and spontaneous release. Nature neuroscience 18:935-941.

Schreurs A, Sabanov V, Balschun D (2017) Distinct Properties of Long-Term Potentiation in the Dentate Gyrus along the Dorsoventral Axis: Influence of Age and Inhibition. Sci Rep 7:5157.

Serantes R, Arnalich F, Figueroa M, Salinas M, Andres-Mateos E, Codoceo R, Renart J, Matute C, Cavada C, Cuadrado A, Montiel C (2006) Interleukin-1beta enhances GABAA receptor cell-surface expression by a phosphatidylinositol 3-kinase/Akt pathway: relevance to sepsis-associated encephalopathy. J Biol Chem 281:14632-14643.

Serrano-Pozo A, Frosch MP, Masliah E, Hyman BT (2011) Neuropathological alterations in Alzheimer disease. Cold Spring Harb Perspect Med 1:a006189.

Shaw GM, Hunter E (2012) HIV transmission. Cold Spring Harb Perspect Med 2.

Shin AH, Thayer SA (2013) Human immunodeficiency virus-1 protein Tat induces excitotoxic loss of presynaptic terminals in hippocampal cultures. Mol Cell Neurosci 54:22-29.

Shin AH, Kim HJ, Thayer SA (2012) Subtype selective NMDA receptor antagonists induce recovery of synapses lost following exposure to HIV-1 Tat. Br J Pharmacol 166:1002-1017.

Shioda T, Levy JA, Cheng-Mayer C (1991) Macrophage and T cell-line tropisms of HIV-1 are determined by specific regions of the envelope gp120 gene. Nature 349:167-169.

Shipton OA, Paulsen O (2014) GluN2A and GluN2B subunit-containing NMDA receptors in hippocampal plasticity. Philos Trans R Soc Lond B Biol Sci 369:20130163.

Siliciano JD, Kajdas J, Finzi D, Quinn TC, Chadwick K, Margolick JB, Kovacs C, Gange SJ, Siliciano RF (2003) Long-term follow-up studies confirm the stability of the latent reservoir for HIV-1 in resting CD4+ T cells. Nature medicine 9:727-728.

Silverberg MJ, Chao C, Leyden WA, Xu L, Tang B, Horberg MA, Klein D, Quesenberry CP, Jr., Towner WJ, Abrams DI (2009) HIV infection and the risk of cancers with and without a known infectious cause. Aids 23:2337-2345.

Simmons DL, Botting RM, Hla T (2004) Cyclooxygenase isozymes: the biology of prostaglandin synthesis and inhibition. Pharmacological reviews 56:387-437.

Snyder EM, Nong Y, Almeida CG, Paul S, Moran T, Choi EY, Nairn AC, Salter MW, Lombroso PJ, Gouras GK, Greengard P (2005) Regulation of NMDA receptor trafficking by amyloid-beta. Nature neuroscience 8:1051-1058.

Sodhi A, Montaner S, Gutkind JS (2004) Viral hijacking of G-protein-coupled-receptor signalling networks. Nat Rev Mol Cell Biol 5:998-1012.

Spencer DC, Price RW (1992) Human immunodeficiency virus and the central nervous system. Annual review of microbiology 46:655-693.

Stocca G, Vicini S (1998) Increased contribution of NR2A subunit to synaptic NMDA receptors in developing rat cortical neurons. J Physiol 507 (Pt 1):13-24.

Stocca G, Schmidt-Hieber C, Bischofberger J (2008) Differential dendritic Ca2+ signalling in young and mature hippocampal granule cells. J Physiol.

Straiker A, Hu SS, Long JZ, Arnold A, Wager-Miller J, Cravatt BF, Mackie K (2009) Monoacylglycerol lipase limits the duration of endocannabinoid-mediated depolarization-induced suppression of excitation in autaptic hippocampal neurons. Molecular pharmacology 76:1220-1227.

Strazielle N, Ghersi-Egea JF (2005) Factors affecting delivery of antiviral drugs to the brain. Reviews in medical virology 15:105-133.

Taghibiglou C, Martin HG, Lai TW, Cho T, Prasad S, Kojic L, Lu J, Liu Y, Lo E, Zhang S, Wu JZ, Li YP, Wen YH, Imm JH, Cynader MS, Wang YT (2009) Role of NMDA receptor-dependent activation of SREBP1 in excitotoxic and ischemic neuronal injuries. Nature medicine 15:1399-1406.

Tang YP, Shimizu E, Dube GR, Rampon C, Kerchner GA, Zhuo M, Liu G, Tsien JZ (1999) Genetic enhancement of learning and memory in mice. Nature 401:63-69.

Tham CS, Whitaker J, Luo L, Webb M (2007) Inhibition of microglial fatty acid amide hydrolase modulates LPS stimulated release of inflammatory mediators. FEBS Lett 581:2899-2904.

Thaney VE, Sanchez AB, Fields JA, Minassian A, Young JW, Maung R, Kaul M (2018) Transgenic mice expressing HIV-1 envelope protein gp120 in the brain as an animal model in neuroAIDS research. J Neurovirol 24:156-167.

Thomas SA (2004) Anti-HIV drug distribution to the central nervous system. Curr Pharm Des 10:1313-1324.

Thompson KA, Cherry CL, Bell JE, McLean CA (2011) Brain cell reservoirs of latent virus in presymptomatic HIV-infected individuals. Am J Pathol 179:1623-1629.

Toggas SM, Masliah E, Mucke L (1996) Prevention of HIV-1 gp120-induced neuronal damage in the central nervous system of transgenic mice by the NMDA receptor antagonist memantine. Brain Res 706:303-307.

Toggas SM, Masliah E, Rockenstein EM, Rall GF, Abraham CR, Mucke L (1994) Central nervous system damage produced by expression of the HIV-1 coat protein gp120 in transgenic mice. Nature 367:188-193.

Tong L, Prieto GA, Cotman CW (2018) IL-1beta suppresses cLTP-induced surface expression of GluA1 and actin polymerization via ceramide-mediated Src activation. J Neuroinflammation 15:127.

Tong L, Prieto GA, Kramar EA, Smith ED, Cribbs DH, Lynch G, Cotman CW (2012) Brain-derived neurotrophic factor-dependent synaptic plasticity is suppressed by interleukin-1beta via p38 mitogen-activated protein kinase. J Neurosci 32:17714-17724.

Tozzi V, Balestra P, Bellagamba R, Corpolongo A, Salvatori MF, Visco-Comandini U, Vlassi C, Giulianelli M, Galgani S, Antinori A, Narciso P (2007) Persistence of neuropsychologic deficits despite long-term highly active antiretroviral therapy in patients with HIV-related neurocognitive impairment: prevalence and risk factors. J Acquir Immune Defic Syndr 45:174-182.

Trujillo JR, Navia BA, Worth J, Lucey DR, McLane MF, Lee TH, Essex M (1996) High levels of anti-HIV-1 envelope antibodies in cerebrospinal fluid as compared to serum from patients with AIDS dementia complex. J Acquir Immune Defic Syndr Hum Retrovirol 12:19-25.

Tu W, Xu X, Peng L, Zhong X, Zhang W, Soundarapandian MM, Balel C, Wang M, Jia N, Zhang W, Lew F, Chan SL, Chen Y, Lu Y (2010) DAPK1 interaction with NMDA receptor NR2B subunits mediates brain damage in stroke. Cell 140:222-234.

Turrigiano G (2011) Too many cooks? Intrinsic and synaptic homeostatic mechanisms in cortical circuit refinement. Annual review of neuroscience 34:89-103.

Turrigiano G (2012) Homeostatic synaptic plasticity: local and global mechanisms for stabilizing neuronal function. Cold Spring Harb Perspect Biol 4:a005736.

Turrigiano GG (1999) Homeostatic plasticity in neuronal networks: the more things change, the more they stay the same [Review]. Trends in neurosciences 22:221-227.

Turrigiano GG, Nelson SB (2004) Homeostatic plasticity in the developing nervous system. Nat Rev Neurosci 5:97-107.

Tyagarajan SK, Fritschy JM (2014) Gephyrin: a master regulator of neuronal function? Nat Rev Neurosci 15:141-156.

Ueda N, Tsuboi K, Uyama T, Ohnishi T (2011) Biosynthesis and degradation of the endocannabinoid 2-arachidonoylglycerol. Biofactors 37:1-7.

Valcour V, Shikuma C, Shiramizu B, Watters M, Poff P, Selnes O, Holck P, Grove J, Sacktor N (2004) Higher frequency of dementia in older HIV-1 individuals: the Hawaii Aging with HIV-1 Cohort. Neurology 63:822-827.

Vanhems P, Dassa C, Lambert J, Cooper DA, Perrin L, Vizzard J, Hirschel B, Kinloch-de Loes S, Carr A, Allard R (1999) Comprehensive classification of symptoms and signs reported among 218 patients with acute HIV-1 infection. J Acquir Immune Defic Syndr 21:99-106.

Vera JH, Guo Q, Cole JH, Boasso A, Greathead L, Kelleher P, Rabiner EA, Kalk N, Bishop C, Gunn RN, Matthews PM, Winston A (2016) Neuroinflammation in treated HIV-positive individuals: A TSPO PET study. Neurology 86:1425-1432.

Vesce S, Bezzi P, Rossi D, Meldolesi J, Volterra A (1997) Hiv-1 Gp120 Glycoprotein Affects the Astrocyte Control of Extracellular Glutamate By Both Inhibiting the Uptake and Stimulating the Release of the Amino Acid. FEBS Letters 411:107-109.

Vezzani A, Maroso M, Balosso S, Sanchez M-A, Bartfai T (2011) IL-1 receptor/Toll-like receptor signaling in infection, inflammation, stress and neurodegeneration couples hyperexcitability and seizures. Brain, behavior, and immunity 25:1281-1289.

Viader A, Blankman JL, Zhong P, Liu X, Schlosburg JE, Joslyn CM, Liu QS, Tomarchio AJ, Lichtman AH, Selley DE, Sim-Selley LJ, Cravatt BF (2015) Metabolic Interplay between Astrocytes and Neurons Regulates Endocannabinoid Action. Cell Rep 12:798-808.

Viviani B, Corsini E, Binaglia M, Galli CL, Marinovich M (2001) Reactive oxygen species generated by glia are responsible for neuron death induced by human immunodeficiency virus-glycoprotein 120 in vitro. Neuroscience 107:51-58.

Viviani B, Gardoni F, Bartesaghi S, Corsini E, Facchi A, Galli CL, Di Luca M, Marinovich M (2006) Interleukin-1 beta released by gp120 drives neural death through tyrosine phosphorylation and trafficking of NMDA receptors. J Biol Chem 281:30212-30222.

Viviani B, Bartesaghi S, Gardoni F, Vezzani A, Behrens MM, Bartfai T, Binaglia M, Corsini E, Di Luca M, Galli CL, Marinovich M (2003) Interleukin-1b Enhances NMDA Receptor-Mediated Intracellular Calcium Increase through Activation of the Src Family of Kinases. J Neurosci 23:8692-8700.

Vlahov D, Graham N, Hoover D, Flynn C, Bartlett JG, Margolick JB, Lyles CM, Nelson KE, Smith D, Holmberg S, Farzadegan H (1998) Prognostic indicators for AIDS and infectious disease death in HIV-infected injection drug users: plasma viral load and CD4+ cell count. Jama 279:35-40.

Waataja JJ, Kim HJ, Roloff AM, Thayer SA (2008) Excitotoxic loss of post-synaptic sites is distinct temporally and mechanistically from neuronal death. Journal of neurochemistry 104:364-375.

Wallace JM, Rao AV, Glassroth J, Hansen NI, Rosen MJ, Arakaki C, Kvale PA, Reichman LB, Hopewell PC (1993) Respiratory illness in persons with human immunodeficiency virus infection. The Pulmonary Complications of HIV Infection Study Group. The American review of respiratory disease 148:1523-1529.

Wallace JM, Hansen NI, Lavange L, Glassroth J, Browdy BL, Rosen MJ, Kvale PA, Mangura BT, Reichman LB, Hopewell PC (1997) Respiratory disease trends in the Pulmonary Complications of HIV Infection Study cohort. Pulmonary Complications of HIV Infection Study Group. American journal of respiratory and critical care medicine 155:72-80.

Walsh JG, Reinke SN, Mamik MK, McKenzie BA, Maingat F, Branton WG, Broadhurst DI, Power C (2014) Rapid inflammasome activation in microglia contributes to brain disease in HIV/AIDS. Retrovirology 11:35.

Walter L, Stella N (2004) Cannabinoids and neuroinflammation [Review]. British Journal of Pharmacology 141:775-785.

Wang P, Barks JD, Silverstein FS (1999) Tat, a human immunodeficiency virus-1-derived protein, augments excitotoxic hippocampal injury in neonatal rats. Neuroscience 88:585-597.

Wang Z, Pekarskaya O, Bencheikh M, Chao W, Gelbard HA, Ghorpade A, Rothstein JD, Volsky DJ (2003) Reduced expression of glutamate transporter EAAT2 and impaired glutamate transport in human primary astrocytes exposed to HIV-1 or gp120. Virology 312:60-73.

Wierenga CJ, Walsh MF, Turrigiano GG (2006) Temporal regulation of the expression locus of homeostatic plasticity. Journal of neurophysiology 96:2127-2133.

Wilen CB, Tilton JC, Doms RW (2012) HIV: cell binding and entry. Cold Spring Harb Perspect Med 2.

Willey RL, Bonifacino JS, Potts BJ, Martin MA, Klausner RD (1988) Biosynthesis, cleavage, and degradation of the human immunodeficiency virus 1 envelope glycoprotein gp160. Proc Natl Acad Sci U S A 85:9580-9584.

Wilson RI, Nicoll RA (2001) Endogenous cannabinoids mediate retrograde signalling at hippocampal synapses. Nature 410:588-592.

Woodward DF, Pepperl DJ, Burkey TH, Regan JW (1995) 6-Isopropoxy-9-oxoxanthene-2-carboxylic acid (AH 6809), a human EP2 receptor antagonist. Biochem Pharmacol 50:1731-1733.

Wu MM, Zhang X, Asher MJ, Thayer SA (2019) Druggable targets of the endocannabinoid system: Implications for the treatment of HIV-associated neurocognitive disorder. Brain Res 1724:146467.

Wu Y, Yoder A (2009) Chemokine coreceptor signaling in HIV-1 infection and pathogenesis. PLoS pathogens 5:e1000520.

Wu Z, Guo Z, Gearing M, Chen G (2014) Tonic inhibition in dentate gyrus impairs long-term potentiation and memory in an Alzheimer's [corrected] disease model. Nat Commun 5:4159.

Xing HQ, Hayakawa H, Izumo K, Kubota R, Gelpi E, Budka H, Izumo S (2009) In vivo expression of proinflammatory cytokines in HIV encephalitis: an analysis of 11 autopsy cases. Neuropathology 29:433-442.

Yang J, Hu D, Xia J, Liu J, Zhang G, Gendelman HE, Boukli NM, Xiong H (2013) Enhancement of NMDA receptor-mediated excitatory postsynaptic currents by

gp120-treated macrophages: implications for HIV-1-associated neuropathology. J Neuroimmune Pharmacol 8:921-933.

Yu XM, Salter MW (1999) Src, a molecular switch governing gain control of synaptic transmission mediated by N-methyl-D-aspartate receptors. Proc Natl Acad Sci U S A 96:7697-7704.

Zhang J, Hu M, Teng Z, Tang YP, Chen C (2014) Synaptic and cognitive improvements by inhibition of 2-AG metabolism are through upregulation of microRNA-188-3p in a mouse model of Alzheimer's disease. J Neurosci 34:14919-14933.

Zhang X, Thayer SA (2018) Monoacylglycerol lipase inhibitor JZL184 prevents HIV-1 gp120-induced synapse loss by altering endocannabinoid signaling. Neuropharmacology 128:269-281.

Zhang X, Green MV, Thayer SA (2019) HIV gp120-induced neuroinflammation potentiates NMDA receptors to overcome basal suppression of inhibitory synapses by p38 MAPK. Journal of neurochemistry 148:499-515.

Zhao ML, Kim MO, Morgello S, Lee SC (2001) Expression of inducible nitric oxide synthase, interleukin-1 and caspase-1 in HIV-1 encephalitis. J Neuroimmunol 115:182-191.

Zhao P, Waxman SG, Hains BC (2007) Extracellular Signal-Regulated Kinase-Regulated Microglia-Neuron Signaling by Prostaglandin E2 Contributes to Pain after Spinal Cord Injury. J Neurosci 27:2357-2368.

Zhou Y, Liu J, Xiong H (2017) HIV-1 Glycoprotein 120 Enhancement of N-Methyl-D-Aspartate NMDA Receptor-Mediated Excitatory Postsynaptic Currents: Implications for HIV-1-Associated Neural Injury. J Neuroimmune Pharmacol 12:314-326.

Zink MC, Uhrlaub J, DeWitt J, Voelker T, Bullock B, Mankowski J, Tarwater P, Clements J, Barber S (2005) Neuroprotective and anti-human immunodeficiency virus activity of minocycline. JAMA 293:2003-2011.

Zorrilla de San Martin J, Delabar JM, Bacci A, Potier MC (2018) GABAergic over-inhibition, a promising hypothesis for cognitive deficits in Down syndrome. Free Radic Biol Med 114:33-39.